Lifetime Prediction of PVC Push-fit Joints

André Marques Arsénio

Lifetime Prediction of PVC Push-fit Joints

Proefschrift

ter verkrijging van de graad van doctor
aan de Technische Universiteit Delft,
op gezag van de Rector Magnificus Prof.ir. K.C.A.M. Luyben,
voorzitter van het College voor Promoties,
in het openbaar te verdedigen

op woensdag 27 november 2013 om 10.00 uur

door André MARQUES ARSÉNIO,
Master in Biological Engineering,

geboren te Sesimbra, Portugal.

Dit proefschrift is goedgekeurd door de promotor:
Prof.dr.ir. L.C. Rietveld

Copromotor: dr.ir. J.H.G. Vreeburg

Samenstelling promotiecommissie:

Rector Magnificus	voorzitter
Prof.dr.ir. L.C. Rietveld	Technische Universiteit Delft, promotor
Dr.ir. J.H.G. Vreeburg	Wageningen Universiteit, copromotor
Dr.P.Eng. B. Rajani, Principal	Rajani Consultants Inc., Canada
Prof.dr.ing. S. Sægrov	NTNU, Noorwegen
Prof.dr.ir. F.H.L.R. Clemens	Technische Universiteit Delft
Prof.dr.ir. R.F. Hanssen	Technische Universiteit Delft
Prof.ir. J.W. Bosch	Technische Universiteit Delft
Prof.dr.ir. J.P. van der Hoek, MBA	Technische Universiteit Delft, reservelid

This work was performed in the TTIW-cooperation framework of Wetsus, centre of excellence for sustainable water technology (http://www.wetsus.nl). Wetsus is funded by the Dutch Ministry of Economic Affairs. The author like to thank the participants of the research theme "Water Distribution and Water Quality" for the fruitful discussions and their financial support.

Typeset in LaTeX
Printed by Gildeprint Drukkerijen
Cover by Miguel Carvalho / www.miguelcarvalho.eu
Original photo of Pegões Acqueduct by Duarte Fernandes Pinto

ISBN 978-94-6186-217-4

Summary

Background

Despite the role played by joints in the failures occurring in drinking water networks, scientific literature has focused on barrel failure. Therefore, it can be assumed that the significance of these appurtenances has been disregarded.

The objective of this work is to create a procedure to predict the remaining lifetime of PVC push-fit joints. PVC was selected due to it being the most used material in the Netherlands and resistant to corrosion which facilitates condition assessment due to the absence of tuberculation. Finally, working with PVC, for example, in the laboratory, does not incur the inherent safety/health risks as with, for example, AC.

Failure modes of push-fit joints

In this thesis, failure is defined as leakage; a joint fails when it begins leaking. Seven failure modes for push-fit joints are presented with joint bending and axial pull-out being the most relevant for PVC push-fit joints. Failures due to physical-chemical degradation, although significant, are not considered in this thesis. This decision was made because non-destructively characterizing the physical/chemical condition of PVC in the field is difficult to achieve.

Non-destructive evaluation of PVC push-fit joints

The alignment of both pipes inside the joint is assumed to be a surrogate measurement for the joint's condition. When two pipes are connected with a double-socket PVC joint, the two pipes are separated by a gap. The alignment of a joint can be determined if the gap is measured at four different locations: 3 h (springline), 6 h (invert), 9 h (springline) and 12 h (crown). Two angles are calculated, one for the 12h-6h pair of gap values and a second for the 9h-3h pair. This can be achieved using a non-destructive evaluation (NDE) tool.

Several NDE tools were surveyed whereby the most promising for the assessment of PVC push-fit joints were selected and tested in the laboratory including ultrasound, CCTV and Panoramo® with CCTV consistently considered as the best, delivering both accurate and reproducible results.

Real-time pipe monitoring

This component of the work was projected as an alternative to inspections employing NDEs, for example, in the case of important assets where the risk of failure is minimal, *i.e.*, consequences of failure are exceptionally high*. For this, a PVC 250 mm drinking water pipe supplying water to approximately 1,250 customers was continuously monitored from September 2011 until June 2013. The aggregated data encapsules strains registered on pipes and joints in operation; soil temperatures next to the pipe; and strains registered on non-loaded coupons of isolated PVC and also installed next to the pipe.

The data exhibit an expected positive correlation between temperatures and strains. Daily water demand patterns were ascertained with the strain gauges affixed to the pipes and joints. Two confirmed episodes of water-hammer were also detected by the sensors. This demonstrates the accuracy of the strain gauges and their potential in detecting dynamic loads that can be detrimental to a pipe. This work also demonstrates that a pipe can be continuously monitored for expansion/contraction when other assessment methods are not available.

Destructive laboratory tests with PVC

Only minimal information is available regarding the limit conditions of joints in operation (*e.g.* the limit bending angle before leakage). Therefore, laboratory tests with PVC were planned. Pipes and joints of two diameters, 110 and 315 mm, were tested under two different conditions: water pressure (4 bar) and air sub-pressure (0.2 bar). Both joint bending and axial pull-out tests were performed. To monitor the behavior of the joint, its stiffness (bending moment vs. bending angle) was monitored in real-time employing a force sensor.

First, it was concluded that joint stiffness increases with bending angle, insertion, diameter and inner-pipe pressure. An increase in stiffness is considered dangerous because the joint becomes less able to bend. However, joint stiffness does not increase linearly with the bending angle (for the same diameter and pressure). The joint becomes stiffer after a threshold angle of 3° for 110 mm and 5° for 315 mm joints. These results are, for 10 m barrel pipes, more conservative than the limit defined by the AWWA (34° for 110 mm; 12° for 315 mm) and nearer to the limit defined by the Dutch PVC manufacturers of 6° for both diameters.

Second, the role played by insertion in the increase of joint stiffness demonstrates that the pipes should not be installed completely inserted inside the joints.

*An example is a pipe installed in a dyke.

Finally, for a rubber ring in good condition, leakage/intrusion can only be expected at bending angles above 10° and with complete pull-out of the pipe from the joint. Such extreme angles have not yet been detected in the field (Chapter 3).

The index for joint condition

The index for joint condition (IJC) was developed by employing installation guidelines and data aggregated from the aforementioned laboratory tests with the intention of exploiting it to assess *in-situ* joint conditions. The IJC affords a quantitative comparison of results obtained from different inspections and selecting the pipe in the worst condition. With the IJC, it is feasible to grade both the entire pipe and each joint separately which makes the results less prone to subjective interpretation.

Correlating failures & soil movement

Soil movement is one of the factors cited as a possible explanation for the failure of an underground infrastructure. Nevertheless, to the knowledge of the author, an investigation of the impact of soil movement in the occurrence of failure in drinking water networks had yet to be attempted.

Therefore, failure registration data was retrieved from USTORE (Section 1.6.3); the data encapsulated a period of 40 months during which 868 failures were registered. These data were exploited collectively with empirical ground movement data obtained from radar surveys. The results clearly demonstrated that the failure rates for PVC, CI and AC increase with the level of soil movement. For the study-area, while CI is the material most affected by soil movement, AC has the highest failure rates. Furthermore, there is a clear increase in the failure rate in the AC pipes installed prior to and following the 1960s. These conclusions were the beginning point in creating a risk map for the study-area. This map pin-points areas inside the distribution network that are expected to be more failure-prone. These riskier areas should either be inspected more often (pro-active on-condition AM) or replaced more often (pro-active routine replacement).

Concluding remarks

This thesis presents a four-step procedure to predict failure in PVC push-fit joints. The **first step** is selecting the best candidates for condition assessment, for example, employing a risk map that indicates failure-prone areas. The **second step** is to evaluate the joint condition through gap sizing by using non-destructive evaluation equipment (*e.g.* CCTV). The **third step** is to utilize the IJC, having the data retrieved from the condition assessment as input, and evaluating the condition of the pipe and the joints. A decision can subsequently be made to either replace the entire pipe or only a section of it or to schedule another inspection. The fourth and **final step** is to recommence the process: the lifetime prediction procedure is an iterative process, and the same pipe and joints should be inspected several times

throughout their lifetime. When their condition is below a certain threshold, they should be replaced.

Samenvatting

Achtergrond

Verbindingen in drinkwaterleidingen spelen een belangrijke rol in het geregistreerd falen van het drinkwaterleidingnet. Ondanks dit aanzienlijke aandeel, concentreert de wetenschappelijke literatuur zich op het falen van de leidingen. Hierdoor kan worden aangenomen dat de rol die verbindingen spelen bij storingen is onderschat.

Het doel van dit onderzoek is het opstellen van een procedure waarmee de resterende levensduur van PVC spie-mof verbindingen kan worden voorspeld. PVC is gekozen omdat dit het meest voorkomende materiaal is in Nederland. Daarnaast is PVC immuun voor corrosie. Dit vergemakkelijkt de conditiebepaling van de verbinding. Tevens vereist het werken met PVC, bijvoorbeeld in een laboratorium, geen speciale veiligheids- of gezondheidsrisico's in tegenstelling tot bijvoorbeeld AC.

Faalmechanisme van spie-mof verbindingen

In dit onderzoek is falen gedefinieerd als lekkage: een verbinding faalt als hij begint te lekken. Zeven faal-mechanismen voor spie-mof verbindingen zijn gepresenteerd, waarvan het verbuigen van de verbinding en het axiaal uit elkaar trekken de meest relevante zijn voor PVC spie-mof verbindingen. Falen als gevolg van fysisch-chemische aantasting zijn weliswaar belangrijk, maar zijn niet beschouwd in dit onderzoek. Deze keuze is gemaakt omdat het niet-destructief bepalen van de fysisch/chemische conditie in het veld erg moeilijk is te realiseren.

Niet-destructief onderzoek aan PVC spie-mof verbindingen

De uitlijning van beide leidingdelen binnen in de verbinding is beschouwd als een surrogaat parameter voor de conditie van de verbinding. Als twee leidingen zijn verbonden met een dubbele PVC mof verbinding, zijn de leidingdelen gescheiden door een spleet. De uitlijning van de verbinding kan worden bepaald door het meten

van de spleetwijdte op vier plaatsen: op 3 uur (horizontaal), 6 uur (bodem), 9 uur (horizontaal) en 12 uur (top). Twee hoeken worden bepaald: één voor de 12u-6u combinatie en één voor de 3u-9u combinatie.

Enkele NDE technieken zijn onderzocht waarvan de meest veelbelovende voor de conditiebepaling van PVC spie-mof verbindingen zijn geselecteerd en getest in het laboratorium: ultrasound, CCTV en Panoramo®. CCTV was de beste, omdat deze zowel accurate als reproduceerbare resultaten leverde.

Real time leiding monitoren

Dit gedeelte van het onderzoek is gericht op een alternatief voor de inspecties met de NDE technieken, voor toepassing op belangrijke leidingen die niet mogen falen (bijvoorbeeld een leiding in een dijk). Hiervoor is een 250 mm PVC drinkwater leiding, die water levert aan ongeveer 1250 aansluitingen, permanent gemonitord in de periode van september 2011 tot juni 2013. De verzamelde gegevens betreffen de spanningen op de leidingdelen en de verbindingen in bedrijf, bodem temperatuur naast de leiding en spanning op onbelaste coupons van PVC die geïsoleerd geplaatst waren naast de leiding.

De gegevens laten een positieve relatie zien tussen de temperatuur en de spanning, zoals verwacht. Het dagelijks waterverbruikspatroon kon worden herkend met de aan de buis vastgemaakte rekstrookjes. Ook zijn met de sensoren twee waterslag gebeurtenissen waargenomen die later zijn bevestigd. Dit laat de accuratesse zien van de rekstrookjes en de mogelijkheid om dynamische spanningen te meten die een risico kunnen vormen voor een leiding. Het werk laat ook zien dat het mogelijk is om een leiding permanent te monitoren op uitzetten/inkrimpen als er geen andere methoden beschikbaar zijn.

Destructieve laboratorium testen met PVC

Er is weinig informatie beschikbaar over de grenswaarde voor de conditie van verbindingen in het veld (bijvoorbeeld de grenswaarde voor de buiging, juist vóórdat het gaat lekken). Daarom zijn laboratorium testen met PVC uitgevoerd. Leidingen met verbindingen in twee diameters, 110 en 315 mm, zijn getest onder twee verschillende omstandigheden: water druk (4 bar) en lucht onderdruk (0,2 bar). Er zijn testen met zowel buiging als axiale uittrekking uitgevoerd. Een continue krachtsensor is gebruikt om de stijfheid van de verbinding te meten waarmee het gedrag van de verbinding is bepaald.

Ten eerste is geconcludeerd dat de stijfheid van de verbinding toeneemt met de buigingshoek, de insteekdiepte in de mof, de diameter en de druk in de leiding. De toename van de stijfheid wordt als gevaarlijk beschouwd omdat de verbinding minder vrijheid heeft om te bewegen. De stijfheid van de verbinding neemt echter niet lineair toe met de buigingshoek (voor dezelfde diameter en druk). De stijfheid wordt groter nadat een zekere limietwaarde is overschreden: 3° voor de 110 mm en 5° voor de 315 mm. Deze resultaten zijn voor 10 m leiding lengtes conservatiever dan de grenswaarde die door de AWWA is bepaald (34° voor 110 mm en 12° voor

315 mm) en dicht bij de grenswaarde die is bepaald door de Nederlandse fabrikanten: 6° voor beide diameters.

Ten tweede, de rol die de insteekdiepte speelt bij de toename van de stijfheid van de verbinding laat zien dat de leidingdelen niet volledig ingestoken moeten worden bij installatie.

Tenslotte, als de rubberring in goede conditie is kun je alleen lekkage of indringing verwachten bij buigingshoeken van meer dan 10° en bij complete uittrekking van de leidingdelen van de verbinding. Zulke extreme buigingshoeken zijn niet waargenomen in het veld (Hoofdstuk 3).

De index voor de verbindingsconditie

De index voor de verbindingsconditie (IJC) is ontwikkeld op basis van installatie richtlijnen en de gegevens van de eerdergenoemde laboratorium testen met als doel om het *in-situ* toe te passen. De IJC maakt het mogelijk om de resultaten van verschillende inspecties kwantitatief met elkaar te vergelijken en de leiding met de slechtste conditie te bepalen. Met de IJC is het mogelijk om de hele leiding te classificeren, maar ook iedere verbinding apart, waardoor de resultaten minder makkelijk verkeerd zijn te interpreteren.

De relatie tussen falende verbindingen en bodem beweging

Bodembeweging wordt beschouwd als een oorzaak voor het falen van de ondergrondse infrastructuur. Desalniettemin is, naar de kennis van de auteur, nog nooit geprobeerd om onderzoek te doen naar de invloed van bodembeweging op het voorkomen van falen van drinkwaterleidingnetten.

Om dit te doen zijn gegevens gebruikt van de USTORE database (paragraaf 1.6.3). De gegevens hebben betrekking op een periode van 40 maanden waarin 868 lekkages zijn geregistreerd. Deze gegevens zijn gebruikt in combinatie met empirische gegevens van de bodemdeformatie verkregen uit radar waarnemingen. De resultaten laten duidelijk zien dat de faalfrequenties van PVC, GIJ en AC toenemen met een toenemende bodemdeformatie. In het studiegebied had AC de hoogste faalfrequentie, maar GIJ is het materiaal dat het meest wordt getroffen door de bodemdeformatie. Daarnaast is er een duidelijke toename van faalfrequentie bij AC leidingen geïnstalleerd voor 1960. Deze conclusies vormen de basis voor een risicokaart die is gemaakt voor het studiegebied. Deze kaart laat zien in welke gebieden van het distributienetwerk er meer falen kan worden verwacht. Deze meer risicovolle gebieden zouden ofwel vaker geïnspecteerd kunnen worden (proactief AM) ofwel vaker vervangen kunnen worden.

Afsluitende opmerkingen

In dit onderzoek is een faal-voorspellings-procedure voor PVC spie-mof verbindingen gepresenteerd. De procedure kan in vier stappen worden geïmplementeerd. De eerste stap is het selecteren van de beste kandidaten voor het bepalen van de conditie, door bijvoorbeeld een risicokaart te gebruiken zoals hiervoor beschreven. De tweede stap is het bepalen van de conditie van de verbinding door de spleetwijdte te bepalen met behulp van de CCTV. De derde stap is het met behulp van de IJC, gebaseerd op de gegevens van de conditiebepaling, de leiding te classificeren. Dan kan de beslissing genomen worden om de leiding geheel of gedeeltelijk te vervangen of om een volgende inspectie te plannen. De vierde en laatste stap is het opnieuw starten van het proces. Het voorspellen van de restlevensduur is een iteratief proces waarin dezelfde verbinding verscheidene keren geïnspecteerd wordt gedurende de levensduur. Als de conditie een zekere grenswaarde overschrijdt, kan deze worden vervangen.

. . .

So grab your things
And stumble into the night
So we can shut the door
And shut the door on terrible times, oh

Yeah, do it right
And head again into space
So you can carry on and carry on
And fall all over the place

. . .

LCD Soundsystem - Home

To my Family.

Preface

From early on, I indicated that I would obtain a Ph.D., but that was even before beginning secondary school. After my first year at university, I was certain that I did not want to otbain a Ph.D. - in fact, I was not even sure if I wanted to complete my current degree. Now, approximately twenty years later, I am, indeed, a Ph.D. candidate which proves that it is the first impression that matters (even when it is ill-informed). Of course, I was not alone in this endeavour, and many people have assisted me throughout the years.

First and foremost, I would like to thank my sponsors which include the Dutch Drinking Water Companies that funded this project through the joint research program (BTO) and Wetsus that funded the project through the TTIw program. Without their assistance, none of this would have been achievable.

I owe much to Jan Vreeburg who always believed in me and in my capacities - many times, even more than myself. Jan certainly was not the most available supervisor[†] but was, beyond any doubt, always supportive both from a technical and, especially, from a personal perspective. I also wish to thank my promotor, Luuk Rietveld, for all of the assistance and help provided throughout the final year of my project. It is clear now that the arrival of Luuk as a second supervisor was a significant encouragement to complete everything (almost) on time. I also wish to acknowledge my first promotor, Hans van Dijk, for his role during the first years of the project.

It was a wonderful experience to write articles with so many different co-authors. I would like to thank them all for bringing their knowledge and opinions and helping to enrich my work.

It has been a delight for me to work with everyone at the Water Infrastructure group of KWR: George, Nellie, Ad, Martin, Ralph, Jos, Peter, Marcel, Mirjam, Cláudia, Joost, Andreas and Ronald, thank you for being wonderful colleagues. Ilse: thank you for being, from day one, the most encouraging and helpful person that has ever been involved in the project and for pushing me to plan and schedule my work and be more organized - I can assure you that not all was in vain and that something did remain imprinted in my mind (*please*, believe me). Hendrik, thank you for all of the help given to wire the monitoring set-up and to retrieve the data. Thank you,

[†]Maybe an *available supervisor* is the perfect oxymoron, a chimera, the Moby Dick of research.

Kim, for all of the help given with GIS. One final word must to go to Irene: thank you for being the best roomy that I have ever had and thank you for introducing me to Mr. Fuzzy and all his *fuzzyfied* friends - I will never see fuzzy-logic in the same manner as before (and thank you for that as well).

I would like to also thank the following people at the water companies: Eelco Trietsch and Jan Pot at Vitens; Rob de Jong and Rob de Bont at Dunea; Marcel Wielinga, Peter Schaap and Peter Horst at PWN and Henk de Kater at Evides; and Petra Holzhaus at WMD for always being available and cooperative. To all the pipe-fitters at the water companies that somehow helped me throughout this project, in sunny and in rainy days: from working with you, I understand how one builds a country such as the Netherlands.

Once again, I wish to acknowledge all of the members of the TTIw program table for all of the meetings, the valuable input and for the thorough and insightful reviews on my papers.

At DYKA, I would like to thank Mr. Freddie Bouma and Mr. Henk Meerman for affording me the opportunity to use their installations. Thank you, Jarig Bangma, for all of the support and comments derived from your deep practical knowledge. Finally, I wish to thank all of the people at DYKA's workshop for making me feel welcomed at all times - it was always a pleasure to travel to Steenwijk.

I wish to thank everyone at TU Delft - Mieke, Jennifer, Anouk, Jorge, Dara, Sam, Diana, Maria, Ran, David and Gang - and everyone at KWR - Roberto, Andreas, Helena, Sara and Diego - for these great four years.

To everyone at *Shelter Productions*: Baka, Mike[‡], Sofia, Nuno, Rodrigo, António and Seta, thank you for reminding me daily that true friendship overcomes both barriers and distance.

Mum and Dad: thank you for always having encouraged even my strangest ideas and having taught me to follow my dreams and to be happy. Once again: thank you very much.

Mãe e Pai: obrigado por me terem apoiado sempre de maneira incondicional e desde cedo me terem incentivado a seguir os meus sonhos. Uma vez mais: obrigado.

I wish to dedicate a final word to my lovely partner, Elisa, a central pillar in my life. Without her support, love and comprehension, I would not have achieved any of this.

André Marques Arsénio
Utrecht, November 7, 2013

[‡]Beautiful cover, *sócio*!

Contents

chapter 1

Introduction

Qualcosa doveva cambiare perché tutto restasse com'era prima.

Il Principe di Salina

These words, derived from the classic film *Il Gattopardo* (1963) by the Italian master Luchino Visconti, can be roughly translated as *something had to change, so everything could stay the same*. The film was localized during a troublesome period, the times were changing and Burt Lancaster, the Prince of Salina, had to make a decision.

Everyday, throughout the world, asset managers must also make decisions: "replace or repair?", "inspect or not?". Something must change so that everything can remain the same, *i.e.*, the supply of safe drinking water continues. If nothing changes, assets will fail more frequently, and this will imply additional costs for water companies. These costs, whether direct, indirect or social (Gaewski and Blaha, 2007; Makar and Kleiner, 2000) may, in time, become financially unsustainable.

In order to assist in decision making and help utilities to minimize their expenses, the objective behind this thesis is to develop a procedure that can be employed to predict the remaining lifetime* of PVC push-fit joints. This work comprises both condition assessment techniques for joints and the development of a lifetime prediction model. These topics will be briefly introduced in this first chapter that addresses the Dutch drinking network as the beginning point in order to discuss general concepts of asset management (AM).

*In this thesis, lifetime is interpreted as service life.

1.1 The Dutch drinking water network

1.1.1 Characteristics

The Association of Dutch Water Companies (VEWIN) publishes reports offering valuable information regarding the operations of Dutch drinking water companies. According to the most recent report (Geudens, 2012), more than 51% of the total network length is made of PVC with asbestos cement (AC) being the second most common material (approximately 28%), and cast iron (CI) as the third most used material (approximately 8% of the total length). An overview of the variation of the piped network composition since the 1950s is given in Figure 1.1. It can be clearly seen that, while the percentage of PVC has been steadily increasing, the opposite has been occuring with both AC and CI.

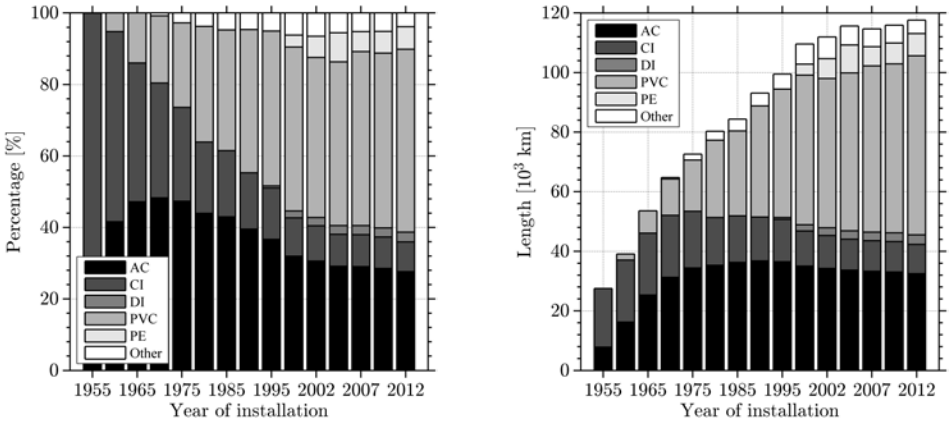

Figure 1.1: Length of drinking water network per pipe material in the Netherlands. In the country, the percentage of PVC has been increasing since the 1950s. The percentage of AC, after peaking in the 60s, as has been decreasing as has that of CI. The use of polyethylene (PE) used for house connections and ductile iron (DI) used for pipes beneath heavy-traffic roads, have been on the rise. Adapted from Geudens (2012).

1.1.2 Non-revenue water

In 2012, the ten largest Dutch water companies produced a total of 1,136 million m^3 of drinking water. The total non-revenue water (NRW) was 54 million m^3, or 4.8% of the total (Geudens, 2012). Although not representative of just leakage (Farley et al., 2003), leakage is frequently the most significant component of NRW (Methods et al., 2003).

In certain low-income countries, NRW represents 50-60% of supplied water with a global average estimated at 35% (Farley et al., 2008). Therefore, the Dutch NRW level is minimal even when compared to other developped countries. Collaborative work between Dutch and British research institutes was performed to investigate

this (UKWIR, 2006). The authors concluded that the Dutch companies have a lesser leakage percentage for the following reasons (Ofwat, 2007):

- Low operating pressures due to the flat terrain and the tall buildings being equipped with their own pumps;
- A newer, post-war infrastructure system when compared with England and Wales and typically made of non-corrosive PVC;
- The mains tend to be situated under footpath paving blocks and in sandy soils which signifies that leaks cause the pavement to subside which facilitates easy leak location and easy repair access;
- Existence of fewer joints as a single connection generally supplies a number of buildings; and
- Quick repair of reported leaks.

1.2 Failure rate

A typical performance indicator to characterize drinking water networks is the failure rate (Moglia et al., 2008; Tabesh et al., 2009). This parameter is represented by Equation 1.1.

$$\lambda = \frac{f}{\sum L \times \Delta t} \tag{1.1}$$

Where λ is the failure rate [#.km^{-1}.yr^{-1}], f is the recorded number of failures [#] during the time period of observation Δt [years]; and $\sum L$ is the pipe network length [km]. Certain authors present the values of λ per 100 km of pipe network (Burn et al., 2005). According to Rajani et al. (1996), a failure rate greater than 0.05 #.km^{-1}.year^{-1} is "undesirably high". O'Rourke (2010) employs a similar parameter entitled repair rate [# repairs.km^{-1}]. This formulation, solely normalized in reference to network length, is of use in episodic situations such as earthquakes. However, for the long-term analysis of network performance, the normalization, in respect to time, becomes necessary.

Rajani et al. (1993) exploited data from 21 Canadian water utilities to calculate failure rates in PVC pipes. Summing all PVC failures over the total PVC pipe length yields an average failure rate of 0.07 (#.km^{-1}.year^{-1}). Per utility, the failure rate figures varied from 0.009 (Windsor) to 0.03 (Ottawa-Carleton).

In their work, Mackellar and Pearson (2003) compiled data from 17 utilities across the UK. The authors demonstrated that, for those utilities, the average failure rate for 5 years (1998-2002) was 0.16 (#.km^{-1}.year^{-1}) for AC, 0.053 for DI, 0.20 for CI, 0.032 for PE, 0.073 for PVC and 0.11 for steel.

Burn et al. (2005) surveyed 44 water utilities in Australia, Canada and in the USA with significant volumes of PVC in their systems. The authors reported a broad range of failure rates (0.0004 to 0.11 #.km^{-1}.year^{-1}) with an average of 0.046.

Vloerbergh and Blokker (2010) indicated that, for the Netherlands, the overall failure rate (for all pipe materials together) was in the range of 0.06 #.km^{-1}.year^{-1}. This demonstrates that the Dutch figures are among the lowest worldwide.

Both the reduced failure rate and diminished leakage figures demonstrate that, although natural environment plays a role, proper network management is crucial, *i.e.*, materials used, location of the pipes and response to failures.

1.3 What is asset management?

"AM allows asset-intensive businesses to use limited resources to achieve their stated business objectives in the most cost-effective way" (Edwards, 2010), irrespective of the country's level of development (Parker, 2010). The Institute of Asset Management argues that "AM is emerging as a 'mainstream' expectation for competent organisations" (IAM, 2012). AM at utility level is thoroughly addressed in Deadman (2010), and its importance has been clearly identified in Bernstein and Laquidara-Carr (2013). Bernstein and Laquidara-Carr (2013) surveyed 451 utilities in the water and infrastructure sector in the US and Canada and ascertained that, for the surveyed utilities, the top three benefits of AM were:

1. Improved ability to explain and defend budgets/investments;
2. Improved focus of priorities; and
3. Improved understanding of risks/consequences of alternative investment decisions.

The EPA (2002) estimated the gap between the projected need and current spending for clean water and drinking water infrastructure over the next 20 years in the US. The authors indicated that the clean water capital payment could be between $73 billion and $177 billion with a point estimate of $122 billion.

Additionally, according to Folkman (2012), over 8% of the installed water mains in the US and Canada are beyond their expected service. The author argues that, given the rapid increase on pipes requiring immediate replacement, improved AM is essential so that all utilities can survive this trend. In fact, Kirby et al. (2006) show that AM allows utilities to cut operating costs, reduce capital expenditure and improve the level of service. These examples demonstrate the importance of AM not only in maintaining a productive operational level but also to avoid disastrous situations.

Nevertheless, AM is a broad field, and there is not one individual recipe for success. Hudson et al. (1997) identified various possible approaches:

- Reactive maintenance where maintenance is performed to repair damage and/or restore infrastructure facilities to satisfactory operation or function following failure;
- Proactive maintenance where maintenance is performed to delay deterioration or failure of a component or system;

  - On-condition maintenance where maintenance is performed in response to condition monitoring indicating impending deterioration or failure; and

- Routine maintenance where maintenance is performed on a regular basis or schedule.

According to Marlow et al. (2009), proactive strategies are generally applied to assets when the consequences associated with failures are significant, for example, pipes installed in dykes (typical Dutch situation) or alongside important transport routes (*e.g.* highway or railways). In these situations, "there is the potential for authorities, municipalities and other segments of society to incur high costs (tangible and/or intangible) if failure occurs. For such assets, the economics of preventing failure are advantageous".

In Figure 1.2, a possible on-condition maintenance approach is presented. It requires up-to-date and accurate information about the asset's condition (Costello et al., 2007) that can be obtained with a non-destructive assessment of the asset. The remaining lifetime is then modeled taking the current condition as input:

1. Select the best pipe for inspection. This can either be accomplished by employing practical knowledge - areas where the pipe-fitters are aware that the failure rate is greater than average - or be a data-driven decision as discussed in Kleiner and Rajani (2008). An alternative approach will be presented in Chapter 7;
2. Inspect the pipes using the most appropriate inspection tool. This topic will be extensively discussed in Chapter 3;
3. With the information aggregated during the inspection, either:
   (a) If the condition of the asset is below a previously defined threshold, repair/replace;
   (b) Otherwise, predict the remaining lifetime, indicated as t, of the asset exploiting an appropriate model (Section 1.5); and
4. Finally, schedule a new inspection after a period, t', shorter than t. The actual condition of the asset at t' can be exploited to re-calibrate the model used in step 3b.

1.4 Non-destructive assessment

Recently Liu et al. (2012) argued that "information on the current structural condition of individual water mains [and joints], combined with a good understanding of failure modes and deterioration models, can greatly enhance the ability of water utilities to manage their assets in a cost-effective manner", which was confirmed by Bernstein and Laquidara-Carr (2013). The authors demonstrated that this approach was the most effective AM practice with 53% of the surveyed utilities practicing this approach.

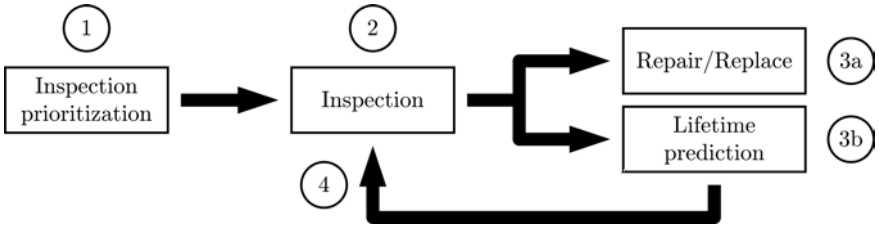

Figure 1.2: Scheme of a proactive AM approach. 1) pipes are selected for inspection; 2) the inspection is performed, and the condition of the pipes is evaluated; 3a) if the pipes are in poor condition, they are repaired/replaced; 3b) if they are in poor condition, their expected remaining-lifetime is calculated employing an appropriate model. Finally, 4) a new inspection is scheduled, and the output of the pipe condition is utilized to calibrate the prioritization model used in 3b.

One manner in which to perform condition assessment is by utilizing non-destructive evaluation (NDE) equipment. NDEs are powerful tools that, collectively with failure models, can play an important role in a proactive approach to the management of water assets. According to Najjaran et al. (2004), NDE tools can be exploited on two levels: first, to provide a snapshot of the pipe condition at a given time in order to determine if immediate intervention is required; and, second, NDE tools can be deployed in subsequent inspections to assess the rate of deterioration and calibrate certain parameters of the lifetime prediction models and improve their accuracy (Rajani and Kleiner, 2002).

Many researchers have devoted their work in developing innovative NDE tools that can be applied to a multitude of pipe materials in various conditions. Certain research has been conducted on the condition assessment of wastewater networks: Andrews (1998), Makar (1999) and Feeney et al. (2009). The work of Dingus et al. (2002), Reed et al. (2006) and Liu and Kleiner (2012) are examples of research conducted on the inspection and condition assessment of drinking water networks.

1.5 Modeling remaining asset life

Modeling remaining asset life is an important instrument in proactive AM and is indissociable from condition assessment.

Kleiner and Rajani (2001) and Rajani and Kleiner (2001) divided lifetime prediction models into physical-based and statistically-based. Both approaches require information on the asset's condition, either as input (physically based) or to validate the assumptions made by the model (statistically based). Therefore, although condition assessment exists without lifetime prediction procedures - the water utility can exploit the results of an inspection program to immediately replace a pipe - the opposite is not true. The same utility should not replace a pipe just because a given model predicts it to be "old". This is even more the case for very important pipelines for which the cost of replacement can easily surpass the cost of inspection.

More recently, Marlow et al. (2009) reviewed the different approaches to model the remaining lifetime of assets. The authors distinguished the various models into deterministic, statistical, physical and soft-computing or artificial-intelligence based approaches.

1.5.1 Deterministic modeling

In deterministic models, the relationship between external factors and asset failure are assumed to be certain. These are relatively simple to develop and apply. However, they usually rely on a number of simplifying assumptions. Additionally, they do not account for the uncertainty that is associated with asset deterioration and failure. Deterministic models can be further divided into physical deterministic and empirical deterministic.

Physical deterministic models

These models have been primarily applied to model corrosion in metallic water pipes. One example is a linear model based on the assumption that corrosion pit depth has a constant growth rate (Randall-Smith et al., 1992) (Equation 1.2).

$$\rho = \left(\frac{g}{P_e + P_i} \delta \right) - g \tag{1.2}$$

Where ρ is the remaining life [years], g is the age of the water main [years], δ is the thickness of the original pipe wall [m], P_e is the external pit depth and P_i is the internal pit depth [m]. This model requires the pipe age, wall thickness and depths of internal and external corrosion pits. This information is typically obtained from a condition assessment of pipe samples that are ascertained following exhumation.

Empirical deterministic

A classic empirical deterministic model was presented by Shamir and Howard (1979): regression analysis was used to create a break prediction model that relates a pipe's breakage to the exponent of its age (Kleiner and Rajani, 2001) (Equation 1.3).

$$\lambda\left(t\right) = \lambda\left(t_0\right) \times e^{A(t+g)} \tag{1.3}$$

Where $\lambda(t)$ is the failure rate [$\#.\mathrm{km}^{-1}.\mathrm{yr}^{-1}$] at time t elapsed from present [years]. $\lambda(t_0) = \lambda(t)$ when the pipe is new, and A is the coefficient of breakage rate growth [yr^{-1}].

1.5.2 Statistical models

The prediction of pipe failure with statistical models is conducted based on historical performance data (*e.g.* failure data). These models attempt to capture the inherent uncertainty and employ historical data that describes failure rates or service lifetimes in asset cohorts. Statistical models can be used for assets where historical data are readily available for analysis. A classic example of statistical models is the one presented by Herz (1996), *i.e.*, the "Herz distribution".

1.5.3 Physical probabilistic models

Physical probabilistic models are based on a comprehension of the physical processes that lead to asset failure while accounting for realistic uncertainty and are beneficial in those cases where no historical data are available. They are underpinned by a robust understanding of the degradation and failure processes that occur for an asset in service (corrosion, fracture, etc.). Therefore, while the models do not require access to statistical data, availability of physical related data are necessary[†]. However, the models also attempt to account for realistic uncertainty by using appropriate probability distributions for model variables. However, they can be data intensive and, in the event that insufficient data exist to adequately describe model variables, simplifying assumptions are required. Davis et al. (2007) presented a physical probabilistic model developed to estimate failure rates in buried PVC pipelines as they age.

1.5.4 Soft-computing or artificial intelligence-based models

These models are data-driven rather than model driven. One example is the use of Artificial Neural Networks (ANNs) to predict output from input information in a manner that simulates the operation of the human central nervous system (Asnaashari et al., 2013), otherwise known as Fuzzy logic to model pipe degradation (Kleiner et al., 2006b).

1.6 Mains failure databases

Network management relies on accessibility to relevant data. In fact, the decisions to replace, repair or inspect should be *data-driven* and not *hint-driven*, and this is even more the case with important assets. One of the decision-support tools for a network manager is a mains failure database (MFD). In such a database, all failure related data (date, location, material type, cause of failure, etc.) are registered. These databases become more significant with time as the volume of data, together with its statistical significance, increases.

Gaewski and Blaha (2007) collected information on 30 large-diameter (above 20-inch) pipe breaks and demonstrated that the average total cost was approximately $1,700,000. The authors argued that a MFD would be beneficial in assessing the status of buried infrastructure and assist in avoiding such disastrous episodes. Similarly, Grigg (2009) argued that a MFD can improve knowledge on actual conditions in a utility's asset base and offer utilities an efficient manner in which to organize and manage their pipe failure data.

In fact, with access to such databases, a manager is able to, for example, determine failure rates (Equation 1.1), Failure rates can be calculated to determine failure prone materials or areas within the network. Failure registration data are also the input to certain models presented above (for example, Section 1.5.2).

[†]For example, temperature or precipitation series; or soil properties (*e.g.* soil resistivity, chlorides, pH) (Rajani and Kleiner, 2001)

Several countries around the world have attempted to create national MFDs (NMFDs). Such a database stores all available failure data in a country to produce a larger and more significant source of data. Nevertheless, establishing such a database is not a straightforward process as, for example, each utility utilizes its own registration procedure.

To the author's knowledge, worldwide, only the UK and the Netherlands have operational NMFDs.

1.6.1 NMFD of the United Kingdom

The NMFD implemented by the UK Water Industry Research UKWIR (2008) is the result of a cooperative work of the British water companies. In 2006, the database comprised 480,000 failures of approximately 350,000 km of water mains. These failures were recorded by over 95% of the UK companies from approximately 1995 forward (Mackellar, 2006).

UKWIR (2008) harmonized the plethora of data formats received from the participating utilities and produced an anonymous database. The database was implemented to allow access and analysis of the data employing readily available MS Office® tools. Several companies had used the data to support their AM business plans to the British Regulator, OFWAT.

According to Grigg (2009), pipe data attributes included in the database include an identification number, diameter, material type, location, lining, ground surface type, installation year and whether the main has pumped or gravity flow. Failure data items include type of failure, whether third-party damage was involved, location and other related information. The British database and respective website have been operational since 2009 (Cima and Peters, 2009).

1.6.2 NMFD of the United States

The British NMFD was adapted to the American situation (*i.e.* types of pipe, national specifications) and consists of a website where utility staff could upload their mains inventory and their failure related data. The company's data would then be anonymized and pooled. Basic reports can be created or data can be extracted and exploited for additional advanced analysis elsewhere (Grigg, 2013; Hodgins, 2013).

Grigg (2009) identified the main challenges in adapting the British database to US conditions and practices, which vary widely among utilities:

- How to include geographical information: the US has a state plan coordinate system, but it does not provide a unified national grid system,
- How to import soil data; and
- How to coordinate the main different practices for collecting and managing pipe data among US utilities.

Initially, 20-30 utilities were contacted to participate in the project. All utilities were from medium to larger cities (not the top-10 largest), and only two utilities participated. The explanations for such low participation were (Hodgins, 2013):

- Inexistence of a regulatory driving force as is evident in the UK (OFWAT);
- The larger utilities most likely already possessed a pipe-analysis system;
- Lack of funding and manpower. On the one hand, most utilities did not have available staff to compile and upload the data (difficult economic times) and, on the other hand, the researchers did not have personnel to manage the project more closely; and
- Lack of quality on certain utility's data.

Nevertheless, Hodgins (2013) argues that one of the two participating utilities, despite the necessary work to compile and upload the data, realized that the system afforded them an improved understanding on i) the type of data and the data-quality necessary for such project, and ii) the analysis process and overall support for the utility in repair/replace/maintenance decisions.

A report including all of the conclusions of this project and authored by Neil Grigg (Colorado State University) is due to be published by the Water Research Foundation.

1.6.3 NMFD of the The Netherlands

Seven Dutch water companies, collectively with KWR - Watercycle Research Institute[‡], have developed a NMFD to uniformly register water mains failure data. This data can then be exchanged, analyzed and exploited in order to improve AM in the country.

When a failure occurs in the network, a work order is placed, and one of the fitters receives the order. The pipe fitter travels to the failure location, repairs the failure and registers at least the mandatory questions on the form. The questions on the form pertain to information about the failure (date, location, cause and nature), about the asset (appurtenance, material, age, diameter, etc.) and about the surroundings (presence of trees, type of soil, etc.).

To exchange the failure data, a secure database system with web access, referred to as USTOREweb, has been developed. USTOREweb combines the individual databases into a composite database. In addition to the failure databases, databases of network lengths are provided by each water company to enable the calculation of failure rates. Prior to the failure data being entered into the central database, each record is examined for omissions and duplicates. Records that lack certain (mandatory) fields or are already in the database are excluded from the database and reported back to the company for checking. Improved or completed records can be uploaded again. All participants can download an anonymous composite database. Despite containing all uploaded failures, the downloaded database does not contain company name, address or coordinates of the failure. Asset managers can employ the database to perform their own specific analyzes or compare their data with the complete data-set.

The complete data-set encompasses the period of 2009-2013, and the length of the network available on the database is over 50,000 km more than 42% of the total

[‡]The Dutch Drinking Water Research Institute

national length of 117,585 km (Geudens, 2012). USTORE will be exploited as input for the lifetime prediction procedure (Chapter 7) and is thoroughly discussed in Vloerbergh and Blokker (2010) and Vloerbergh et al. (2012).

1.7 PVC in operation

1.7.1 Aging & degradation of PVC

Different pipe materials behave (and fail) in different ways. For example, for metallic pipes, the typical failure mechanism - corrosion - is fairly well known and described (Doleac et al., 1980; Randall-Smith et al., 1992). On the contrary, the characterization of failure modes in polymeric pipes is more difficult and, in fact, little is known about their long-term deterioration mechanisms. According to Rajani and Kleiner (2001), these "are not as well documented [as for other materials], mainly because these mechanisms are typically slower than in, for example, metallic pipes and also because PVC has been used commercially only in the last 35-40 years". Nevertheless, some degradation mechanisms for PVC may include chemical or mechanical degradation, oxidation and biodegradation of plasticisers and solvents (Rajani and Kleiner, 2001).

Visser (2009) developed an NDE method to determine the residual lifetime in unplasticised PVC (uPVC) - an older and more brittle version of the modern PVC. The author employed a procedure specified as micro-indentation to quantify the hardness and, therefore, the resistance against plastic deformation. His observations induced that this technique can be employed for the assessment of the current state of uPVC. This material, according to Burn et al. (2005), in spite of registered premature failures, when properly designed and installed should have a lifetime of at least 50 years. Some experts suggest that even 100 years is a conservative estimate.

The Dutch research institute TNO produced a series of reports entitled "Long term performance prediction of existing PVC water distribution systems" (Boersma, 2002; Boersma and Breen, 2003, 2006; Breen, 2005, 2006; Breen and Etsu, 2003; Lange, 2003) in which producers of PVC and PV material as well as representatives from water companies participated in the investigation. The authors concluded that the lifetime of a plastic product is determined by the intrinsic properties of the polymer applied, the processing of the polymer into a product, and the final operation conditions. The authors argued that, with properly installed pipes and scratches less than 1 mm in depth, the expected residual lifetime should surpass 100 years. Nevertheless, the reliability of the lifetime of PVC water systems is strongly correlated with the uncertainty regarding the future loadings to be experienced by the PVC pipes. In fact, external loadings and non-uniform soil settlements can cause significant local stresses in PVC pipes and subsequent preliminary failure. A lifetime of less than 10 years is feasible when a calamity occurs (Breen, 2006).

1.7.2 PVC joints in the field

One possibility of characterizing the behavior of PVC pipes and joints is by investigating failure registration databases (Section 1.6) and information aggregated

through surveys sent to drinking water companies.

Folkman (2012) surveyed 188 Canadian and American utilities. While corrosion was a main cause for water breaks, PVC pipes demonstrated having the lowest failure rates (0.016 #.km^{-1}.year^{-1}) with CI pipes having the highest (0.15 #.km^{-1}.year^{-1}).

Dingus et al. (2002) remitted surveys to the 100 most significant AwwaRF member utilities whereby 46 companies filled out a questionnaire and returned it. For the transmission systems, the number one problem was joint leaks/failures (35%), irrespective of the pipe material. For the PVC distribution systems, less than 15% of the total number of problems was due to a problem in a joint.

Burn et al. (2005) discussed data collected through a survey from utilities in Australia (nine utilities), Canada (four utilities) and in the US (four utilities). The total length of pipes in the collective networks was over 97,000 km, of which approximately 12,000 km was PVC. For the networks with PVC, the percentage of failures registered as a joint leak ranged from 1% up to 38% and averaging 16%.

The data analyzed by Reed et al. (2006) were obtained from a questionnaire to seven utilities from the UK (one), USA (four), and Canada (two). The total mains population was 33,247 km consisting mainly of CI (40% of length) and PVC as the fourth most used material (11%). PVC joint failures were dominated by gasket/seal failure (55%). The primary cause of joint failure for mechanically joint non-metallic pipes (AC, reinforced concrete and PVC) was ground movement.

Arai et al. (2010) surveyed Japanese water companies and gathered information on leakages related to water distribution pipelines that occurred during 2004 and 2005. The Japanese network is composed of approximately 600,000 km of water pipelines. More than 40% of the entire number of failures was detected at joints. When focusing on PVC, more than 60% of the failures were detected at joints.

USTORE (Section 1.6.3) shows that, in the Netherlands, of the total number of failures, approximately 29% are detected at joints (irrespective of pipe material), and over 9% of all failures are detected at PVC joints.

1.8 Problem definition

In Section 1.7.2, it was clearly demonstrated that joints play a major role in the failure in a network comprised of PVC. However, given the focus of literature on pipe barrel deterioration, it can be assumed that this role might have been disregarded.

Additionally, although the importance of on-condition pro-active AM has been thoroughly motivated in Section 1.3, at a utility level, the *status quo* has been reactive AM for low-importance/risk assets and routine maintenance AM for high-importance/risk assets.

Therefore, the current work is focused on developing a novel pro-active on-condition AM procedure for PVC push-fit joints. PVC is selected for three main reasons: i) it is the most used material in the Netherlands (Section 1.1.1); ii) it does not corrode and PVC walls remain clean (easy to inspect) throughout its lifetime; and iii) working with PVC does not pose the inherent safety/health risks as with, for example, AC. The objectives of this thesis are:

1. Define the failure modes of PVC joints. This will cast light on the origins of joint failure and determine how joint condition can be assessed;
2. Develop a condition assessment method. The failure modes will be the beginning point in creating the condition assessment method;
3. Choose the best NDE tool for this application. This tool will be selected from commercially available tools; and
4. Implement a lifetime prediction procedure. Since not all pipes can be inspected, this procedure will assist in precisely defining which pipes in a network should be inspected first.

1.9 Layout of this thesis

The seven failure modes for push-fit joints derived from literature are presented in **Chapter 2**: joints fail in various ways and due to different reasons. To cast some light on this issue, a literature review and a collection of failure modes for joints, irrespective of material type, are presented.

In **Chapter 3**, all of the work performed with NDE tools is covered. A thorough literature review was performed bearing in mind the condition assessment of PVC pipes and joints. The three most promising NDE tools were tested both in the laboratory and in the field; those results are also discussed.

Condition assessment can also be performed in real-time without the use of NDE tools. In **Chapter 4**, a possible approach is presented: several sensors (strain gauges, thermometers) were installed on barrels, joints, and in the soil adjacent to them. This pipe is employed to supply drinking water to Dutch customers. This set-up allows monitoring the behavior of the pipe in real-time for daily (*e.g.* effect of water demand pattern) and seasonal (*e.g.* air temperature) changes.

One of the knowledge gaps before beginning this work was the lack of information on limit condition before failure, especially maximum joint angle before leakage. To characterize this, destructive laboratory tests were conducted with hundreds of PVC joints and pipes. All data are discussed in **Chapter 5**.

The index for joint condition (IJC) is introduced in **Chapter 6**. The IJC is a graphical framework that can be utilized to characterize the condition of PVC push-fit joints *in-situ*. The IJC is a result of the aforementioned laboratory tests and has an enormous practical potential: characterizing the condition of a newly installed pipe or deciding which one of the two pipes should be replaced.

An approach to determine failure-prone areas within drinking water networks is surveyed in **Chapter 7**. This work was conducted by correlating failures in drinking water networks obtained from USTORE (Section 1.6.3) with ground movement data obtained through satellite surveys.

Finally, the general conclusions are presented in **Chapter 8**.

chapter 2

Failure modes of push-fit joints[†]

This chapter was the first section of this work and was initiated by Ilse Pieterse. Nevertheless, due to being the foundation of the thesis, it was continuously updated. The objective was to review scientific and technical literature and collect as much information about joint failure as possible.

In fact, "joint failure" has a very broad definition. Two situations, *i.e.*, a pipe that is completely pulled-out from the joint or a joint that is fractured, can both be registered as "joint failure" (Section 1.6) by a pipe-fitter. Given the difference between both failures, it is important to register more information about the failure - the mode. This additional information is valuable: knowing the areas inside of a distribution network where certain failure modes occur or which type of materials (or of what age) fail in specific ways is of the utmost importance both for scientists and network managers.

Nevertheless, it is recognized by the author that improving failure registration is not an easy feat: filling out a 10-20 question form on a -5°C day after having spent 2 hours fixing a burst pipe burst is hardly a priority. Nevertheless, creating a framework to improve failure registration is an initial step.

In this chapter, seven failure modes for joints are presented and discussed.

[†]This chapter is based on the following articles:

Arsénio, A. M., Pieterse-Quirijns, E. J., and Vreeburg, J. H. G. (2009a). Failure mechanisms of joints in water distribution networks and its application on asset management. In *Leading Edge on Strategic Asset Management (LESAM)*, Miami (Florida, USA)

Arsénio, A. M., Vreeburg, J. H. G., Pieterse-Quirijns, E. J., and Rosenthal, L. (2009b). Overview of failure mechanism of joints in water distribution networks. In Boxall, J. and Maksimović, C., editors, *Computing and Control in the Water Industry (CCWI)*, pages 607–612, Sheffield (UK). CRC Press

Arsénio, A. M., Pieterse-Quirijns, I., Vreeburg, J. H. G., de Bont, R., and Rietveld, L. (2013c). Failure mechanisms and condition assessment of PVC push-fit joints in drinking water networks. *Journal of Water Supply: Research and Technology-AQUA*, 62(2):78

2.1 Introduction

The reason for this work was thoroughly motivated in Section 1.7.2: it was demonstrated that joints play a major role in the failures registered in a network comprised of PVC pipes. However, given the focus of literature on pipe barrel deterioration, it can be assumed that the role played by PVC pipes may have been disregarded.

During an NDE inspection and/or afterwards during analysis, operators and analysts should focus on detecting distress indicators on the pipes or joints. According to Rajani and Kleiner (2004), these are forms of deterioration that have not yet led to pipe or joint failure. Among the distress indicators presented by the authors are cracks in cement, plastic or metallic pipes; corrosion pits in metallic pipes; and broken prestressing wires in prestressed concrete cylinder pipes. However, no distress indicators were defined for PVC joints. This might be explained by the fact that PVC has only been employed on a large scale since 1960 and that long-term deterioration mechanisms are not well documented for PVC mainly because the deterioration occurs slowly (Rajani and Kleiner, 2001). Breen et al. (2004) also argued that the lifetime of PVC material that is well processed, well installed, and applied under relative mild service conditions will exceed 50 years and even possibly 100 years.

Therefore, the objectives of this chapter are identifying the appropriate distress indicators - failure modes - for PVC joints. This chapter is also the beginning point for the development of the inspection procedure presented in Chapter 3.

2.2 Types of push-fit joints

It is not the objective of this work to present an exhaustive description of all of the joint systems employed for all pipe materials as this topic is thoroughly discussed elsewhere (Reed et al., 2006). Nevertheless, it is necessary to differentiate between the various types of push-fit joints that are commercially available for PVC pipes. The term push-fit joints, in this work, defines any type of joint that is not fixed with bolts or screws and is not glued. There are two primary types of these joints including bell-and-spigot joints and the double-socket joint which is used only in the Netherlands.

2.2.1 Bell-and-spigot joints

Around the world, pressurized drinking-water PVC pipes are usually connected using the bell-and-spigot system (Reed et al., 2006). In these systems, the straight spigot end of one section is inserted in the flared-out end of the adjoining section (Figure 2.1). The system is sealed with rubber gaskets.

2.2.2 The double-socket PVC joint

In the Netherlands, PVC pipes are connected with stand-alone joints*. These have two rubber gaskets and connect two pipe-barrels (Figure 2.2). While the rubber

*The same system is employed for water, gas and wastewater networks.

gaskets keep the system sealed, the pipes are separated inside of the joint by a ring. For smaller diameters (< 250 mm), this ring is a loose piece that separates both pipes inside the joint (Figure 2.2, in the center in black). For larger diameters, the ring is molded with the joint. This ring creates a gap between the pipes, ensuring that the pipe ends are not touching each other and are symmetrically situated inside the joint during installation. The sizing of this gap is the principle behind the assessment procedure presented in Chapter 3.

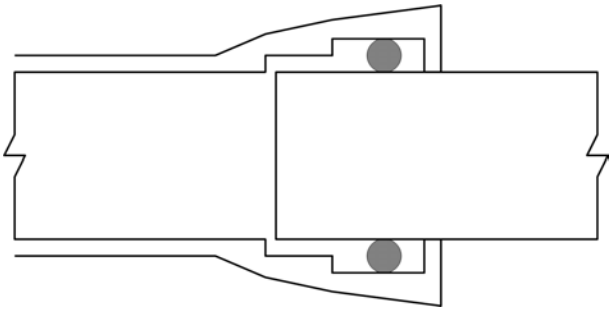

Figure 2.1: Schematic of a bell-and-spigot joint. In this system, the straight spigot end of one section is inserted in the flared-out end of the adjoining section. The rubber gasket (grey circles) seals the system.

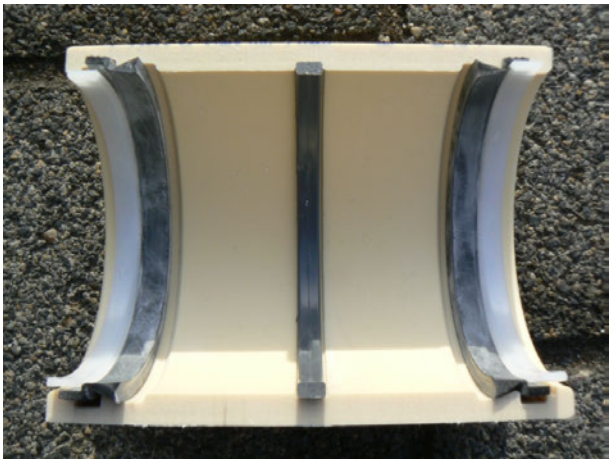

Figure 2.2: Longitudinal cut of a double-socket DN110 PVC joint. At the center, a ring (black) separates both of the two pipes inside the joint. For joints below 250 mm, the ring is a stand-alone piece. For larger diameters, the joint is molded with a ring. At each end, a rubber gasket (black) keeps the system sealed. In this figure, on each side of the joint, two white/light-blue rings are visible on top of the rubber gaskets. For joints of this diameter, this is the system to fix the rubber gaskets in place; for joints above 250 mm, the rubbers gaskets are fixed to the joint.

2.3 Joint condition & failure

2.3.1 Ideal & threshold conditions of a joint

A PVC joint is designed to accommodate changes in alignment - to bend - and the threshold bending angle varies with diameter and with the shape of the joint.

The ideal condition or alignment of a joint can be defined as the alignment inside the joint that minimizes the occurrence of stress within the joint and allows for a certain movement of both pipes inside the joint. In this situation, the pipes are perfectly aligned along their axis and are not touching each other or the joint's inner-wall (Figure 2.3). Reversely, the threshold condition of a joint is an alignment inside the joint for which a slight variation in the joint's alignment leads to a failure. This situation can be, for example, an extreme bending angle or an almost pipe pull-out. A joint in this situation is considered "at risk".

2.3.2 Joint failure

A failure is defined as leakage. In the case of joint bending, the limit condition is indicated as an angle. In the case of axial pull-out, the limit condition is indicated as a distance. A joint is considered to have failed only in the following situations: i) the joint is fractured (circular or longitudinal break); ii) the rubber gaskets are leaking; or iii) a part of the pipe wall inserted into the joint is broken.

2.4 Failure modes of joints

Even considering the ubiquity of joints in water networks, their failure modes have never been described for common situations. Many drinking water pipelines, irrespective of the actual pipe material, use the push-fit joint technique, where the system is sealed with rubber gaskets. Push-fit joints (bell-and-spigot and double-socket) are flexible joints that prevent leaks and permit slight axial movement and rotation of the joint (3-4°) that accommodates limited movement of the soil bedding. However, aging of these components tends to impose some movement restrainment. Also, pressure fluctuations, long term exposure to working pressure, and incompletely inserted sockets may weaken the capacities of the joints (Bailey and Kaufmann, 2006; Rajani and Tesfamariam, 2004).

For these reasons, additional insight on the failure modes of joints is necessary. To accomplish this, a preliminary overview of possible failure modes is developed based on a review of scientific literature, reports from the joint research programme of the Dutch water companies and failure registration databases.

In this chapter, seven failure modes of push-fit joints are introduced: angular deviation, joint bending, axial displacement, torsion by slight rotation, vertical displacement, horizontal displacement, and vertical deflection. The phenomena of the failure modes are applicable for any type of PVC push-fit joints, bell-and-spigot or double-socket. It is also assumed that, since the push-fit joints are applied in pipelines of other material types, these failure modes are universal.

2.4.1 Joint bending

Underground structures (pipes and joints) are compelled to move with the surrounding soil. Some of the major causes of bending or beam action in a pipeline are (Moser and Folkman, 2008):

- Uneven bedding support. This can result from unstable foundation materials, uneven settlement due to overexcavation and non-uniform compaction or scouring, for example, due to a leaking joint (Rajani and Tesfamariam, 2004);
- Differential settlement. This effect is especially important in wastewater networks when a pipe is rigidly connected to a manhole and both structures settle at different rates; and
- Ground movement. This can occur due to earthquakes or expansive soils. Frost heave can also play a role.

Soil movement can usually be mitigated with an appropriate selection of the pipe material that is most appropriate in a specific soil, proper preparation and compaction of the foundation and bedding materials of the pipe to be installed. In fact, the soil properties employed in the embedment and the compaction of the backfill are the most important factors; the greatest deflections are expected in subsiding sensitive backfills such as peat and clay (Lange, 2003). If the movement of the soil is uniform, no problems will occur to the pipe since the entire pipe will move as a single structure. However, in the presence of differential soil settling, different sections of the pipe will experience different levels of settlement. When the bending angle exceeds a threshold value, contact points arise between the pipe and the joint or, in extreme situations, between the two pipes inside the joint. Figure 2.3 presents some contact points inside a joint. These contact points lead to increased bending moments as well as longitudinal tensile stresses in the pipe and in the joint which may induce bursting of pipes or joints (Rajani et al., 1996).

A push-fit joints allows a slight bending of the pipes connected to it. The maximum bending angle depends on the material type and on the inner shape of the joint. This inner shape depends on the manufacturer, on its pressure rating, and on its diameter. Special types of PVC joints also allow greater bending angles due to their inner conformation. To the knowledge of the authors, no laboratory tests have been performed to determine the maximum bending angles for PVC push-fit joints. The standard procedure to test PVC joints (ISO 13783, 1997) is not aimed at determining the maximum limit condition of a joint (*e.g.* maximum bending angle) before breakage/leakage but, instead, the minimum tolerable conditions (*e.g.* minimum applied bending force) without leakage.

2.4.2 Vertical displacement

Vertical displacement has numerous origins (Figure 2.4) and can occur in weak or young soils such as peat, sedimental and alluvial soils and in delta areas which are dominant in the Netherlands. For example, in certain areas in the region of Gouda (a Dutch city), the smooth peat soil subsides approximately 1 cm per year.

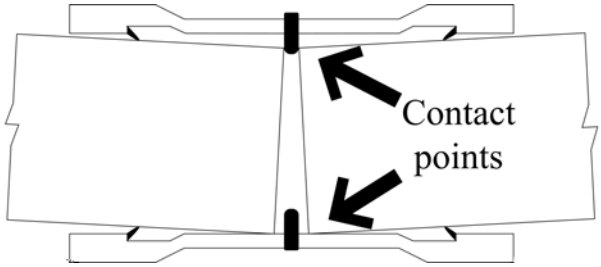

Figure 2.3: Joint bending. Contact points between the pipe and the inner-joint wall are annotated.

Seismic movements of the soil can also induce vertical displacement of a pipe by ground rupture (Tan and Yang, 1988). Interface between two media with different properties can also cause vertical displacement of the pipes.

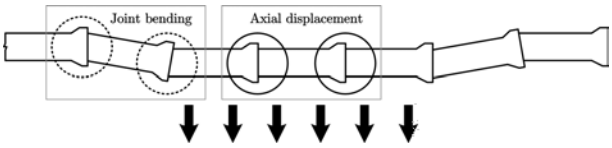

Figure 2.4: Schematic of vertical displacement where two joints subjected to joint bending and two joints subjected to axial displacement are highlighted and annotated.

Vertical displacement of the pipe is bound to induce joint bending at the inflection points and axial displacement (Figure 2.4). Moreover, it is possible that torsion plays a role due to soil movements. Vertical displacement is a composite failure mode since various joint failure modes such as angular deviation, axial displacement and torsion are involved depending upon the magnitude of vertical displacement. Nevertheless, vertical displacement is included in the overview as a separate failure mode since its cause is different. Moreover, the displacement can be easily measured, which makes the cause for this type of failure easy to distinguish.

2.4.3 Horizontal displacement

Transverse movement of pipes occurs mainly due to the influence of a third party. In Groningen (a region of the Netherlands), a significant amount of soil was placed near the distribution network, leading to a prominent horizontal displacement of pipes. The consequences of these displacements are similar to that of vertical displacement since comparable movements occur though on a different plane. Therefore, horizontal displacement is also a composite failure, a combination of angular deviation, axial displacement and torsion. The dominance of a failure mode will be dependent upon the magnitude of horizontal displacement.

2.4.4 Pipe bending

Pipe bending is not a failure mode for joints but may be related to joint bending. Two consecutive bent joints may be connected through a bent pipe. Longitudinal bending of a long tube on a horizontal plane will produce vertical ring deflection due to the induced bending moments (Reissner, 1959). The level of this deformation is mainly governed by the installation procedure and is related to the material employed in the embedment and its compaction. With pressurization, the pipe tends to reacquire its round shape with decrease of the deflection (Lange, 2003).

Typically, tensile hoop strains would be anticipated when a pipe is subjected to water pressure. However, large hoop stresses can arise either as a result of radial internal/external loads, temperature changes and axial stress (Rajani et al., 1996). External loads can be caused by soil or traffic (Rajani and Kleiner, 2001). Freezing of moisture in the soil causes an increase of the ring stress due to the expansion of the soil (Rajani and Kleiner, 2001). Another cause for increased hoop stress is the response of water mains to pressure surge (Rajani et al., 1996).

Due to the increase in hoop stress, longitudinal breaks can occur in the pipes and in joints (Bailey and Kaufmann, 2006; Lange, 2003; Rajani et al., 1996). Due to the differences in stiffness between the pipe and the joint, hoop stress will have more influence on the pipe than on the joint, which may subsequently lead to leakage of the joint.

2.4.5 Axial displacement

Longitudinal tensile stresses in water mains causing axial movements may be induced through temperature changes, ground movements, and tensile forces. For example, water mains will contract (axially, and to a minor extent, circumferentially) in response to a subsequent drop in water and ground temperatures (Rajani and Zhan, 1996). The same authors demonstrated that the axial strain due to the contraction or expansion of pipes is not constant throughout the pipe length. As expected, the portion of the pipe near the joint is freer to move than is the center of the pipe. Axial displacement can also occur due to the Poisson Effect or due to the installation procedure (Figure 2.5).

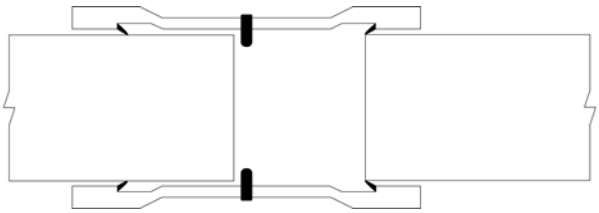

Figure 2.5: Alignment of a joint during axial displacement. The pipe on the right-hand side is almost pulled-out from the rubber-gasket. The images are not to scale.

In fact, with an axial contraction of the pipe, a complete pull-out of the pipe from the inside of the rubber ring can occur. This leads to joint leakage. The pipes

can also move toward each other (*e.g.* pipe expansion due to temperature increase), and this may lead to contact between the pipe and joint and between the two pipes and to joint/pipe breakage. The length of a 10 m PVC barrel can vary 8 mm over a temperature variation of 10 ℃ to 25 ℃, considering a linear expansion coefficient for PVC of 54 $m.m^{-1}.K^{-1}$ (AWWA, 2002).

2.4.6 Torsion by slight rotation/vibration

A sustained rotation of the pipe during a torsional type of failure is due to the formation of a failure zone in the sand at the pipe and soil interface (Singhal, 1984) (Figure 2.6).

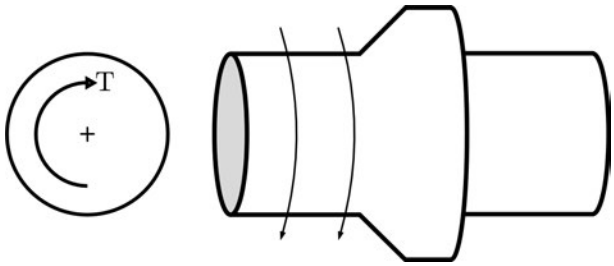

Figure 2.6: Torsion of the joint. Adapted from Singhal (1984).

Torsional tests demonstrate an increase of the torque at thr failure with the increase of the burial depth and the increase of the pipe diameter (Singhal, 1984). No information is known on this type of failure mode of joints under the condition in the Netherlands. It might be expected that, with a rigid connection in the pipeline, torsion leads to a longitudinal or spiral breakage of the pipe and joint. On the other hand, torsion of the pipe in a push-fit joint might cause the slippage and leakage of the joint due to separation of the segments.

2.4.7 Pipe ovalization

The soil load on a flexible pipe causes a decrease in the vertical diameter and an increase in the horizontal diameter of the pipe, an effect that is more significant is larger diameter pipes (Howard, 1977). The level of this deformation is mainly governed by the installation procedure and related to the material employed in the embedment. Pressurization of the pipe results in re-acquiring its round shape with decrease of the deflection (Lange, 2003). Typically, tensile hoop strains would be anticipated when a pipe is subjected to water pressure. However, large hoop stresses can arise either as a result of radial internal/external pressure, temperature change, and axial stress (Rajani et al., 1996). External load is caused by soil or by traffic (Rajani and Kleiner, 2001). Freezing of moisture in the soil causes an increase of the ring stress due to the expansion of the soil (Rajani and Kleiner, 2001). Another cause for increased hoop stress is the response of water mains to surge pressure (Rajani et al., 1996). Due to the increase in hoop stress, longitudinal breaks can occur in the

pipes and in the joint (Bailey and Kaufmann, 2006; Lange, 2003; Misiunas, 2005; Rajani and Kleiner, 2001). Moreover, due to the differences in stiffness between the pipe and the joint, hoop stress will have more influence on the pipe, which may lead to leakage of the joint.

2.5 Conclusions

Seven failure modes of joints are derived from literature and from practice. For the first time, to the author's knowledge, the failure modes of joints are surveyed, leading to a uniform nomenclature of the topic of joint failure.

This overview elucidates the importance of ground movement in the failure of joints. The overview is essential for the water companies as well as for scientific purposes. First, it facilitates and improves the failure registration of the water companies which is currently incomplete and ambiguous. The improved registration will determine the most significant joint failure mode in the Netherlands. From a scientific perspective, the modes are crucial in modeling the failure of joints as a function of a great number of material-related and environmental variables. The models render insight in the failure modes which will result in limits for the joint displacement before failure occurs.

Joints are considered to be particularly affected by bending that can originate, for example, from differential soil movement. Bearing this in mind, an inspection procedure for joints was developed. This procedure is presented and discussed in the next chapter.

chapter 3

Non-destructive evaluation of PVC push-fit joints†

This chapter addresses a very important component of this thesis: the selection of the most accurate and reproducible non-destructive evaluation (NDE) tool for the condition assessment of joints in the field. Following a literature review, three NDE tools were selected: ultrasound, closed-circuit television (CCTV), and Panoramo®.

Tests were projected in order to characterize the tools on accuracy and reproducibility. The work began in the laboratory at KWR. Afterwards, the best two tools were taken to an AC research pipe of Vitens in the north of the Netherlands and tested side-by-side. Finally, the best tool was thoroughly tested in the field in three field inspections of PVC pipes.

The chapter is divided into two main sections. The first section presents the general concepts and the second section discusses all of the characterization performed to the three tested NDE tools.

†This chapter is based on the following articles:

Arsénio, A. M., Vreeburg, J. H. G., van Doornik, J., Dijkstra, L., and van Dijk, H. (2010). Assessment of PVC Joints Using Ultrasound. In *Water Distribution Systems Analysis (WDSA)*, Tucson (Arizona, USA). ASCE

Arsénio, A. M., Vreeburg, J. H. G., de Bont, R., and van Dijk, H. (2011). Real-life inline inspection of PVC push-fit joints using NDE equipment. In *Leading Edge on Strategic Asset Management (LESAM)*, Mülheim an der Ruhr (Germany)

Arsénio, A. M., Vreeburg, J. H. G., de Bont, R., and van Dijk, H. (2012b). Real-life inline inspection of buried PVC push-fit joints. *Water Asset Management International*, 8(2):30–32

Arsénio, A. M., Vreeburg, J., and Rietveld, L. (2013d). Quantitative non-destructive evaluation of push-fit joints. *Urban Water Journal*, pages 1–11

3.1 Introduction

Recently, Liu et al. (2012) argued that "information on the current structural condition of individual water mains [and joints], combined with a good understanding of failure modes and deterioration models, can greatly enhance the ability of water utilities to manage their assets in a cost-effective manner". It could be added that this information should be as accurate as possible, and that, with the currently available technology, this can only be obtained from in-line inspections with NDE equipment. During an NDE inspection and/or afterwards during analysis, operators and analysts should focus on detecting distress indicators on the pipes or joints (Chapter 2).

Paramount work has been published on the topic of employing NDE tools for the inspection of drinking and wastewater pipes. Beuken et al. (2011) have presented business cases regarding the inspection of drinking water pipes. Feeney et al. (2009); Liu et al. (2012); Makar (1999) and Reed et al. (2006) have all published work presenting and discussing state of the art equipment and an overview of their conclusions is depicted in Table 3.1.

According to Rajani and Kleiner (2004), NDE equipment can be exploited on two levels: first, to provide a snapshot of the pipe condition at a given time in order to determine if immediate intervention is required. NDE tools can also be deployed at a later date in subsequent inspections to determine the rate of deterioration.

In 2002, no vendors possessed field-ready methods to examine polymer pipes such as PE and PVC (Dingus et al., 2002). The authors continued by stating that polymer pipe inspection was lagging behind NDE for other piping materials. Also NETTWORK (2002) and Grigg (2006) argued that little, if any, research had been devoted to the development or investigation of the use of NDE tools for the inspection of polymeric pipes or their respective jointing components. More recently, Liu and Kleiner (2012) concluded that in-line visual tools (*e.g.* CCTV and Panoramo®) and ultrasound are those that can be used with the widest range of material types such as metallic, cement pipes and also "might work" with polymeric pipes.

However, little information is available on the capacities of each of these NDE tools in order to quantitatively measure the width of joint gaps and on their true potential for inspection of polymeric pipes.

Visual inspection is usually presented as being inaccurate and prone to interpretation (Dirksen et al., 2013). It is also defined as only able to deliver surface scanning. Nevertheless, surface analysis is expected to be adequate for gap sizing, especially since it can be performed in any pipe material. Inspections using ultrasound are usually presented as being able to detect a wide array of defects during the inspection of water pipes. Even so, little information is available regarding this type of application.

Vangdal et al. (2011) provided an example of a field inspection that was performed using ultrasound. However, the results seem to lack the accuracy necessary to measure a joint's gap, and the tool has not yet been tested in polymeric pipes. Reed et al. (2006) tested ultrasound to perform gap sizing at a laboratory scale using ductile iron pipes.

Therefore, in order to select the best tool for joint-gap sizing in the field, an

accurate and reproducible tool is required. In this chapter, a number of laboratory, field and full-scale tests with visual tools (CCTV and Panoramo®) and ultrasound are presented. The tests were performed at laboratory scale (PVC pipes and joints), in the field (AC pipes and joints), and in three full-scale tests (PVC pipes and joints) inside of pipes used to supply drinking water to customers. In the laboratory tests, both accuracy and reproducibility were evaluated. In the field and full-scale tests, only reproducibility of the tools was tested.

3.2 Inspection procedure

Most of the failure modes presented in Chapter 2 can be detected by analyzing the alignment of the pipes inside of a joint. Other failure mechanisms (*e.g.* slow crack growth) cannot be detected when employing this approach. Inside of a joint, there is a gap (Figure 3.1). For double-socket PVC joints, the gap is the separation between the two pipes connected inside a joint. Different alignments of the pipes will correspond to different shapes of the gap.

Figure 3.1: Left: image of the interior of a 315 mm PVC joint. The gap is signaled with an arrow. Right: underwater image of the interior of the same PVC joint obtained with CCTV. Please note the difference between this joint and the one presented in Figure 2.2: in this situation the ring separating both joints (white) was molded with the joint and is not a stand-alone piece.

The shape of the gap can be obtained through measuring its width at different positions. If the width of a gap is obtained at four different locations, pipe crown, 12 h; invert, 6 h; and both spring-lines, 3 h and 9 h (Figure 3.2), its 3D-orientation can be determined (Figure 3.3). The angle α between positions i and j is calculated using Equation 3.1. Furthermore, the current shape of the gape is indicative for the condition of the joint. The development of the gap over time, observed with repeated inspection, is indicative for the lifetime expectancy of the joint.

$$\alpha_{i-j} = 2 \times sin^{-1}\left(\frac{gap\,width_i - gap\,width_j}{2 \times Do}\right) \tag{3.1}$$

Where Do is the outside pipe diameter [mm]. In employing this expression, it is assumed that both pipe ends were cut perfectly perpendicular to the pipe's axis.

Therefore, for the pipe alignment inside of a joint, several situations are hypothesized:

Various alignments of the pipes will correspond to different shapes of the gap, for example:

1. Ideal alignment: the joint will exhibit the same gap at the four measured points. It is assumed that the pipe is installed with the joints perfectly aligned. This assumption is made due to the lack of information regarding the alignment of pipes following installation;
2. Axial pull-out: the angle for the pair 12h-6h and for the pair 9h-3h is equal to zero. The threshold distance depends on the joint's dimensions;
3. Joint bending: the angle calculated with Equation 3.1 is nonzero. For the 12h-6h pair, a positive angle is calculated when the gap at 12 h is wider than the gap at 6 h. For the 9h-3h, a positive angle is calculated when the gap at 3 h is wider than the gap at 9 h. Joint bending can be decomposed into pure bending and axial pull-out; and
4. Pipe-bending: a pipe can be considered to be bent when both of the joints to which it is connected have angles with the same sign.

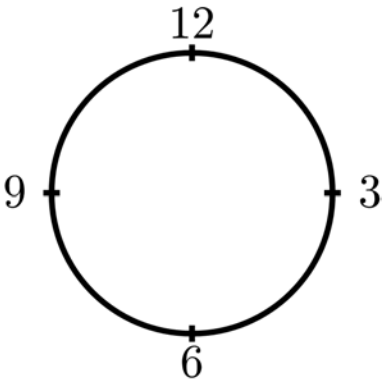

Figure 3.2: Four in-pipe locations. 12 h: pipe crown; 6 h: invert invert; 3 h and 9 h both spring-lines

3.3 NDE equipment

3.3.1 Ultrasound

Operating principle

Ultrasound is based on the measurement of transit times of high frequency sound waves through objects (Rajani and Kleiner, 2004). In this manner, alterations on the surface (*e.g.* a gap after the pipe barrel) or inside the body under inspection (*e.g.*

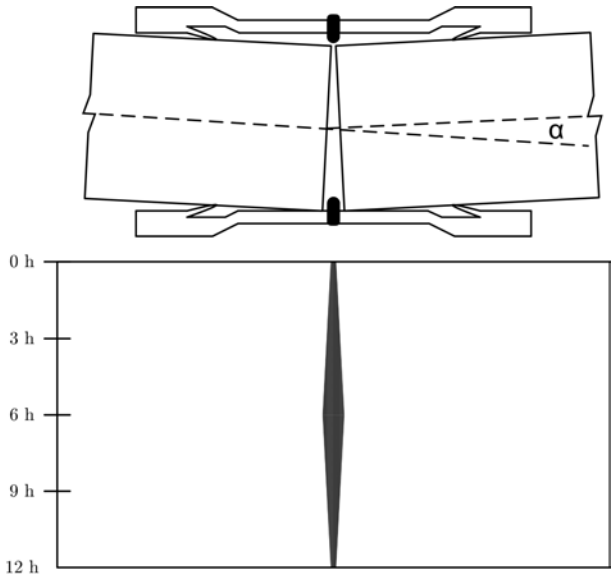

Figure 3.3: Downward bent joint and corresponding unfolded image of its interior (below). This situation is identified by a negative angle α. The schematic would be similar for a bell-and-spigot joint. The unfolded images show the shape of the gap for the complete perimeter of the pipe.

a pipe crack) can be detected due to the changes in the travel path of the sound. An ultrasound system is usually composed of a pulser/receiver and a transducer (typically piezoelectric). The pulser/receiver is an electronic device that generates high voltage electrical pulses. Whereby the transducer generates high frequency ultrasonic energy that propagates in the form of waves. When there is a flaw in the wave path, a portion of the energy will be reflected back from the flawed surface. The reflected wave signal is transformed into an electrical signal by the transducer and is displayed on a screen. Signal travel time can be directly related to the distance that the signal traveled. With this approach, information regarding the location, size and orientation of the flaw can be obtained. Additionally, the ultrasound requires a couplant between the sensor and the test specimen. The couplant is usually a liquid (*e.g.* water) that facilitates the transmission of the sound waves sensor into the test specimen. The principles of the technique are thoroughly discussed by Hellier and English (2001).

By employing ultrasound, the gap width is measured analyzing both the A and the B-scans produced by the ultrasound equipment as presented by Reed et al. (2006). A-scans consist of reflections from the inner and outer walls of the pipe; B-scans are created with A-scans stacked next to each other. In Figure 3.4, part of a B-scan is exhibited. This scan was obtained during laboratory tests (top of the pipe). The ultrasound tool can be imagined at the bottom of the figure with the ultrasound

waves travelling upwards, detecting the pipe (horizontal lines) after a given time of flight (Figure 3.4, Y-axis) and reflecting back to the receiving tool. Knowing the time of flight and the propagation speed of the ultrasound in the element that separates the tool and the pipe (water), the distance between the pipe and the tool can be determined. While the tool travels inside the pipe, a calliper arm determines the in-pipe axial position. Given the information recorded by the calliper arm, the size of this gap can be determined.

Materials that can be assessed

Theoretically, as long as there is good contact at the interface between the sensor and the material to be inspected, the pipes can consist of different materials (Rajani and Kleiner, 2004). Nevertheless, according to the same authors, an ultrasound is most suitable for metallic pipes such as ductile and CI but is not suitable for AC pipes as the acoustic waves are likely to significantly attenuate in a deteriorated (softened material) pipe. The authors suggest that it "may work" with polymeric pipes such as PE and PVC. Misiunas (2005) also argues that this technique is solely applicable to metallic pipes. Nevertheless, it should be considered that the inspection of metallic pipes might be problematic. The internal pipe wall must be very clean so that all of the materials between the sensor and pipe wall have known and well-defined acoustic properties. In corroded metallic pipes, irregular profiles of tuberculation make it difficult to transmit ultrasonic waves which are likely to rapidly scatter and attenuate through the much softer tubercles thus making it difficult to detect and conduct signal processing of the reflected waves (Rajani and Kleiner, 2004).

Detected failures

It has been reported that defects greater than 3 mm can be detected as well as pipe deflections and cracks (Feeney et al., 2009). In steel pipes, this technology is capable to detect metal loss and cracks (Reed et al., 2006). As mentioned previously, the detected failures are dependant on the frequency of inspection. The ultrasonic technique can, theoretically, detect 3D geometry of corrosion pits, voids and cracks (Rajani and Kleiner, 2004).

Possible problems

Makar (1999) argues that the technique is capable of detecting pits, voids and cracks, although certain crack orientations are much more difficult to detect than others. In fact, the ultrasonic wave reflects most easily when it crosses an interface between two materials that are perpendicular to the wave. As an example, cracks that lie perpendicular to the wave are easily detected, but cracks that lie parallel to the beam are usually not identified by an ultrasonic examination. Therefore, if an ultrasonic transducer is located in the center of a pipe, cracks in sewer walls would tend to lie perpendicular to the beam and, therefore, be difficult to detect. One report suggests that cracks as fine as 5 mm can be ascertained, if very fine, slow scans are conducted; however, normal operation will cause such defects to go undetected (Makar, 1999).

The influence of this downside of the technology in the assessment of plastic pipes has yet to be studied.

Another disadvantage of using ultrasonic inspection in water filled (or flushed pipes) is the existence of a significant difference in material properties between water (or air) and the pipe wall. Therefore, almost all of the sound beams that hit the wall are reflected away from it, rather than penetrating and reflecting off of defects inside the pipe wall (Makar, 1999).

In their work, Rajani and Kleiner (2004) argued that the internal pipe wall must be very clean so that all materials between the sensor and pipe wall have known and well-defined acoustic properties. However, this might not be a problem with PVC pipes. Air entrainment, at least during the assessment of sewer pipes, is another potential problem with this technique, since the air tends to block or scatter the ultrasonic signal (Makar, 1999).

Reported uses of the technology

Although this technique has been most frequently used for oil and gas pipelines, it is now being employed to examine the deformation of plastic sewer pipes (Makar, 1999). Demma et al. (2004) mentioned the use of a guided wave technique capable of screening long lengths of pipes for corrosion. The equipment was aimed at detecting corrosion defects by removing 5-10% of the total cross sectional area at a particular axial location. Inspections using ultrasound are normally presented as being able of detecting a wide array of defects during the inspection of water pipes and are usually used mounted on a pig (Dingus et al., 2002). Even so, little information is available on this type of application. Vangdal et al. (2011) provided an example of a field inspection performed using an ultrasound. However, their results appear to lack the accuracy that is necessary to size a joint's gap, and the tool has not yet been tested in polymeric pipes. Also Reed et al. (2006) tested ultrasound to perform gap sizing at laboratory scale using ductile iron pipes.

3.3.2 CCTV

A CCTV consists of a television camera and a method of illuminating the interior of the pipe mounted on a remotely operated vehicle (ROV) (Costello et al., 2007). An operator controls the ROV and, on a computer screen, can see the inside of the pipe in real-time. A CCTV for pipe inspection is usually equipped with software that measures the distance between any two points on the screen. In the present case, the gap widths can be calculated. This is the most common inspection technology in wastewater networks (Figure 3.5).

3.3.3 Panoramo®

Panoramo® is also a visual tool and uses two high-resolution digital photo cameras with 186° wide-angle lenses fit into the front and rear section of the housing as exhibited in Figure 3.6. The system is also mounted on a ROV. The images taken by the two cameras at 5 cm intervals result in an unwrapped 360° image of the pipes' interior. From these, two different views are generated for analysis in the office - an

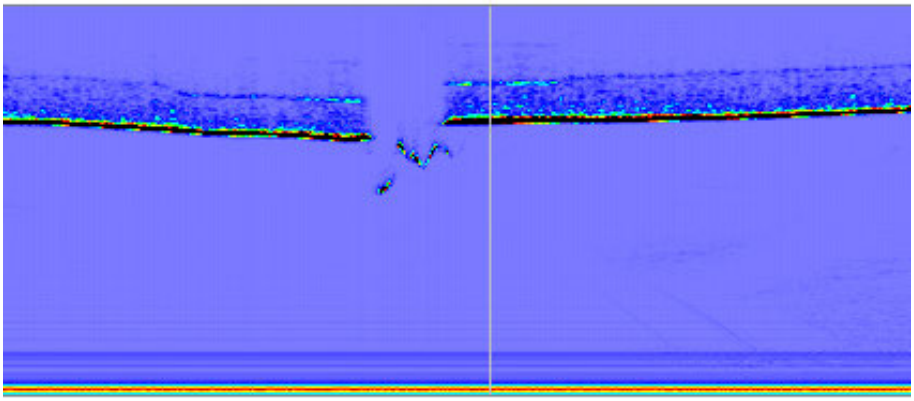

Figure 3.4: B-scan data. The x-axis represents an in-pipe axial position. The y-axis represents sound travel time (or travel distance). In the middle of the image, a discontinuity in the horizontal lines between the two vertical black lines is seen - the gap. Courtesy of Applus RTD.

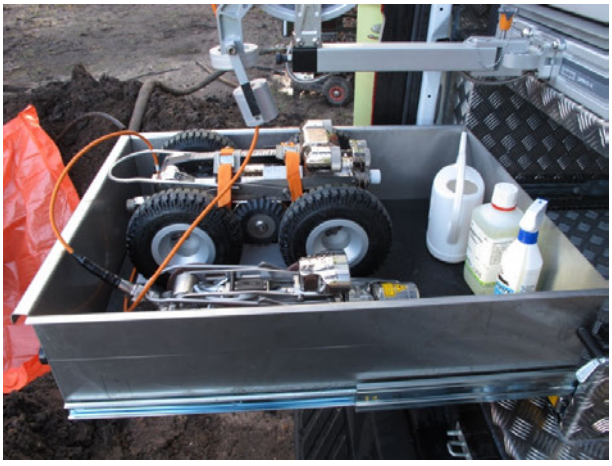

Figure 3.5: Photography of a CCTV camera used during the tests. Courtesy of MJ Oomen.

unfolded two-dimensional view of the entire section and a three-dimensional view of the pipe which permits the viewer to pan the angle of view in all directions (IBAK, 2012). Using the 2D unfolded image, the distances between two points can be calculated at the office. Therefore, unlike CCTV, the analysis is conducted *a posteriori* and not in real time.

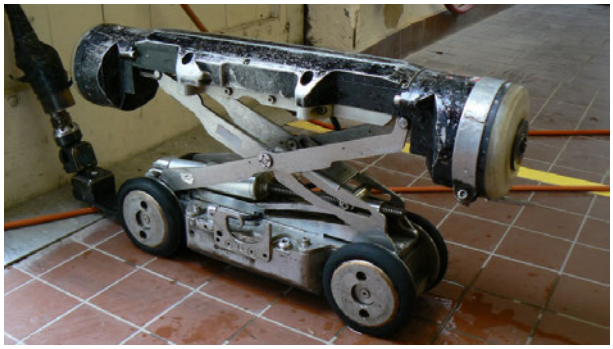

Figure 3.6: Photograph of a Panoramo® tool. Courtesy of MJ Oomen.

3.3.4 Laser scanner

Principle

According to Feeney et al. (2009), laser profiling generates a profile of the interior surface of the pipe wall. The laser is utilized to create a line of light around the pipe wall, highlighting its shape. This technique allows detection of changes to the pipe's profile which may be caused by deformation, corrosion, or siltation. This equipment is often used to complement other inspection methods, most commonly CCTV and/or sonar (Feeney et al., 2009).

Materials that can be assessed

According to Feeney et al. (2009), any pipe material can be inspected using laser equipment.

Detected failures

According to Makar (1999), laser scanning systems are capable of finer resolution than ultrasonic systems and are better at the detection of cracking. Moreover, the information from the laser scans is automatically recorded and analyzed by a computer, substantially reducing operator errors. While the initial equipment may be more expensive than the CCTV system discussed later, the reduced operator time that is necessary to use the technique may also signify that its operation will be more economical. It has also been claimed that laser is more effective since finer defects can be detected and less subjective than CCTV.

Possible problems

Laser inspection can only be employed above water to inspect the sections of a pipe wall that are, as well, above the water line. Therefore, to assess the entire internal surface of a pipeline requires the pipe to be taken out of service (Feeney et al., 2009). In addition to this, laser equipment is not yet commercially available as ultrasound equipment or CCTV (Makar, 1999).

Reported uses of the technology

Both Makar (1999) and Feeney et al. (2009) extensively discuss the technical characteristics of commercially available laser equipment.

3.3.5 Ground-penetrating radar

Principle

Ground-penetrating radar (GPR), also known as georadar, operates by transmitting pulses of ultra-high frequency radio waves (microwave electromagnetic energy) into the ground through a transducer or antenna. The waves travel through the ground until they reach a material which has a different conductivity and dielectric constant than the earth. The signal is then reflected and recorded by a separate receiving antenna. The amount of time it takes for the electromagnetic radio waves to be reflected by surface materials can be analyzed to determine the position and depth of features below the earth's surface (Feeney et al., 2009). Moreover, the GPR can also be operated from the inside of a dry pipe. For in-pipe use, significant physical characteristics between the air, the pipe wall, and the soil lead to the attainment of valuable results.

Materials that can be assessed

Any pipe material can be assessed using GPR (Feeney et al., 2009). Moreover, (Misiunas, 2005) considers GPR a proven NDE for inspection and location of buried objects.

Detected failures

According to Makar (1999) and Feeney et al. (2009), GPR has the ability to evaluate the properties of the soil (*e.g.* detect subsurface voids). Moreover, with this technique, voids, rocks and regions of water saturation produced by exfiltration should all be readily detectable by the technique. If used in-pipe, GPR can also provide information regarding the physical characteristics of the pipe wall. Maierhofer (2003) argued that GPR is capable of locating tendon ducts (depths<50 cm), voids and detachments, and measuring thickness of structures that are only accessible from one side. According to Slaats et al. (2004) and Mesman and Wielen (2005), GPR is a suitable, non-destructive method for determining the degree of internal leaching from AC pipes. Similarly, Smolders et al. (2009) demonstrated that GPR is a beneficial tool for assessing the condition of AC force mains: the authors estimated a maximum and average deterioration speed of the wall thickness of the pipe.

Possible problems

One of the disadvantages of the technique is the difficulty of measurement interpretation. Additionally, GPR inspection does not provide extensive information regarding the condition of the pipe (Misiunas, 2005). Moreover, in a test performed by Makar (1999), many problems with the surface use of GPR were reported. First, a very high

level of both false positive and false negative results was obtained. In addition, GPR results appear to be significantly dependent on local soil conditions, thus making it necessary to adapt the inspection approach for each location. In addition to this, the use of GPR was not in any way recommended for locations with clay soils. Finally, Makar (1999) concluded that surface use of GPR with the current technology would not be able to detect actual problems in sewer pipes. What is more, the detection of water saturated soil regions in permanently water saturated soils, for example, in the Netherlands, might be impossible.

Reported uses of the technology

In their extensive review, Feeney et al. (2009) indicated that there are a number of commercially available GPR systems. Some are designed for locating underground utilities. Others have been employed to date in North America for internal pipe inspection, which actually could be considered more in the prototype stage than in commercial use. Research into exploiting GPR for sewer and bedding condition inspections is ongoing (Feeney et al., 2009).

3.3.6 Multi-sensor systems

Principle

Many multi-sensor systems (MSS) have been presented for wastewater networks. According to Costello et al. (2007), the different condition assessment technologies described above have specific characteristics, strengths, and weaknesses that make them suitable for the detection of particular defects. Nevertheless, such defects reflect only a limited subset of anomalies. A possible approach for wastewater networks is the combination of CCTV and sonar mounted one above the other on the same tractor. While CCTV captures the information above the waterline, the information below the waterline is captured by sonar. Therefore, some of the disadvantages of both systems are surmounted. At the completion of the inspection, the images from both systems can be subsequentely superimposed to form a full profile of the pipeline.

Materials that can be assessed

At least in theory, any pipe material can be assessed using this inspection equipment.

Detected failures

The equipment provides more reliable data and is capable of producing a continuous profile of the pipe walls. An increased benefit/cost ratio was also anticipated by some authors (Makar, 1999).

Possible problems

Some of the projects have been abandoned. Despite the aforementioned high benefit/cost ratio, the initial investment cost is high when compared to the cost of the

individual tools.

Reported uses of the technology

Two developments are worth mentioning: KARO, a German robot (Eiswirth et al., 2001), and PIRAT (Pipe Inspection Real-time Assessment Technique), a robot developed by the Commonwealth Scientific and Industrial Research Organisation (CSIRO) of Australia (Kirkham et al., 2000). KARO comprises a broad range of inspection and navigation sensors, specifically, a microwave sensor and a 3D optical sensor. These complemented the standard video camera and ultrasound transducers. The PIRAT robot included a camera and a laser scanner. The laser could be replaced by sonar while inspecting flooded pipes. However, according to personal communications from the developers, PIRAT and KARO are no longer in use.

Table 3.1: Summary of advantages and disadvantages of ultrasound, CCTV and Panoramo®. Adapted from: Feeney et al. (2009); Liu et al. (2012); Makar (1999) and Reed et al. (2006)

Tool	Advantages	Disadvantages
Ultrasound	Inspect all pipe materials Some models do not rely on the existence of an umbilical chord Together with surface inspection, can perform physical evaluation of the pipe's wall (*e.g.* embrittlement in PVC) Inspection is done in one run	Data analysis can only be done after the retrieval of the equipment Can only be used in fully filled water pipes
CCTV	Inspect all pipe materials Data analysis can be done *in-situ* Can be employed in empty, partially or completely filled pipes	Can only perform surface inspection The inspection has to be stopped in order to focus on attention points
Panoramo®	Inspect all pipe materials Produces an unfolded 360° image of the pipe's interior Data analysis can be done *in-situ* Inspection is done in one run	Can only perform surface inspection Preferably used in empty pipes. Cannot be used in partially filled water pipes
Laser scanner	Inspect all pipe materials Very accurate geometry and defect measurement Can be used to create a 3D model of the pipe Accurate comparison between various evaluations Multiple evaluations would allow to determine rate of damage	Can only perform surface inspection Only usable above the water line
GPR	Inspect all pipe materials **Surface use:** Does not require entering the pipe Theoretically capable of detecting voids near the pipe **In-pipe use :** Detection of voids, rocks and other objects in bedding Detection of exfiltration	**Surface use:** Highly dependent on soil conditions No evidence of a consistent ability to detect voids Tests have produced false positive results **In-pipe use:** More field tests required to prove technique
MSS	Inspect all pipe materials Production of more reliable data than CCTV alone	Projects have been abandoned Highly dependent on soil conditions

3.3.7 Characterization of the NDE equipment

The three NDE tools were tested in three different occasions: laboratory, field, and full-scale tests. Each of these tests had a specific objective:

1. Laboratory tests: characterize the accuracy and reproducibility of the ultrasound, CCTV, and Panoramo® and select the two most promising tools for gap sizing to be employed in the field tests;
2. Field tests: characterize the reproducibility of the two selected tools in the laboratory tests and select the most promising tool for gap sizing to be used in the full-scale tests. The inspected pipe was selected so that an ultrasound could be used; and
3. Full-scale tests: perform several inspections in various PVC pipes used to supply drinking water and further characterize the reproducibility of the NDE tool selected in Point 2. Although following a similar approach as the field tests, which were a one-day experiment with the same operator, the full scale tests attempted to characterize the reproducibility of the CCTV through the inspection of different pipes, in different days, and with different operators.

   During the field tests and the full scale tests, the accuracy of the measurements was not calculated because it was not possible to non-destructively confirm the gap sizes, *i.e.*, without exhuming the pipes.

3.4 Materials & methods

3.4.1 Laboratory tests

Equipment

The ultrasound equipment is composed of 8 ultrasound probes connected to a waterproof core where batteries are kept and data are stored. The probes are aligned on a star-shaped head. Each probe is separated from each other by 45° (Figure 3.7). To record the exact position of the ultrasound a calliper arm is attached to the end of the tool (Figure 3.7, left). Certain technical characteristics of the equipment are depicted in (Table 3.2). The equipment travels inside the pipe attached to a foam pig (Figure 3.8) using water pressure (in the Netherlands, typically 3 bar). This is similar to the cleaning pigs typically employed in drinking water network flushing (Vreeburg, 2007).

The CCTV used was an Argus 4 manufactured by the German company IBAK. A typical pan and rotate CCTV camera is mounted on a ROV. The system has integrated halogen lighting (2×35 W) which pans and rotates in accordance with the direction of view. It can be operated in 200 mm pipes and higher IBAK (2012).

Panoramo® was also manufactured by IBAK. The system is mounted on a ROV, and it operates in pipes that are 200 mm and larger. It has a maximum scanning speed of 35 $cm.s^{-1}$ IBAK (2012).

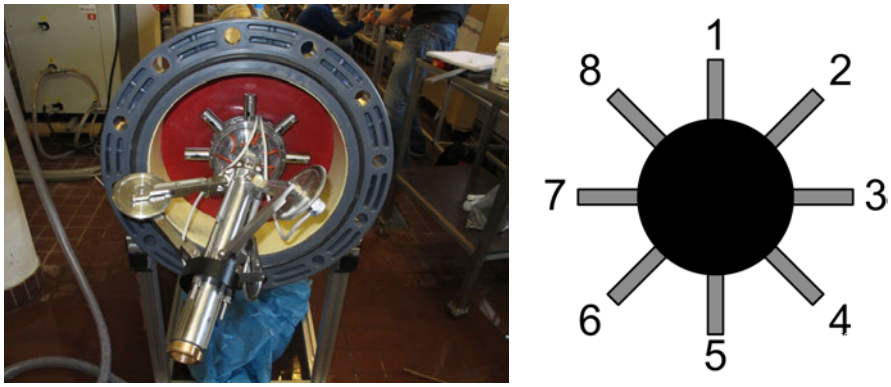

Figure 3.7: Ultrasound equipment being introduced inside the pipe during a laboratory test (left). The red foam pig is visible inside the pipe. The calliper is outside the pipe fixed to the ultrasound tool. Schematic of the 8 ultrasound probes each numbered consecutively from one to eight (right).

Figure 3.8: Photograph of the ultrasound tool used in the tests attached to a foam pig. Courtesy of Applus RTD.

Table 3.2: Operational characteristics of the ultrasound equipment used in the laboratory tests. This information was supplied by Applus RTD.

Minimum internal diameter	300 mm
Optimal operation speed	20 $cm.s^{-1}$
Resolution	0.5 mm
Frequency	2.25 MHz

Table 3.3: Overview of the equipment and set-up of the laboratory tests. The inspected pipe was PVC DN315 equipped with double-socket push-fit joints.

NDE	Positions	Repetitions [#]	Nr tests [#]
US	0 cm, 3 cm, 6 cm and 10 cm 4 positions	2	8
CCTV	0 cm to 10 cm; 1 cm steps	3	33
Panoramo®	11 positions	2	22

Operation & set-up

With CCTV and Panoramo®, gap sizing was accomplished at 12 h and 6 h. With Ultrasound performed gap sizing is performed with eight different ultrasound probes (Figure 3.7, right). Probe one is facing the 12 h position; probe five is facing the 6 h position. The tests with the ultrasound and with CCTV were duplicated; the tests with Panoramo® were triplicated. The total number of laboratory tests conducted with each of the NDE tools is illustrated in Table 3.3.

A metallic loading frame was constructed for this project to test all NDE equipment. A schematic of the loading frame is provided in Figure 3.9, and photos are demonstrated in Figure 3.10. The metallic frame supports two 2-meter DN315 PVC pipes coupled with a double-socket PVC push-fit joint. On the left hand side, the pipe could be accessed through a flange. On the right hand side, a 45° elbow allowed the pipe to remain filled with water while open to the exterior. This elbow was also the way of retrieving the foam pig used during the ultrasound inspection and to grant access to the pipe's interior when using the CCTV and Panoramo®. The height of the pipe support can be varied from 10 cm (0° angle) to 0 cm (5° downward angle) in 1 cm increments (11 positions). This arrangement allows variation in the gap width between the two barrels. Fixed points were marked on the pipe's outer wall at a fixed location, 0.5 m away from the beginning of the joint (dotted lines in Figure 3.9). The exact length of pipe inside the joint at the top and at the bottom was also known. Thus, both the lengths of pipe from the fixed points until the beginning of the joint and the length of pipe inside the joint were known. During downward bending while the gap at the top increases, the gap at the bottom becomes smaller; during upward bending, the opposite occurs. Using these fixed points, the gap width at the top and at the bottom was calculated for each pipe support height.

3.4.2 Field tests

Equipment

The ultrasound and CCTV equipment used on this inspection were the same as in the laboratory tests.

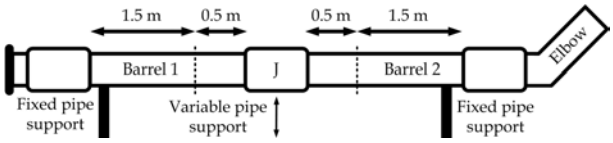

Figure 3.9: Schematic of the loading frame. Two 2 m-barrels (1 and 2) are connected with a double-socket push-fit joint (J). The dotted lines represent the fixed points on the pipes' walls used to calculate the joint's width. These were located 0.5 m away from the joint. The variable pipe support (below the joint) allowed the pipes to be bent on the joint from a horizontal position to 5° (downward) in 11 increments. On the left-hand side, the loading frame was equipped with a flanged door while, on the right-hand side, a 45° elbow was installed. Image not to scale.

Figure 3.10: Photos of the loading frame. Top left: overview of the frame. Top right: variable pipe support. Bottom left: 45° elbow. Bottom right: flanged door.

Operation & set-up

The CCTV and ultrasound inspections were performed in one run and were not duplicated. For the CCTV, control measurements were made in the office using frames obtained from the inspection. The control measurements were obtained by a different operator. With the ultrasound, the complete pipe length was inspected (620 m). With the CCTV, only 420 m of the pipe's entire length was inspected. This limitation was caused by the drag created by the umbilical chord connecting

the CCTV to the inspection van.

An overview of the characteristics of the inspected pipe and of the NDE tools employed in the field tests is presented in Table 3.4.

A DN300 620 m long AC pipe was used. The first 20 m of pipe were PVC. This pipe was selected for the following reasons. First, it possessed all of the adaptations necessary to perform an ultrasound inspection using a foam pig - an entry and an exit point. The entry point was a flange connected to the network through a hose (Figure 3.11, left). The exit was a sliding door above ground level (Figure 3.11, right). Second, the barrels of this AC pipe were also connected with push-fit double-socket joints. Finally, an inspection of another pipe material proves that this assessment procedure can be applied to any pipe material connected with push-fit joints.

Figure 3.11: Entry point with flange and hose (left). Exit point with sliding door above ground level (right).

3.4.3 Full scale

Equipment

The Panoramo® and CCTV equipment employed for this inspection were the same as in the laboratory tests and in the field test.

Operation & setup

All inspections were duplicated (run 1 and run 2). The runs were re-analyzed in the office by a different operator (control 1 and control 2). An overview of the characteristics of the inspected pipes and of the CCTV used in the full-scale tests is depicted in Table 3.4.

Three inspections were performed in PVC pipes used in the Dutch drinking water supply network.

Table 3.4: Overview of the equipment and set-up of the field test and of the full-scale tests. Field test: the inspected pipe was AC DN300 equipped with double-socket push-fit joints. Full scale tests: all inspected pipes were PVC DN315 equipped with double-socket push-fit joints. Only CCTV was used.

	Tool or test	Access	Length [m]	Repetitions [#]	Joints [#]	Age [years]
Field	Ultrasound	Flange	600	Run	132	47
	CCTV		420	Run + Control	90	47
Full scale	1st	Cut	350	2 runs + 2 controls	48	37
	2nd	Flange	70	2 runs + 2 controls	10	37
	3rd		250	2 runs + 2 controls	14	42

3.5 Statistical analysis

3.5.1 Accuracy

At maximum accuracy, the measured gaps using an NDE and the calculated gaps using a ruler should have the same value. In a plot with measured gaps, against calculated gaps the values should align along an x=y line. In a genuine situation, deviations will occur between measured and calculated gaps. In the laboratory, these deviations will be quantified using the root mean squared error (RMSE). The RMSE (Equation 3.2) provides information about the tool's accuracy - the tool with the lowest RMSE (minimum = 0) measures the gap width most accurately.

$$RMSE = \sqrt{\frac{1}{m} \times \sum_{i=1}^{m} (calculated - measured)^2} \tag{3.2}$$

Where *calculated* is the calculated gap width using a ruler [mm], *measured* is the measured gap width using the NDE [mm], m is the number of laboratory tests [#], and i refers to the i^{th} test. RMSE will have the same units as the measurements.

3.5.2 Reproducibility

Consecutive runs performed with an NDE were compared employing the Wilcoxon Rank Sum Test which is a non-parametric statistical test. The parametric equivalent

is the Student's t-test. Corder and Foreman (2009) have thoroughly discussed non-parametric statistics and the Wilcoxon Rank Sum Test. The Student's t-test and other traditional tests follow certain assumptions called parameters - parametric tests. One of the assumptions in traditional statistics is that samples approximately resemble a normal distribution. If a sample breaks one of these rules, all of the assumptions of a parametric test are violated, and parametric tests cannot be used. To avoid violating the normality assumption, the non-parametric Wilcoxon Test was selected.

The null hypothesis in the Wilcoxon Rank Sum Test is that two data sets which are independent samples from identical and continuous distributions with equal medians are compared against the alternative that they do not have equal medians. The returned p-value rejects or fails to reject the null hypothesis. A high p-value (over the significance level of 5 % for the current work) demonstrates that the probability that the alternative hypothesis was obtained by chance is very high; impossibility of rejecting the null hypothesis, H value equal to 0. A low p-value (< 0.05) demonstrates that the probability that the alternative hypothesis was obtained by chance is very low. Therefore, the null hypothesis is rejected; the H value is equal to 1. Also in the current work, the null hypothesis was that two consecutive measurements are statistically similar (reproducible), against the alternative hypothesis that they are not. In this work, the p-values are not expressed as a percentage.

3.6 Results

3.6.1 Laboratory tests

In order to compare the ultrasound and the visual tools, only the measurements made with the ultrasound at the top (probe 1, Figure 3.7, right) and the bottom (probe 5) are presented.

The gaps measured at the top and at the bottom with each one of the three tools are plotted together with the calculated gaps employing the marks on the pipe exterior. The results for the ultrasound, CCTV and Panoramo® are respectively presented in Figure 3.12, Figure 3.13, and Figure 3.14. In these figures, certain calculated gap values are negative because, at a maximum bending angle, the pipes overlap inside the joint. The error-bars are representations of the standard deviation of the measurements. The results of the RMSE and of Wilcoxon Rank Sum Tests are depicted in Table 3.5.

Ultrasound

In Figure 3.12, a valuable agreement between measured and calculated gaps can be seen. RMSEs of 2.2 mm and 2.4 mm were obtained respectively for the set of measurements made at 6 h and at 12 h. No statistical difference (Wilcoxon Rank Sum Test) was ascertained between the gaps measured during each of the two runs. The results were reproducible. Additionally, the ultrasound could perform a complete inspection in one run without interruptions.

CCTV

In Figure 3.13 a very good agreement between measured and calculated gaps can be seen. RMSEs of 2 mm were obtained both for 6 h and 12 h. This demonstrates that the CCTV was more accurate than the ultrasound. No statistical difference at 95% confidence level (Wilcoxon Rank Sum Test) was ascertained between the gaps measured with CCTV in the different runs. The results were reproducible.

Panoramo®

In Figure 3.14, a deviation between measured and calculated gaps is shown. This is confirmed by the RMSEs: 5.6 mm and 2.5 mm respectively for 6 h and 12 h. these are the largest RMSE obtained during the tests. This shows that Panoramo® struggled to deliver accurate results. No statistical difference at 95% confidence level (Wilcoxon Rank Sum Test) was found between the gaps measured with Panoramo® in the different runs. The results were reproducible.

From Figures 3.12, 3.13, and 3.14, it is also evident that all three tools fail to size negative gaps (overlapping pipes), which was expected given their characteristics. Nevertheless, this is the reason why all three tools seem more accurate for wider gaps.

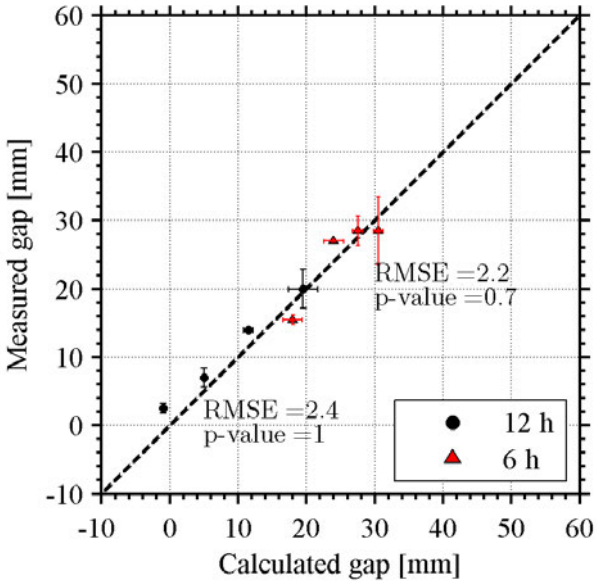

Figure 3.12: Results of the NDE inspection with the Ultrasound. The measured gap with the ultrasound is plotted against the gap calculated using the marks on the pipe's outer wall. For the 12 h data points, the support height increases from left (0 cm support) to right (10 cm support). For the 6 h data points, the support height increases from right (0 cm support) to left (10 cm support).

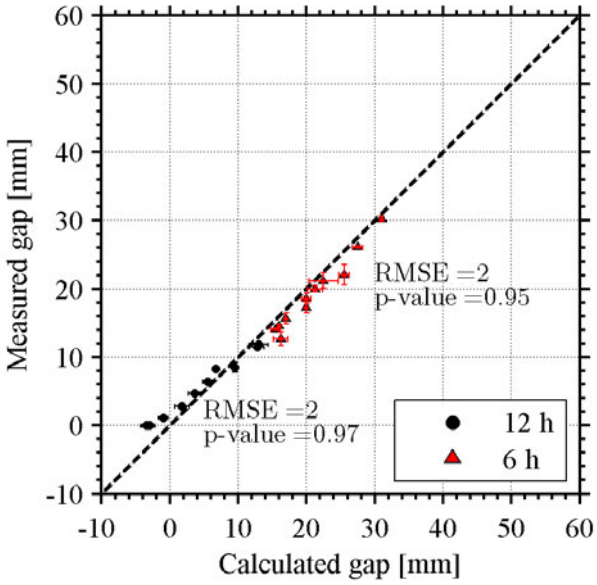

Figure 3.13: Results of the NDE inspection with the CCTV. The measured gap with CCTV is plotted against the gap that is calculated using the marks on the pipe's outer wall. For the 12 h data points, the support height increases from left (0 cm support) to right (10 cm support). For the 6 h data points, the support height increases from right (0 cm support) to left (10 cm support).

3.6.2 Field tests

The gaps measured by the eight ultrasound probes are provided in Figure 3.15 (left). The gaps measured by the CCTV at 3 h, 6 h, 9 h and 12 h are depicted in Figure 3.15 (right). In Figure 3.15 (right), the error bars represent the standard deviation of the measurements. The results of the Wilcoxon Rank Sum Tests are presented in Table 3.6.

Ultrasound

For the AC sections of the pipe, several gaps appear to be wider than 20 mm with many reaching 30 mm to 40 mm.

The ultrasound tested in this experiment freely flowed inside the pipe during inspection while it rotated axially. Without a gyroscope, it was not possible to know where each probe was focusing during the inspection. However, it is important to note that this problem is intrinsic to this individual ultrasound and not to all ultrasound equipment.

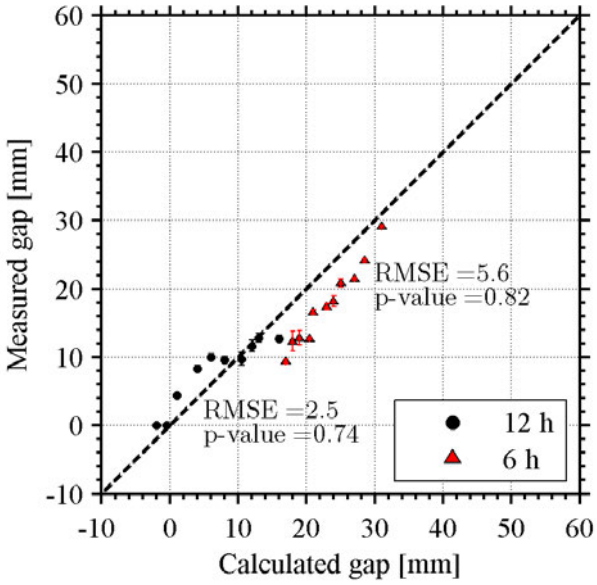

Figure 3.14: Results of the NDE inspection with the Panoramo®. The measured gap with Panoramo® is plotted against the gap calculated using the marks on the pipe's outer wall. For the 12 h data points, the support height increases from left (0 cm support) to right (10 cm support). For the 6 h data points, the support height increases from right (0 cm support) to left (10 cm support).

CCTV

For the first 20 m of pipe (PVC), wider gaps were measured - over 20 mm and reaching 30 mm. For the AC sections, only two gaps were wider than 10 mm. This was explained by the fact that PVC joints allow higher bending angles than AC pipes.

The Wilcoxon Rank Sum Test demonstrated that the hypothesis whereby the sets were different could not be rejected at the 95% confidence level - the CCTV runs and the controls were statistically similar (Table 3.6).

3.6.3 Full-scale tests

The results of inspections one, two, and three are illustrated in Figure 3.16, Figure 3.17, and Figure 3.18, respectively. In these figures, the error bars represent the standard deviation of the measurements. The results of the Wilcoxon Rank Sum Tests are provided in Table 3.7.

Using the Wilcoxon Rank Sum Test, all runs and controls were adjacently compared and, at a 95% significance, all are statistically similar. The exceptions are for inspection 2 at 6 h run 1 and control 1; run 1 and control 2; run 2 and control 1 are statistically different at a 95% significance level (Table 3.7, in bold). This can

Table 3.5: Results of the statistical analysis of the laboratory results. The p-values and the H values were obtained with the Wilcoxon Rank Sum test, at a 95% confidence level. With H=0, the null hypothesis cannot be rejected - the runs are statistically similar. With H=1, the null hypothesis is rejected.

Tool	Location	RMSE	P-value	H
CCTV	12 h	2	run 1/run 2 = 0.97	0
	6 h	2	run 1/run 2 = 0.95	
Ultrasound	12 h	2.4	run 1/run 2 = 1.0	0
	6 h	2.2	run 1/run 2 = 0.70	
Panoramo®	12 h	2.5	run 1/run 2 = 0.74 (min)	0
			run 1/run 3 = 0.89	
			run 2/run 3 = 0.89	
	6 h	5.6	run 1/run 2 = 0.97	
			run 1/run 3 = 0.82 (min)	
			run 2/run 3 = 0.94	

Table 3.6: P-values obtained with the Wilcoxon Rank Sum Test for the CCTV results obtained from the pilot-scale test at 95% confidence level. With H=0 the null hypothesis cannot be rejected - the runs are statistically similar. With H=1 the null hypothesis is rejected.

In-pipe position	P-value	H
12 h	0.66	0
3 h	0.54	0
6 h	0.82	0
9 h	0.13	0

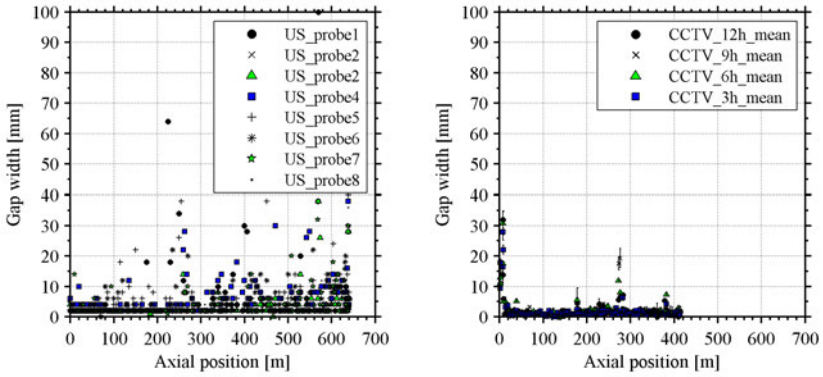

Figure 3.15: Results of the NDE inspection with the ultrasound (left) and CCTV (right). The gap measured with both the ultrasound and the CCTV is plotted against the in-pipe axial position.

be explained with the debris (mostly sand and iron) discovered at the bottom of the pipe (6 h) during this inspection. For some joints, the beginning and the end of the gap was not visible, and the operator, in order to size the gap, had to estimate these boundaries.

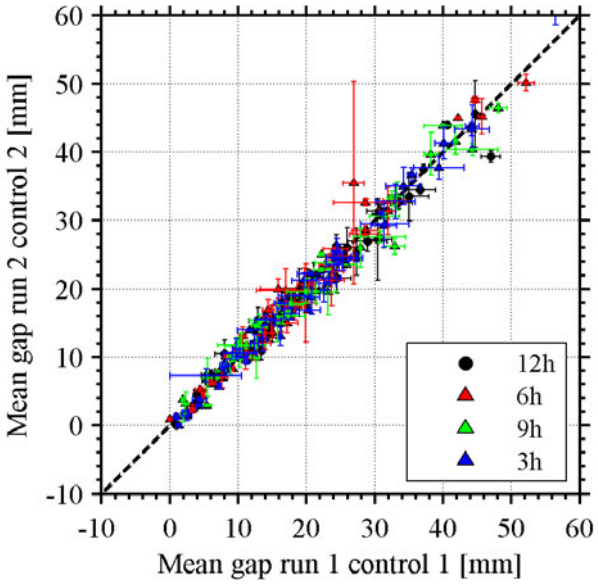

Figure 3.16: CCTV results of inspection one. The mean gap calculated for run 2 and control 2 is plotted against the mean gap calculated for run 1 and control 1. The line x=y is also presented.

Table 3.7: P-values obtained with the Wilcoxon Rank Sum Test for the CCTV results obtained from inspections 1, 2, and 3 were at a 95% confidence level. With H=0, the null hypothesis cannot be rejected - the runs are statistically similar. With H=1, the null hypothesis is rejected. The results differing statistically at a 95% significance level are highlighted in bold.

		Insp. 1		Insp. 2		Insp. 3	
In-pipe location	Compared runs	p-value	H	p-value	H	p-value	H
12 h	run 1/run 2	0.87	0	0.91	0	0.66	0
	run 1/control 1	0.94	0	0.32	0	0.7	0
	run 1/control 2	0.91	0	0.52	0	0.53	0
	run 2/control 1	0.78	0	0.38	0	0.98	0
	run 2/control 2	0.78	0	0.34	0	0.85	0
	run 2/control 2	0.99	0	1	0	0.89	0
3 h	run 1/run 2	0.97	0	0.54	0	0.95	0
	run 1/control 1	0.77	0	0.91	0	0.98	0
	run 1/control 2	0.67	0	0.97	0	0.98	0
	run 2/control 1	0.88	0	0.57	0	0.96	0
	run 2/control 2	0.76	0	0.57	0	0.93	0
	run 2/control 2	0.91	0	0.97	0	1	0
6 h	run 1/run 2	0.99	0	1	0	0.55	0
	run 1/control 1	0.69	0	**0.03**	**1**	0.38	0
	run 1/control 2	0.7	0	**0.05**	**1**	0.43	0
	run 2/control 1	0.76	0	**0.04**	**1**	0.84	0
	run 2/control 2	0.7	0	0.06	0	0.77	0
	run 2/control 2	0.97	0	0.94	0	0.94	0
9 h	run 1/run 2	0.95	0	0.97	0	0.98	0
	run 1/control 1	0.78	0	0.26	0	0.8	0
	run 1/control 2	0.94	0	0.27	0	0.76	0
	run 2/control 1	0.73	0	0.18	0	0.71	0
	run 2/control 2	0.91	0	0.18	0	0.7	0
	run 2/control 2	0.81	0	0.85	0	0.96	0

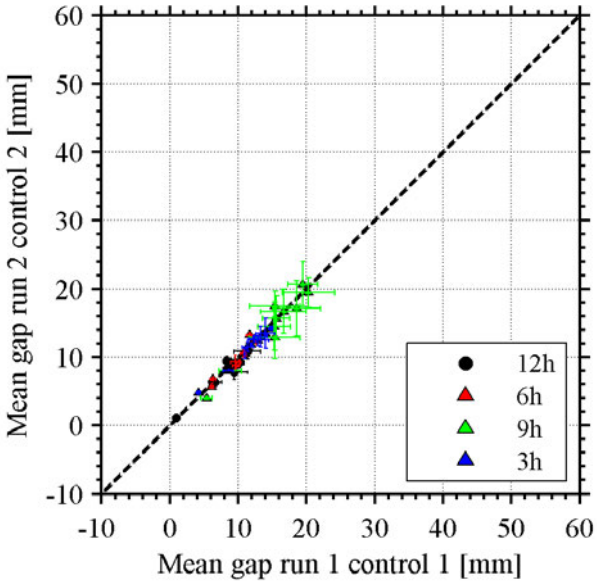

Figure 3.17: The CCTV results of inspection two. The mean gap calculated for run 2 and control 2 is plotted against the mean gap calculated for run 1 and control 1. The line x=y is also presented.

3.7 Discussion

3.7.1 Laboratory tests

The laboratory results clearly demonstrated that both the ultrasound and the CCTV could deliver accurate and reproducible results and performed a quantitative pipe assessment. On the one hand, the ultrasound has a significant advantage when compared to the CCTV; the possibility of performing a complete inspection in one run and in a real-life inspection can be an advantage. In fact, during an inspection, the points of interest had to be focused by the CCTV. On the other hand, in order to operate the ultrasound, it requires a completely water filled pipe. During the laboratory tests, two data points were lost due to the presence of air at the top of the pipe which was only detected after the inspection was completed when the data were analyzed.

Panoramo® also delivered reproducible results. When compared to the CCTV, an advantage of Panoramo® is the ability to inspect a pipe in a single run without the need to focus on points of interest. Another advantage is the production of an unwrapped image of the pipe's interior. Two unexpected deficiencies of Panoramo® were identified in these tests. With this tool, it was impossible to accurately inspect above the water level when the pipe was partially filled due to refraction. In fact, in this situation, the Panoramo® took the image of the top wall (above the water line) from under the water. Furthermore, light reflection on suspended matter complicated being able to obtain a clear image of the pipe's interior. It can be concluded

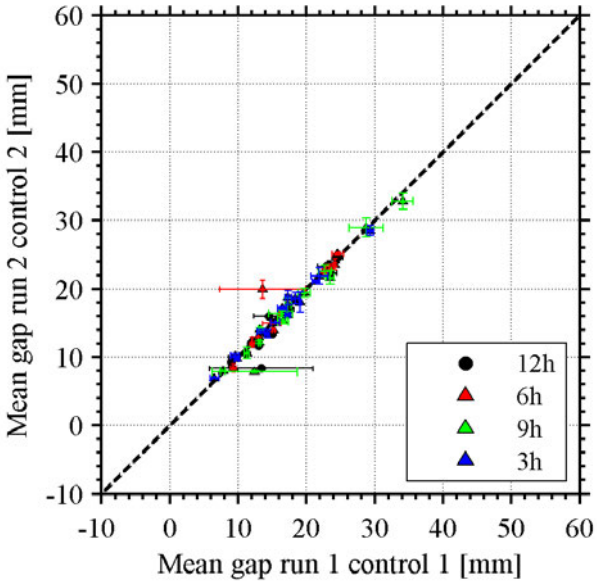

Figure 3.18: CCTV results of inspection three. The mean gap calculated for run 2 and control 2 is plotted against the mean gap calculated for run 1 and control 1. The line x=y is also presented.

that, for accurate readings, Panoramo® should preferably be operated inside empty pipes.

Therefore, the ultrasound and the CCTV were selected for the field tests.

3.7.2 Field tests

While the CCTV was capable of delivering reproducible results, the ultrasound overestimated gap widths, *i.e.*, data with several gaps larger than 20 mm that were not measured with CCTV. These extreme results were considered inaccurate; due to difficulties in analyzing the B-scans originating with operational issues. An example is demonstrated in Figure 3.19: assessing the discontinuity of the horizontal lines was not straightforward and was prone to interpretation. When one operator decides that the gap is the distance between the first and the second black vertical lines, a gap width of 10 mm is ascertained; when a second operator decides that the gap is the distance between the first and the third vertical lines, a 60 mm gap is determined. This only occurred during the field tests and two factors explain this: i) change in flow velocity and consequent loss of data points and ii) presence of air inside the pipe. The effects of these factors were minimized during the laboratory tests which is why the ultrasound performed well. Additionally, the ultrasound was not equipped with a gyroscope and, therefore, it was impossible to know where a given probe was focusing which further complicated the data analysis. The field tests indicated that the tested ultrasound equipment, although promising in the

laboratory, continues to have certain problems in the field.

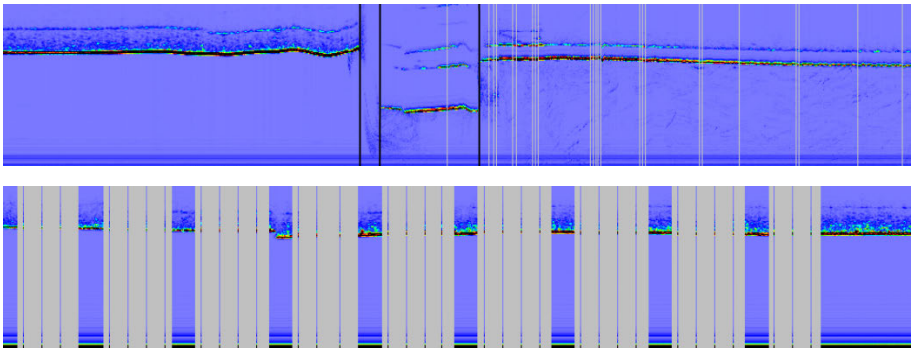

Figure 3.19: B-scans obtained from the ultrasound inspection. Top: sizing the gap width is at times prone to interpretation. Bottom: loss of data due to increased travel speed. Courtesy of Applus RTD.

A disadvantage of the CCTV when compared to the ultrasound, as identified during these tests, was the limited reach. Only a portion of the pipe could be inspected with the CCTV due to the resistance of the umbilical cord. With the ultrasound, an inspection of the complete pipe could be performed.

These results indicate that the tested ultrasound is not as valuable a tool as is the CCTV to accurately measure gaps in push-fit joints. Therefore, the CCTV was selected to perform the full-scale tests.

Although not binding for the selection of the best tool, a comparison with the effort of man-hours to inspect the pipe with the ultrasound and the CCTV will be made. The total time with the ultrasound was one morning including travelling, preparation, inspection (one hour) and packing. The work was performed by two men including one operator and one assistant. Data analysis took one operator five 8-hour days.

The total time with the CCTV was one afternoon: travelling, preparation, inspection (two hours) and packing. The work was performed by two men including one operator and one technician. The office work (report and control of measurements) was made by one man and can be considered to take the same amount of time as the field work.

3.7.3 Full-scale tests

The application of the CCTV to aggregate information regarding the alignment of pipes inside of push-fit joints presented reproducible results as was proven by the Wilcoxon Rank Sum Tests. The comparison between the two runs (both conducted in the field) and between the runs and the controls (conducted in the office) demonstrated no significant statistical difference at a 95% significance. This seems to contrast with the doubts that Costello et al. (2007); Dirksen (2013); Makar (1999); Rajani and Kleiner (2004) and others cast on the CCTV inspection, presenting it

as a subjective and qualitative tool which delivers results that are prone to interpretation. However, it should be mentioned that the application of the CCTV in the present work differed from the typical application of the CCTV described in literature. The CCTV is normally employed in order to screen a multitude of pipe and joint defects - root intrusion, pipe cracks, wall collapses, presence of debris, joint bending, etc. - and, in fact, the detection and quantification of some of these factors can be subjective. In the current work, the CCTV was applied as a measuring tool for a single application - gap sizing - and this application minimized the potential for incorrect interpretations of the CCTV inspections.

3.8 Conclusions

In this chapter, three NDE tools were systematically tested both in a laboratory and in the field. The results delivered by the three tools were analyzed on their accuracy and reproducibility.

In the laboratory tests, both the ultrasound and the CCTV were demonstrated to deliver accurate and reproducible results. Panoramo® was shown to deliver reproducible results but displayed deficiencies when compared to the other two tools, specifically, inconsistent reproducibility and accuracy as well as problems with the inspection of water filled pipes, especially when in the presence of suspended matter.

Both the CCTV and the ultrasound were tested in the field to measure the joint gaps of AC and PVC pipes. The field tests were conducted on a single day, the pipe selected for this portion of the work allowed the CCTV and the ultrasound inspection, which is not standard in water distribution pipes in the Netherlands. The CCTV produced reproducible results. The tested ultrasound demonstrated certain disadvantages including the lack of a gyroscope - a gap can be sized but it is not known to which in-pipe position it is concerned - and production of unexpected and extreme gap values.

The full-scale tests aimed at further testing the reproducibility of the CCTV. Thus, the CCTV was employed over three different days in order to inspect three different pipes. In the full-scale tests the CCTV again delivered reproducible results.

These results indicated that the visual tools tested in this work (CCTV and Panoramo®) could produce reproducible results. In addition to this, the CCTV could be operated to consistently deliver accurate results and was considered the best readily available tool for the inspection of joints and detecting the failure modes described in Chapter 2.

chapter 4

Real-time pipe monitoring[†]

From early on in the project, the author realized two things regarding condition assessment. On the one hand, it provides valuable information and many recognize its importance. On the other hand, it is very intrusive and not all utilities are willing to have pipes closed, inspected, and disinfected.

Therefore, an alternative to condition assessment as described in Chapter 3 had to be developed. An option is installing sensors and monitoring the pipe in real-time. A PVC 250 mm drinking water pipe that supplies water to approximately 1,250 customers was monitored from September 2011 until June 2013. The aggregated data comprises strain registered on pipes and joints, temperature registered adjacent to these appurtenances and strain registered on coupons of PVC isolated and also installed adjacent to the pipe. The data depict an expected positive correlation between temperature and strain on PVC. It also demonstrates that such a set-up is able to detect daily water pattern use and episodes of water-hammer.

In order to compare the monitoring results with the NDE assessments, five CCTV inspections had been planned: one before use and the remaining four throughout the remainder of the year. However, due to safety/public-health issues, these inspections were not performed. Additionally, some practicalities evidenced from early-on as many sensors became inoperative. Nevertheless, the obtained data proves that such a set-up, although complex, can become a valuable approach for important drinking water transport mains that cannot be inspected following a standard condition assessment procedure.

[†]This chapter is based on the following article:

Arsénio, A. M., Vreeburg, J. H. G., Wielinga, M. P. C., and van Dijk, H. (2012c). Continuous assessment of a drinking water PVC pipe. In *Water Distribution Systems Analysis (WDSA)*, Adelaide (Australia)

4.1 Introduction

4.1.1 Background

In Chapter 3, it was demonstrated that the 3D alignment of the pipes connected through a joint can be known measuring the gap between the two pipes connected through a joint at four locations (bottom, top and both springlines). This 3D alignment can be employed as a surrogate measurement for joint condition prior to failure.

In the field, the gap widths and the alignment of the pipes change dynamically. Several external factors influence the change, *e.g.*, seasonal soil-temperature variation, traffic, inner-pipe pressure, and differential soil settling. Changes in pipe alignment can only be detected using an NDE to determine if the pipe can be accessed for inspection and only if the pipe does not require continuous monitoring. In case of, for example, important mains that cannot be placed out-of-service to be inspected or mains that should be monitored permanently, real-time monitoring might be the only solution. Two examples of important mains that should be monitored permanently are large mains installed adjacent to highways or mains installed in dykes, a typical case in the Netherlands.

In several countries, real-time monitoring set-ups have already been tested and implemented. In Canada, real-time pipe monitoring has been used to determine the influence of frost on the behavior of a PVC pipe spanning several years. In Australia, metallic and plastic pipes have been monitored to study the impact of expansive soils in pipe breakage. More recently, also in Australia, pipes have also been monitored using fibre-optics.

Real-time monitoring of dykes in the Netherlands

In the Netherlands, 55% of the territory is located within the dyke rings protected by dunes, dykes, dams, and other artificial structures; with approximately 25% of the country being below sea level (PBL, 2007). In spite of this, according to Van et al. (2009), questions regarding the ammount of time before failure or the maximum load increase that a specific dyke location can withstand are still difficult to answer. Therefore, the IJkdijk project, an international test site for inspection and monitoring techniques for dykes, was established with the following objectives (Van et al., 2009):

1. Develop and validate new sensor techniques;
2. Perform full-scale failure experiments on dykes to understand fundamental behavior in order to be able to increase the quality of the inspection process and safety assessment of dykes; and
3. Study the manner in which to respond timely to an emergency with appropriate measures.

At the IJkdijk test location, three test dykes were collapsed in August and September of 2009 (IJkdijk, 2009). The objective of this project was to study the applicability of employing modern sensor technology to obtain (sub)soil information which could act as an early warning system for dyke failure. Some of the installed

sensors included fibre-optics, humidity sensors, inclinometers and cameras tracking fixed points on the dykes' surfaces (Van et al., 2009). The analysis of the results indicated that "the sensor systems predicted the dyke breaches well in advance" (IJkdijk, 2009). More recently, the IJkdijk's failure mechanism was modeled by Sellmeijer et al. (2012).

The effect of frost in underground infrastructure

The negative impacts of frost in underground infrastructure - pipe freezing or differential frost heave and pavement settlement - have long been recognized by engineers (Kleiner et al., 2007; Selvadurai et al., 1999; Sepehr, 1994). The region of Western Canada is especially affected by frost and, in Edmonton in the province of Alberta, in the mid-1990s, the National Research Council of Canada (NRC) installed sensors on and close to a pipe (Rajani and Kuraoka, 1995; Zhan et al., 1995) with the following objectives (NRC-CNRC, 1997):

- Evaluate the thermal performance and cost effectiveness of the different types of backfill material;
- Determine the modes of failure of PVC water mains exposed to freezing ground conditions by monitoring strains in PVC pipes; and
- Conduct measurements of vertical earth loads in selected backfills and relate the variation of loads to climatic and soil conditions and the type of backfill.

Throughout approximately three years, the sensors monitored temperature; axial, flexural and circumferential strains; earth pressures; thermal conductivity, and moisture (NRC-CNRC, 1997). During the project, the sensors supplied relevant information that enabled the authors to select the most appropriate backfill for frost conditions and modeling the pipe's behavior (Kuraoka et al., 1996; Rajani et al., 1996).

The effect of expansive soils in underground infrastructure

The ground movement which results in pipe failures can be a result of shrinkage and swelling of soil due to seasonal variations of moisture content. According to Gallage et al. (2008), "high stresses produced by the swelling of soil can damage pipelines by introducing cracks and rupture at longitudinal and circumferential directions". Chan et al. (2007) ascertained that there is a strong correlation of water main breaks with climate changes in Australia as there are up to 3 times more failures recorded in a hot, dry season than during relatively wet seasons. A preliminary analysis on the main failure location indicated that a greater proportion of failures occurred within reactive, rather than in non-reactive, soils. Therefore, Australian researchers have studied the effect of soil shrinkage on pipe failure employing sensors. A group from Monash University performed laboratory tests with reactive soils and PE pipes Gallage et al. (2011). This work induced a three dimensional numerical model (Rajeev and Kodikara, 2011). In the field, a 100 mm CI pipe was instrumented and, while Chan et al. (2009) focused on the field instrumentation section of the pipe project, detailed analysis of the aggregated data was discussed by Gallage et al.

(2009). According to Gallage et al. (2009), despite inner-pipe pressure leading to minimal variations in the pipe stresses, these may lead to pipe failure, especially, "when pipes are stressed close to failure due to other factors such as soil stresses and corrosion". The authors also concluded that pipe failure during dry weather is dominated by downward bending (particularly during summer) and that continuous wetting might lead to significant upward bending and increase pipe failures during winter.

For the project "Critical Pipes", Rajeev et al. (2013) reviewed the use of fiber-optics on a drinking water pipe. According to the authors, "traditional electrical sensors* the sensor network becomes more complex, difficult to install and maintain, and expensive". The authors also argued that "the use of these discrete sensors for large civil structures is simply impracticable and not cost effective". Furthermore, according to Rajeev et al. (2013), fiber-optics afford the inclusion of a significant number of sensors in a single optical fibre line owing to the tremendous optical bandwidth and minimal power loss. These systems also have the capability to monitor local strain, temperature, and corrosion rate, etc. at thousands of locations distributed along a single optical fiber over several tens of kilometers (Rajeev et al., 2013). Nevertheless, substantial research efforts are required to implement such a project and realize its full potential (Rajeev et al., 2013).

4.1.2 Objectives

The aforementioned case-studies demonstrate the added-value of monitoring set-ups for real-time pipe monitoring. Therefore, this chapter discusses the installation of electrical sensors for real-time monitoring of pipes and joints to be employed as an alternative to NDE inspection as described in Chapter 3. The objective will be to cast some light on the accuracy, usefulness, and applicability of such a set-up to monitor pipes and joints in real-time. Electrical sensors were selected instead of fiber-optics as it was decided that monitoring short pipe length (40 m) was sufficient. Furthermore, for this work, a field-test was selected instead of a laboratory test for two main reasons:

1. Investigating the feasibility of installing such sensors in the field on a real-life pipe; and
2. Monitoring a pipe subjected to real-life dynamic loads, *e.g.* water-demand patterns and seasonal temperature change.

It had also been planned to asses the condition of the monitored joints utilizing CCTV (Chapter 3). The pipe would be inspected before being in use and, afterwards, four times in the first year. While the first assessment would indicate the initial condition of the pipe, the subsequent inspections would characterize the behavior pipe throughout the year. This procedure would allow comparing the results provided by the CCTV with the results obtained from the sensors and could be interpreted as further validation of the inspection procedure. However, due to safety/public-health reasons, these inspections were not performed.

*For example, strain gauges.

4.2 Materials & methods

4.2.1 Axial strain

The expansion and contraction of a body can be expressed as strain. Strain is a description of deformation in terms of relative displacement of particles in the body and, in the case of a water pipe, it can have its origin in a combination of factors, *e.g.* inner-water pressure, water/ground temperature or traffic. Strain can be calculated using Equation 4.1.

$$\epsilon = \frac{a - A}{A} = \frac{\Delta}{A} \tag{4.1}$$

Where ϵ is the value of strain. Although ϵ is a dimensionless parameter, it is usually given units of $\mu\epsilon$ or mm of deformation per m of initial body length. Therefore, a 1 $\mu\epsilon$ value of strain value indicates that a 1 m length body expanded 10^{-6} m, or 0.001 mm. A [m] and l [m] are, respectively, the initial and the final length of a body subjected to deformation. Δ [m] is the variation in length. Therefore, when a body is stretched ($a > A$ or $\Delta > 0$), the strain is positive (Figure 4.1, left) when a body is compressed ($a < A$ or $\Delta < 0$) the strain is negative (Figure 4.1, right). Using Equation 4.1 and knowing the strain, the expansion/contraction (variation in length) of a body can also be calculated.

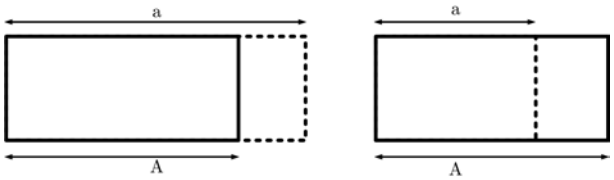

Figure 4.1: Two bodies subjected to deformation. A is the initial body length and a is the final body length. Left: expansion, from Equation 4.1 strain will be positive ($a > A$). Right: contraction; strain will be negative ($a < A$).

To monitor strain on pipes and joints, strain gauges were used (Figure 4.2, top and middle-left). Three monitoring locations were created:

1. Location I: point A, joint 1 and point B;
2. Location II: point C, joint 2 and point D; and
3. Location III: point E, joint 3 and point F.

A general schematic of the complete set-up is illustrated in Figure 4.3. A detailed schematic description of Location I is depicted in Figure 4.4. The set-up is equivalent for Locations II and III. As can be ascertained in Figure 4.4, at each monitoring point, strain is measured at 3 h, 6 h, 9 h and 12 h. Thus, the average axial strain at each monitoring point can be calculated using Equation 4.2.

$$\overline{\epsilon} = \frac{\epsilon_{3h} + \epsilon_{6h} + \epsilon_{9h} + \epsilon_{12h}}{4} \tag{4.2}$$

Where $\bar{\epsilon}$ is the average strain, and $\bar{\epsilon}_i$ is the strain recorded by the gauge at position i.

In this work, hoop strains were not measured.

Figure 4.2: Photos taken during the installation of the sensors. Top left: the strain gauges fixed on the joints. Top right: a strain gauge being fixed on a pipe. Middle left: the dummy strain gauges inside sealed PVC canisters. Middle right: the installation of the pipe. Bottom left: the strain gauges fixed to a joint and two pipes. Bottom right: following the installation, the three cabinets are visible above ground.

Dummy gauges

Strain gauges fixed to pipes and joints monitored the appurtenances responses' to changes in temperature, inner pipe pressure, and external loads. In order to make a distinction between the effect of temperature and the other factors on the pipe/joint

strain dummy strain gauges were also used. To prepare the dummies, strain gauges were glued to small rectangular coupons (10 cm×4 cm) made of PVC similar to the installed pipe. These coupons were then sealed in water proof-canisters to isolate them from the surrounding soil and water (Figure 4.2, middle-right). The PVC canisters were 50 cm sections of 110 mm PVC pipes. These dimensions minimized the friction between the PVC coupons and the inside of the PVC canisters. Therefore, the dummy strain gauges, while being responsive to temperature changes comparable to those experienced by the gauges installed on the pipe and joints, are isolated from all other factors (*e.g.* traffic).

4.2.2 Pipe & joint temperature

The strain gauges also register temperature. The average temperature at each of the monitoring points is calculated using Equation 4.3. The water temperature (inner-pipe) was not monitored.

$$\overline{T} = \frac{T_{3h} + T_{6h} + T_{9h} + T_{12h}}{4} \tag{4.3}$$

Where $\overline{T}$ is the average temperature [°C] and T_i is the temperature recorded by the strain gauge at position i.

4.2.3 Soil temperature

Thermistors (temperature sensors) were installed at each location, 50 cm adjacent to each joint (Figure 4.5), to monitor the soil temperature.

4.2.4 Data logging & power

A relay multiplexer[†] was installed in each cabinet. The multiplexers were connected to the data-logger via a vibrating wire interface[‡]. One datalogger was used to write all data on a 2GB flash drive. The whole system was powered with two 12 V batteries that were replaced every 12 weeks.

4.2.5 Weather data

The weather data presented in this chapter were recorded by the Royal Netherlands Meteorological Institute at the weather station De Kooy, it being the nearest to the monitored pipe (KNMI, 2012), 15 km to the west of the monitoring set-up.

4.2.6 Location & set-up

For this work, a newly installed 250 mm PVC pipe that serves approximately 1,250 customers in the region of North Holland, in the Netherlands, was selected. The installation of the sensors was performed on the 27$^{\text{th}}$ of September 2011 (Figure 4.2,

[†]Among several other advantages, multiplexers significantly increase the number of sensors that a datalogger can measure.

[‡]This equipment allows dataloggers to measure the chosen type of strain gauges.

bottom left), and the pipe began operating in the first week of October. Three joints and four pipe barrels in a row are monitored - a total of 40 m. All pipes are DN250 biaxial PVC with 10 m pipe sections that were installed at 90 cm depth. The pipe sections are connected using double-socket PVC push-fit joints (Section 2.2.2).

Pipes and joints are monitored with strain gauges and, adjacent to each joint, a thermistor and a dummy were installed. Three cabinets were placed above ground 1 m away from the pipe (Figure 4.2, bottom right). A complete list of the installed sensors (per monitoring location) is provided in Table 4.1. All sensors were first checked in the laboratory.

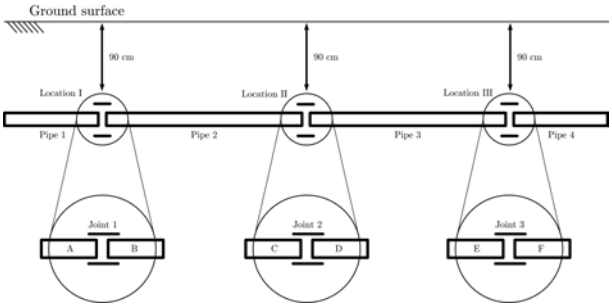

Figure 4.3: Side view of the monitoring set-up. The pipe was buried approximately 90 cm deep. Detailed schematics of Locations I, II, and III are depicted. Location I is composed of position A, joint 1, and position B. Location II is composed of position C, Location 2, and position D. Location III is composed of position E, joint 3, and position F. Image not to scale.

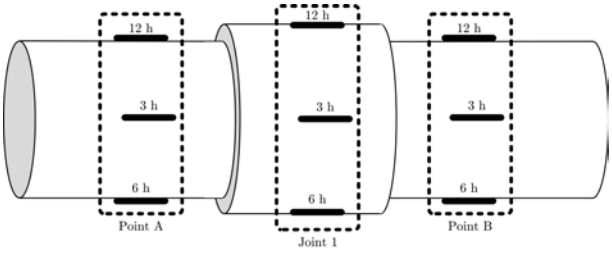

Figure 4.4: Schematic of the installed strain gauges on Location I. The thick, horizontal black-bars represent the strain gauges. In the schematic, the strain gauges installed at 9h are on the other side of the pipe. The strain gauges at points A and B were installed approximately 7 cm away from the joint. The strain gauges installed on the joint were installed approximately in the middle. The set-up is equivalent for locations II and III. Image not to scale.

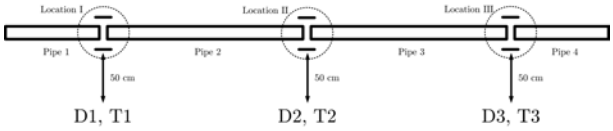

Figure 4.5: Top view of the monitoring set-up. Each pipe section has a length of 10 m. The dummy strain gauges (D1, D2 and D3) and the thermistors (T1, T2 and T3) were installed approximately 50 cm away from the pipe. Image not to scale.

Table 4.1: List of installed sensors at each location.

Sensor	Manufacturer	Model	Number	Data	Position
Strain gauge	Geokon	VK-415	12	$\mu\epsilon$ and temperature	4 gauges glued to the pipe immediately before the joint at 12h, 3, 6h and 9h, 7 cm away from the beginning of the joint. Points A, C and E. 4 gauges glued to the joint also at 12h, 3, 6h and 9h exactly at the center of the joint. Joints 1, 2 and 3 4 gauges glued to the pipe wall at 12h, 3, 6h and 9h, 7 cm away from the end of the joint. Points B, D and F.
Dummy	Geokon	VK-415	1	$\mu\epsilon$ and temperature	Next to the pipe (50 cm away). Glued to a coupon (10 cm×4 cm) of PVC of the same material as the pipe. Isolated inside of a sealed PVC canister. These PVC canisters were 50 cm sections of 110 mm PVC pipes. These dimensions minimized the friction between the PVC coupons and the inside of the PVC canisters.
Thermistor	CS	CS107	1	Temperature	In the ground next to the pipe (50 cm away).

4.3 Results & discussion

The pipe was monitored from late September 2011 until June 2013. Throughout this period, data were lost due to two main reasons: problems with the multiplexers and depleted batteries. Therefore, the included data encompasses the period from March 2012 until March 2013 as this was the one-year monitoring period with the least data interruptions. Nevertheless, the data-set is not complete for every sensor.

4.3.1 Air temperature & soil temperature

The temperatures recorded by Thermistor 3[§] (Temp_3) are depicted in Figure 4.6 together with the maximum air temperatures recorded by the Dutch Metereological Institute. These data can be located on-line (KNMI, 2012). Maximum air temperature was selected in order to demonstrate the maximum potential for pipe warming.

The data demonstrate the effect of soil insulation on the temperature recorded adjacent to the pipe (Figure 4.6). There is a delay; a peak in maximum/minimum temperature is detected in the soil only some days after. Additionally, the soil temperature has a more stable pattern than the air temperature - the soil has a dampening effect. Soil temperature also does not achieve under 7 °C even with minimum air temperatures reaching almost -10 °C and does not reach 20 °C even with air temperatures peaking at 30 °C.

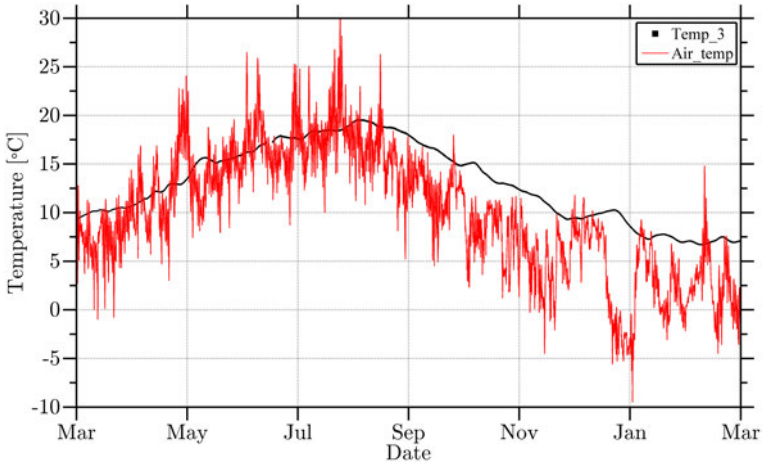

Figure 4.6: Soil temperature recorded by Thermistor 3 (Temp_3) and maximum air temperature. Maximum air temperature data were obtained from KNMI (2012).

[§]Thermistor 3 is located 50 cm away from Location III (Figure 4.5).

4.3.2 Pipes & joints

Temperature

In Figure 4.7, the temperatures recorded by Thermistor 3 (Temp_3) are plotted collectively with the temperatures recorded at point D (3h, 6h, 9h and 12h)[¶]. The temperatures recorded at joint 2 are depicted in Figure 4.8.

Pipe and joint temperatures are consistently lower than the soil temperature (Temp_3).

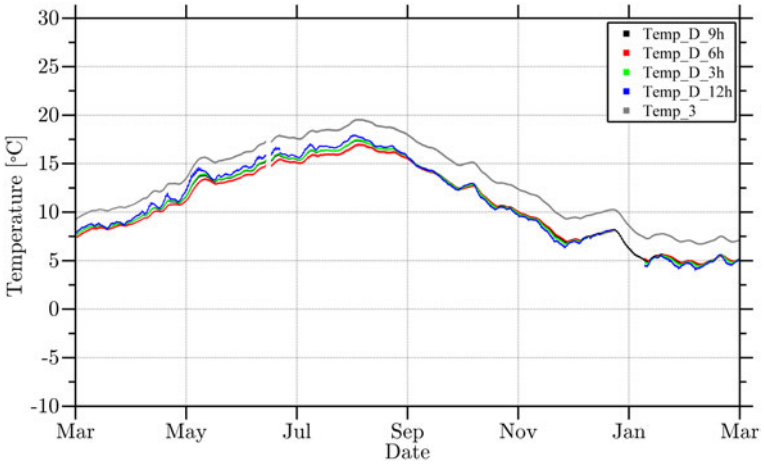

Figure 4.7: The temperature recorded by Thermistor 3 (Temp_3) are plotted collectively with the temperatures recorded at point D (3h, 6h, 9h and 12h).

[¶]Point D is located 7 cm after the joint (Figure 4.4)

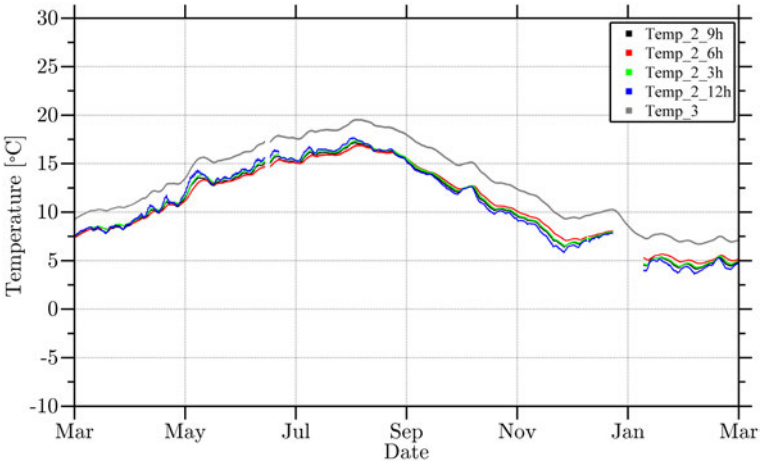

Figure 4.8: The temperature recorded by Thermistor 3 (Temp_3) is plotted together with the temperatures recorded at joint 2 (3h, 6h, 9h and 12h).

Strain

In Figure 4.9, the average temperature at point D (Equation 4.3) is plotted with the strain recorded at point E (3h, 6h, 9h and 12h). The data show that, as expected, there is a correlation between soil temperature and strain, *i.e.*, an increase in temperature leads to an expansion of the pipe.

The spiky pattern obtained for the axial strain on point E is due to the daily water-demand pattern. In Figure 4.10, a detail of Figure 4.9 encapsulating the period from the 31st of May until the 2nd of June is indicated. In Figure 4.10, it is evident that, during the period when the average temperature at point D increases, the strain reaches throughout the day. The strain has its maximum at approximately 12:00 a.m. and a second after 8:00 a.m.. These are probably periods of low water use (lower inner-pipe pressure), during which time the pipe contracts radially and expands axially (Poisson Effect).

In Figure 4.11, the temperature at point D is plotted collectively with the strain recorded at joint 2 (6h and 9h)[‖] and calculated with Equation 4.2. Also, in the joint, the effect of the daily water-demand pattern is obvious.

In late 2011 and beginning of 2012, two episodes of water-hammer were registered by the set-up (Arsénio et al., 2012c). Both episodes occurred before the period of analysis covered in this thesis. Nevertheless, to support the present data-analysis, the first episode is presented in Figure 4.12 (annotated). In this figure, the average strain calculated at point E is plotted together with the average temperature at point E and the temperature recorded by Thermistor 3 (Temp_3). It is obvious that the transient detected by the strain gauges (positive variation of more than 500 $\mu\epsilon$, or 5 mm in 10 m) was not induced by changes in the soil/pipe temperature. According to the utility, a valve was closed when the water-hammer episode was detected.

[‖]The strain gauges installed at 3h and 12h were inoperative.

From the analysis of Figure 4.12, it is also visible that the water temperature (Temp_E_wh) increased after the water-hammer. It can be hypothesized that the origin of the water flowing inside the pipe changed once the valve was closed, and that the water from the new source was warmer than previously.

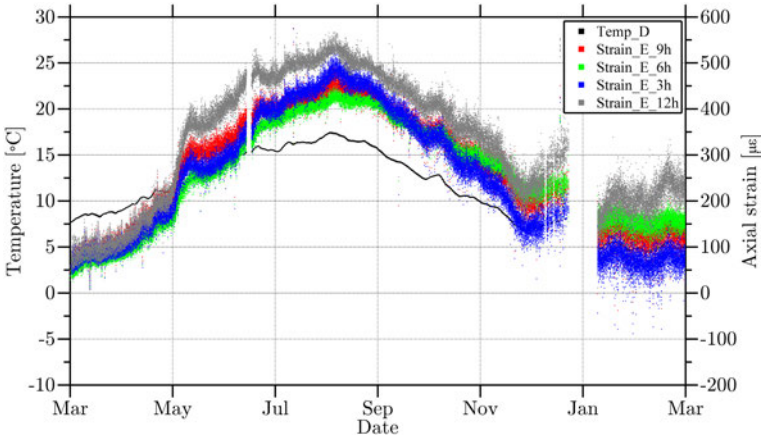

Figure 4.9: The average temperature recorded at position D is plotted collectively with the strain recorded at position E (3h, 6h, 9h and 12h).

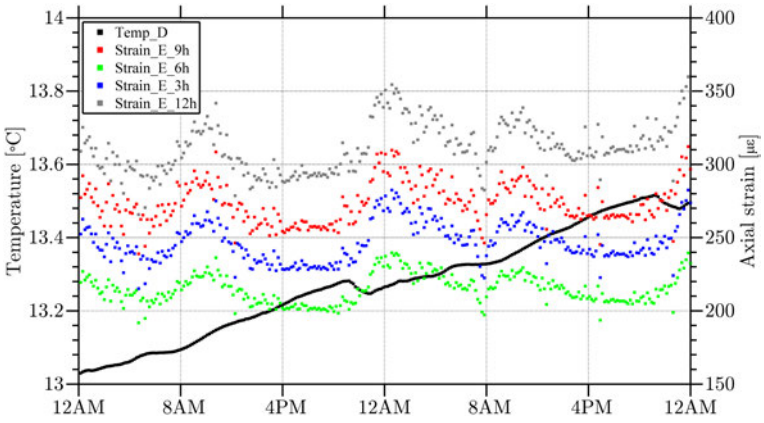

Figure 4.10: Detail of Figure 4.9 encapsulating the period from the 31st of May 2012 until the 2nd of June 2012. The effect of the daily water-demand pattern registered by the strain on the pipe is obvious. Please notice the change in scale from Figure 4.9.

Expansion

In Figure 4.13, the average temperature recorded at point D is plotted with the expansion/contraction values of pipe 2 along its length (Equation 4.1). This value

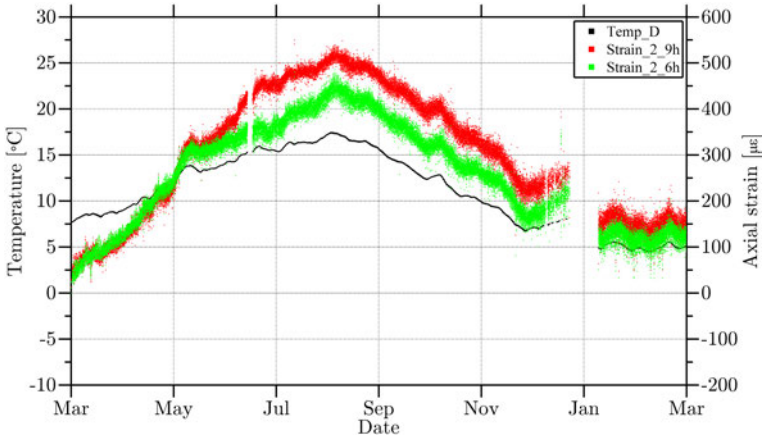

Figure 4.11: The temperature recorded by Thermistors 3 is plotted together with the strain recorded at joint 2 (6h and 9h). The strain gauges positioned at 3h and 12h were inoperative.

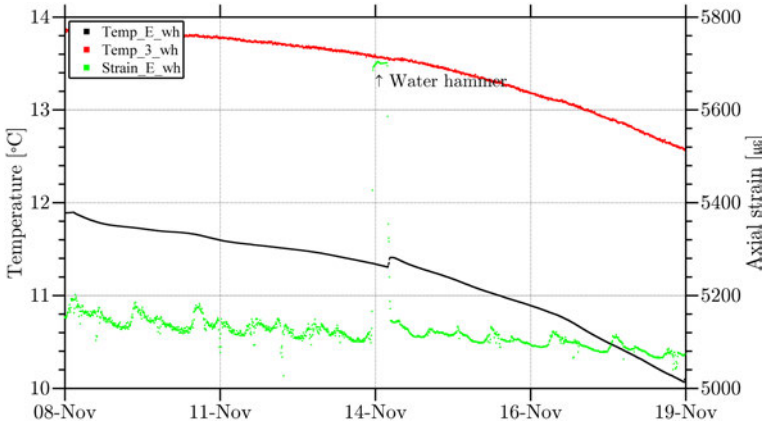

Figure 4.12: One of the water hammer episodes recorded around the 14^{th} November of 2011. The increase in strain is indicated with a black arrow. The water utility confirmed having closed the valves on this day. Please notice the change in scale from Figures 4.11 and 4.9.

was calculated employing the strain values registered at point E.

At each end, the pipe contracts and expands in the order of 3 mm. The daily expansion/contraction range is 1/2 to 1/4 mm at each pipe end due to the daily water-demand pattern and due to the restraining effect of the rubber gaskets.

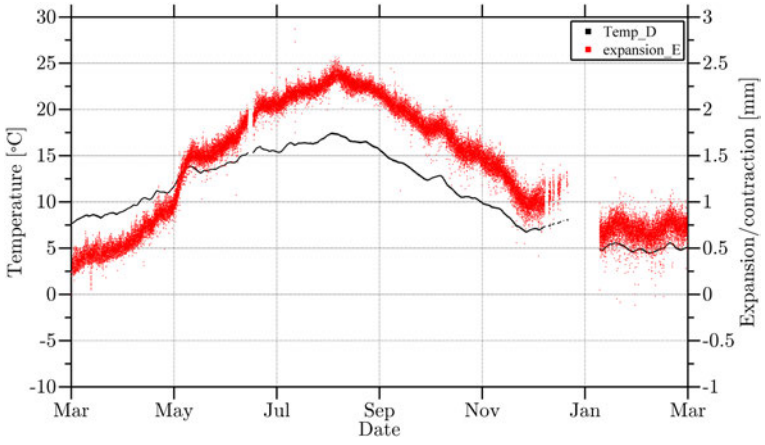

Figure 4.13: The average temperature recorded at position D is plotted together with the average expansion calculated for position E. The expansion is calculated for each pipe-end.

4.3.3 Dummies

Temperature

In Figure 4.14, the temperatures recorded by temperature Thermistor 3 (Temp_3) are plotted collectively with the temperature recorded by Dummies 2 and 3**. As before, the soil temperature is higher than the temperatures registered by the dummies.

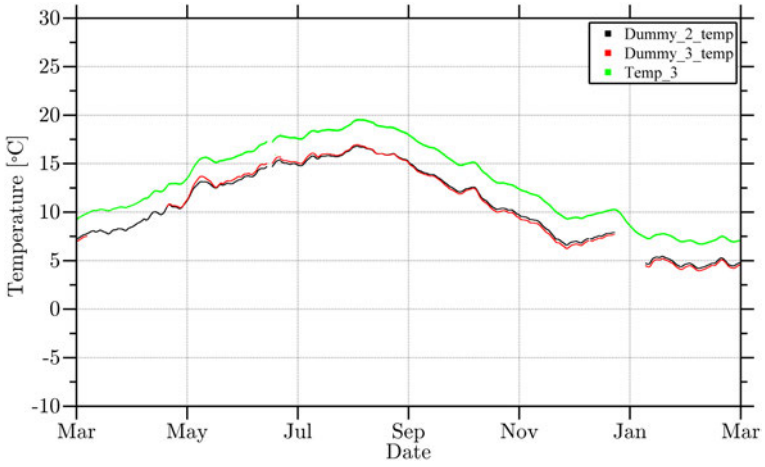

Figure 4.14: The temperature recorded by Thermistor 3 (Temp_3) is plotted together with the temperature recorded at Dummies 2 and 3.

**Dummy 1 was inoperative.

Strain

In Figure 4.15, the strain recorded at point E is plotted with the strain recorded by Dummy 3 where the influence of the temperature in the dummy strain is evident. The effect of the daily water-demand pattern is, as expected, absent on the dummies.

The data demonstrate that the axial strain at joint 2 is less than the strain recorded by the dummy gauges during summer and higher during winter. During winter, the pipe strain is higher than the dummy strain while, during summer, the opposite happens. Expansion due to temperature changes cannot explain this fact since the difference between the temperature registered at position E (the highest) and at Dummy 3 (the lowest) is consistent throughout the year (Figure 4.16).

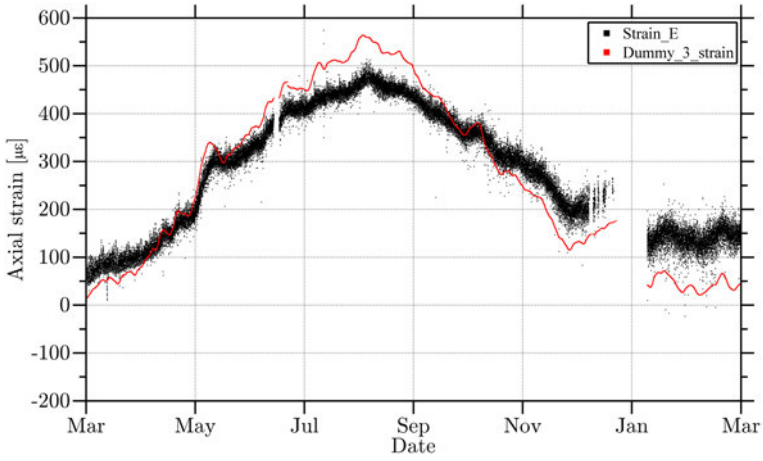

Figure 4.15: The average strain recorded at position E is plotted together with the strain recorded at Dummy 3.

4.3.4 Non-destructive assessment of the pipe

Due to water quality and public-health concerns of the water utility, it was decided not to inspect the pipe. Therefore, no comparison between NDE inspection and monitoring results can be made.

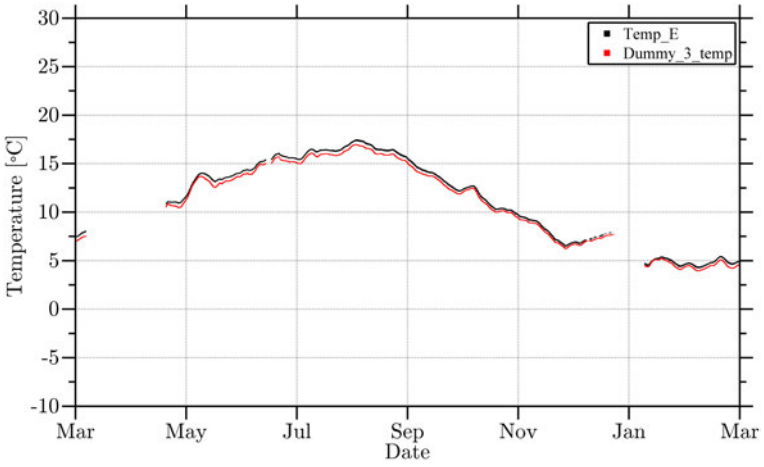

Figure 4.16: The average temperature recorded at position E is plotted together with the temperature recorded at Dummy 3.

4.4 Conclusions

This chapter discusses the application of thermistors and strain gauges to monitor pipes and joints in real-time.

Throughout the monitoring period, daily water-demand patterns and episodes of water-hammer were detected by the strain gauges which demonstrates the accuracy of the equipment.

From the beginning of the monitoring period until the coldest period for which data are available, the pipe contracted more than 2.5 mm at each end due to temperature changes. During the summer season (June-September), the temperature can exceed the installation temperature. At that time, contact points (pipe-pipe and pipe-joint) can begin if one considers that the pipes were installed fully inserted inside the joints[††]. This variation in pipe length can be detected by the CCTV following the procedure outlined in Chapter 3. Additionally, the results also demonstrate that a joint following a winter inspection is considered to be "at risk" with small gaps (Section 3.2) and can be in an even riskier situation during summer after pipe expansion.

This chapter also demonstrates that a pipe monitoring set-up can be implemented for specific situations (*e.g.* high-importance mains). In such cases, specific sections of the pipe can be permanently monitored for expansion/contraction by the utility.

A final note must be dedicated to the problems encountered during the period through which the project ran, from September 2011 until June 2013. Pipe monitoring is not problem-free, and this must be acknowledge by the people projecting such a set-up. As can be seen in all figures except 4.6, portions of the data are always

[††]As will be discussed in Chapter 5, contact points should be avoided as they have a negative impact on a joint's behavior and increase its stiffness.

missing. Several sensors stopped working, and until June 2013:

- Of the 16 strain gauges attached to the joints, only three (one per joint) remained operational;
- Monitoring points C and D only had one operational strain gauge;
- At Location 1 the dummy strain gauge and the thermistor were not operational; and
- At Location 2 the thermistor was not operational.

Most sensors stopped working during the cold period of February 2012 when the maximum air temperature did not rose above 0 °C for more than two weeks (which was great for ice-skating, nonetheless). Due to the cold temperatures, the batteries became depleted, and data was not logged for approximately eight weeks. When new batteries were installed, some of the sensors were inoperative. Two strain gauges installed on the pipes became inoperative following episodes of water-hammer. This further emphasizes that, although such a set-up can produce useful and valuable data, as argued by Rajeev et al. (2013), its complexity is also its *Achilles' heel*.

Furthermore, an unaccomplished objective behind this set-up was to compare results from NDE inspection with results obtained with the sensors; due to water-quality and public health concerns of the water utility, it was decided not to inspect the pipe. At this point, it is noteworthy to mention that no water-quality problem occurred after any of the nine pipe inspections that will be discussed in Chapter 6. This can be explained by the extensive disinfection of the NDEs prior to the inspection and to the thorough pipe flushing and disinfection following the inspection.

chapter 5

Destructive laboratory tests with PVC pipes & joints[†]

This chapter had a clear objective, *i.e.*, defining the limit at which a specified joint begins leaking during bending or pull-out tests. Such information would be an important milestone. With access to the threshold conditions of joints, it becomes possible to accurately detect most failure modes (Chapter 2) by employing the procedure discussed in Chapter 3.

Due to safety reasons, these tests could not be conducted at KWR and were, instead, performed at the workshop of DYKA. Since a testing standard was not being followed, the first steps were projecting, building, and improving the testing frame. The second step was developing a test procedure so that all specimens were tested under the same conditions. With everything finely tuned, more than 200 PVC pipes and joints were tested.

[†]This chapter is based on the following articles:

Arsénio, A. M., Vreeburg, J. H. G., Bouma, F., and van Dijk, H. (2012a). Destructive laboratory tests with PVC push-fit joints. In *Water Distribution Systems Analysis (WDSA)*, Adelaide (Australia)

Arsénio, A. M., Bouma, F., Vreeburg, J. H. G., and Rietveld, L. (2013a). Characterization of PVC joints' behaviour during variable loading laboratory tests (submitted). *Urban Water Journal*

5.1 Introduction

5.1.1 Background information

In Section 1.7.2, it was demonstrated that joints play a major role in the failures occurring in a network with PVC pipes. However, given the focus of literature on pipe barrel deterioration, it can be assumed that this role might have been neglected in the past.

Additionally, in order to characterize the current condition of a joint in the field, information on its threshold conditions was nonexistant.

For joint bending, it is expected that, after a certain bending angle, the joint begins leaking. Leakage is either followed by complete pull-out of the pipe from the joint or by the fracture of either the pipes in the joint or the joint itself. For axial pull-out, it is expected that leakage begins after a certain gap (Section 3.2) followed by the complete pull-out of the pipe from the joint. Therefore, the threshold conditions are both a limit in bending angle and in pull-out distance before leakage, before complete pull-out, and/or before complete burst. Having access to these data, the present condition of a joint can be assessed. Additionally, the results of inspections conducted in different periods can be compared, and a degradation rate can be calculated.

For joint bending, comparable information is provided by pipe manufacturers and in installation guidelines. Some Dutch PVC pipe manufacturers define 6° as the maximum bending angle of a joint during installation (DYKA BV, 2012; Pipelife, 2001). The American Water Works Association (AWWA) defines a maximum joint angle that is a function of the diameter and length of the installed pipe barrels AWWA (2002). This equation calculates the maximum bending angle that is permitted when two consecutive barrels are installed. In the presented work, it is assumed that Equation 5.1, a modified version of the equation presented in AWWA (2002) for bell-and-spigot joints (the original equation was multiplied by a factor 2), can be utilized to calculate the maximum bending angle for a double-socket joint. This assumption is made so that both guidelines can be compared.

$$AWWAL = 2 \times \frac{57.3 \times b}{300 \times Do} \tag{5.1}$$

Where $AWWAL$ [°] is the recommended installation angle, b [m] is the length of a pipe barrel, and Do [m] is the outside pipe diameter. The original equation was developed for the bell-and-spigot system and, during installation, the system will not be stressed if the bending angle is below this limit. Equation 5.1, to be applied to a double-socket joint, was multiplied by 2. Nevertheless, these guidelines are published with the sole purpose of defining optimal pipe-joint alignment during installation and offers no information about allowable bending angles throughout a pipe's lifespan.

Additionally, it is expected that, during bending, due to changes in inner geometry, the stiffness of the joint varies. These changes include: i) contact between the pipes, the inner joint, and the joint ring (Figure 2.2) and ii) between both pipes. In the absence of leakage and/or material fracture, joint stiffness can be exploited

to characterize its condition. In this work, stiffness describes the force required to achieve a certain bending angle in a joint.

Similar work has been presented by several authors. Singhal (1984) performed static experiments on bell-and-spigot rubber gasketed ductile iron joints. Meijering et al. (2004) performed destructive laboratory tests with PVC gas pipes in order to detect leakage during radial deflection of the pipes whereby during the tests, pipes were pressed radially next to the joint. The authors reported that the joint begins leaking when the diameter deflection exceeded 36%. Reed et al. (2006) tested three CI joints and Buco et al. (2008b) characterized the behavior of cement pipes and joints subjected to bending. Both authors concluded that, during bending, the alignment of the pipes inside the joints changes. As discussed in Section 2.4.1, with the increase of bending angle, contact points between the pipe and the joint and between both pipes begins*. Buco et al. (2008b) ascertained that stiffness is greatly influenced by the beginning of these contact points and that these are important in defining a joint's condition. Thus, an increase in stiffness is considered dangerous as the joint can become overstressed which could possibly result in failure.

Additionally, several authors have modeled the behavior of joints exploiting computational methods as is apparent is certain examples in the work of Buco et al. (2008a) with reinforced concrete sewer pipes; Jeyapalan and Abdel-Magid (1987) with reinforced plastic mortar and Scarino (1981) for several pipe materials. According to Rajani and Abdel-akher (2013), O'Rourke and Trautmann (1980) proposed a model to estimate the resisting moment for a lead-yarn joint, assuming that the spigot, given sufficient rotation, mobilizes the adhesion between lead and the cast-iron bell (inside) and spigot (outside) surfaces. Rajani and Abdel-akher (2013) discussed bell split failure, a predominant failure mode in lead-caulked bell-spigot joints of large-diameter cast-iron pipes installed between 1850 and the early 1960s. The authors also presented a mechanistic model and validated it against experimental tests conducted in the mid-1930s (Prior, 1935) on lead-caulked bell-spigot joints. This model was subsequently utilized to develop an additional model to predict the cumulative joint response of two or more contiguous pipe segments resting on an elastic medium and subject to overburden pressure followed by ground movement.

Nevertheless, to the knowledge of the author, a thorough characterization of of the behavior exhibited by water-distribution PVC joints for different loading regimes was lacking. Therefore, PVC push-fit joints and pipes were tested in the laboratory to obtain parameters that can be used to assess the condition of a joint in the field. For pull-out and bending tests, two threshold conditions were investigated. The first is start of leakage and the second is material fracture. During bending tests, force was monitored to characterize the joint's stiffness.

*In Figure 2.2, an example is provided for a double-socket PVC joint.

Table 5.1: Values of D' for the three levels of insertion tested in the laboratory.

	D' [mm]	
Level of insertion	110 mm	315 mm
Minimum	40	70
Half-way	20	35
Maximum	0	0

5.2 Materials & methods

5.2.1 Variables tested

PVC double-socket push-fit joints and pipes were tested in the laboratory under various conditions:

1. Pressure. Tests were performed with 4 bar (absolute) water pressure at 20 °C (water bath) and with 0.2 bar (absolute) air pressure - vacuum. The 4 bar water pressure tests simulate a typical situation in a drinking water network. With the 0.2 bar tests, the objective was to study the possibility of the intrusion of water in a pipe that experiences pressure below the atmosferic. While out-of-service, if the ground water level is above the pipe, the water pressure outside the pipe exceeds the water pressure inside, and intrusion could occur.

2. Level of insertion. Three different insertions of the pipes inside the joints were tested. Maximum insertion: the pipes were touching the inner joint ring (Figure 2.2, in black at the middle of the joint). Half-way insertion: the pipes were at a half-way distance between the center of the joint and the rubber ring. Minimum insertion: minimal insertion inside the joints that still guarantees safety and leak sealed joints. The level of insertion was defined by D' (Figure 5.1), and it is the distance between the extremity of one pipe and the ring at the center of the joint. Due to symmetry, the value of D' is the same for both pipes connected with one joint. The value of D' for each insertion level is depicted in Table 5.1. It is expected that, due to the inner joint geometry, the insertion will play a role when a pipe is being bent: a wider gap between the pipes guarantees that contact points between the pipes and the joint's ring and between both pipes occurs at wider bending angles.

3. Diameter. Pipes and joints of two diameters were tested: new 110 mm and 315 mm PN 10 produced according to the standard of KIWA (2007) and supplied by DYKA BV. Due to geometric differences, it was expected that pipes with different diameters behave differently during the bending tests and that the maximum allowed bending angle also varies with diameter.

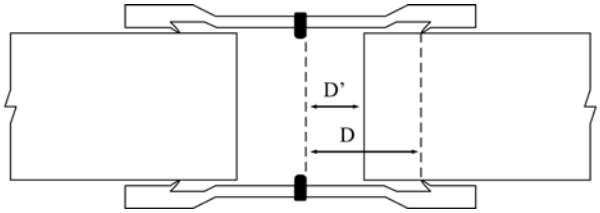

Figure 5.1: Schematic of a double-socket joint. D' is the distance between the extremity of a pipe and the ring at the center of the joint. D is the distance between the rubber o-ring and the ring at the center of the joint. D=50 mm for 110 mm joints and 100 mm for 315 mm joints. The schematic is not to scale.

Table 5.2: Outside diameter (Do) and wall thickness of the pipes and joints used in the laboratory tests.

	Pipe		Joint	
	110 mm	315 mm	110 mm	315 mm
Do	110.15	315.25	131.13	349.5
Thickness	4.2	12.1	10	15

5.2.2 Bending frame

A bending frame was constructed in order to perform these tests (Figure 5.2). Pipe barrels were cut in 1.5 m sections and connected with double-socket joints. The outside diameters and wall thickness of the pipes and joints employed in the laboratory tests are provided in Table 5.2. The system allowed pipes to be bent while being pressurized with water. Screws on each extremity of the pipe were installed to vary the level of insertion.

During testing, the pipe on the frame was pulled sideways using a hydraulic jack (J in Figure 5.2). Bearings installed at the central rotation point allowed the frame to bend more easily. Each of the two pipes rotated along a fixed rotation point (R). The lateral displacement [mm] caused by the jack was measured using a linear variable differential transformer (LVDT) (T). The force applied by the jack to bend the structure was quantified with a force sensor (F). This sensor measures tensile loads or pressure. Both the LVDT and the force sensor were connected to a logger laptop.

The frame might influence the results of the laboratory tests due to two factors. On the one hand, the bearings create a rolling friction during bending. On the other hand, the effect of the end caps affect the force necessary to bend the structure. This influence will be quantified.

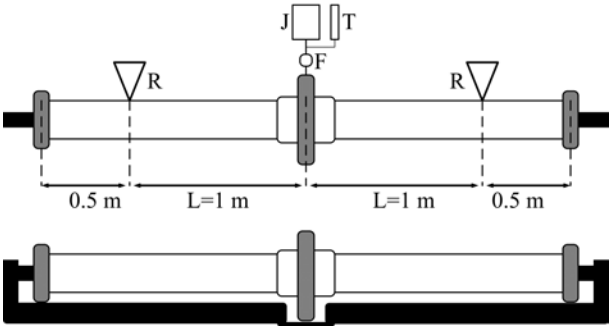

Figure 5.2: Top: top-view schematic of the loading frame. The pulling and monitoring equipment of the frame is composed of a hydraulic jack (J), a force sensor (F) and an LVDT (T). L is the distance between the rotation points (R) and the lip of the pipe inside the joint. Bottom: side-view schematic of the loading frame. Note: images are not to scale.

5.2.3 Bending tests

The LVDT registered and logged the displacement of the set-up. Equation 5.2 converted the displacement into joint angle Figure 5.3.

$$\alpha = 2 \times sin^{-1}\left(\frac{h}{L}\right) \tag{5.2}$$

Where α [°] is the angle between the two pipes inside the joint, h [m] is the displacement recorded by the LVDT, L [m] is the distance (1 m) between the rotation point and the lip of the pipe inside the joint (Figure 5.2).

The joint was bent until 105 mm displacement (12°). This value was selected because it is twice the guideline value indicated for maximum bending angle provided by Dutch pipe manufacturers.

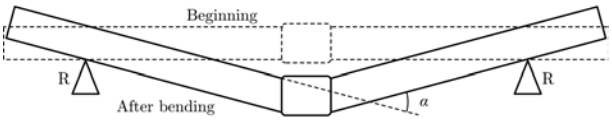

Figure 5.3: Schematic of a joint being bent from an original position until a final position with joint angle α (Equation 5.2). Note: image is not to scale.

5.2.4 Pull-out tests

During the tests, water was continuously pumped into the pipe's interior. The tests were performed without the pipe fixed to the frame at the ends. Both pipes were axially aligned. Pull-out tests with vacuum were not conducted. During these tests,

leakage was the only monitored parameter, and the LVDT and the force sensor were not employed.

5.3 Results

5.3.1 Bending tests

The results of the laboratory tests conducted with 110 mm and 315 mm PVC are depicted in Figure 5.4 and Figure 5.5. The moment of the force [kN] applied by the hydraulic jack and recorded by the force sensor (Figure 5.2) is plotted against the bending angle [°] (Figure 5.3).

The results of six independent tests are collectively indicated (gray line) with the 10-point average (thick black-line) and the sum of inner-pipe force and rolling friction force (*Sum Forces*) (dashed black-line). In Figure 5.4 and Figure 5.5, the tests performed out with water are given in the top row, and the tests conducted with air are demonstrated in the bottom row. The results of the tests performed with maximum, half-way, and minimum insertions are illustrated in the left, middle and right column, respectively.

For the maximum insertion tests (A and D), two vertical dashed lines are illustrated. These lines are at 0° and 3.2° for 110 mm and at 0° and 1.4° for 315 mm. These are the points at which pipe-ring (0°) and pipe-pipe (3.2°) contact occurs. The angles were calculated exploiting Equation 5.2 knowing the initial gap between both pipes inside the joint.

It is clear that stiffness increases with diameter, insertion, and inner-pipe pressure; the force necessary to achieve a specified angle increases. For example, with a 110 mm joint to reach 6°, it was necessary to apply 0.8 kN with maximum insertion, 0.5 kN with half-way, and 0.4 kN with minimum (Figure 5.4 A, B and C).

5.3.2 Pull-out tests

During pull-out tests, leakage was only detected after the complete pull-out of the pipe from the joint.

5.4 Discussion

5.4.1 Destruction of PVC material, leakage & intrusion

Intrusion and leakage were only detected during minimum insertion tests for angles above 10°. This demonstrates the high performance delivered by the PVC double-socket used in the laboratory tests.

Throughout the laboratory tests fracture of material was never observed.

5.4.2 Bending tests: effect of diameter (constant pressure)

The bending tests were up to until 12°. From the analysis of both Figure 5.4 and Figure 5.5, it is evident that joint diameter plays the most significant role in joint

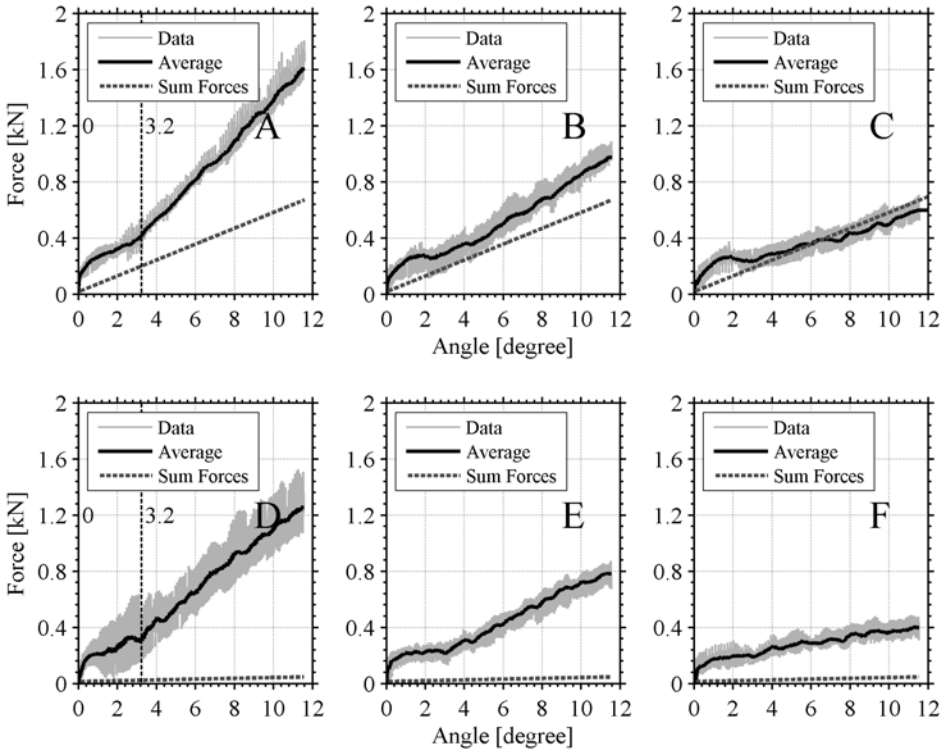

Figure 5.4: Results of the laboratory tests conducted with 110 mm PVC. In all figures, the results of six independent tests are provided (gray) together with the moving average of 10 data points (black). Top row: water pressure. Bottom row: air. Left column: maximum insertion. Middle column: half-way insertion. Right column: minimum insertion.

stiffness; the joint becomes stiffer with the increase of diameter. Several factors influence this, and some are intrinsic to the testing frame while others are intrinsic to the joint itself, *i.e.*, effect of water pressure (intrinsic to the frame), increased weight of the structure (intrinsic to the frame) and increased stiffness of the pipe (intrinsic to the joint).

Effect of water/vacuum (intrinsic to the testing frame)

An increase in the diameter increases the pipe section which subsequently increases the force on the end caps (Equation 5.3).

$$\vec{F_i} = P \times Ai \tag{5.3}$$

Where $\vec{F_i}$ is the internal force [N], P is the inner-pipe pressure [Pa], and Ai is the inner-pipe cross-section area [m^2]. The y component of this force $\vec{F_{iy}}$ has a direction opposed to the force applied by the hydraulic jack (Figure 5.6, Equation 5.4).

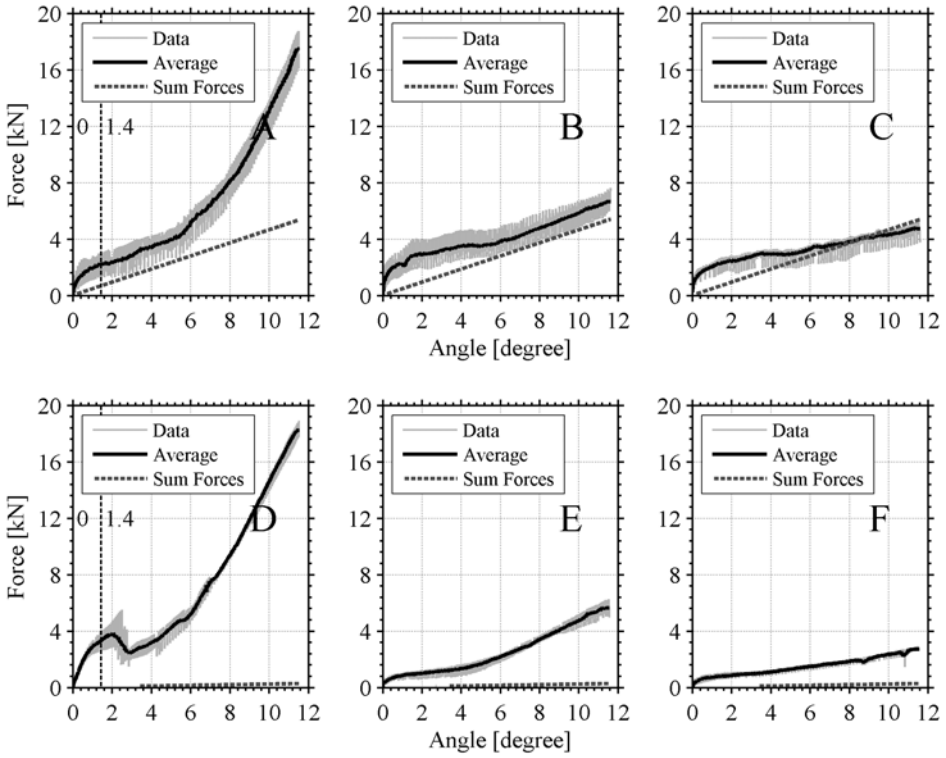

Figure 5.5: Results of the laboratory tests conducted with 315 mm PVC. In all figures, the results of six independent tests are provided (gray) together with the moving average of 10 data points (black). Top row: water pressure. Bottom row: air. Left column: maximum insertion. Middle column: half-way insertion. Right column: minimum insertion.

$$\vec{F_{iy}} = \vec{F_i} \times \left(\frac{\alpha}{2}\right) \tag{5.4}$$

Where $\vec{F_{iy}}$ is the component in y of the internal force [N] and $\vec{F_i}$ [°] is given in Figure 5.6. The effect of inner-pipe pressure is thoroughly discussed ahead for the constant diameter situation.

Effect of structure weight (intrinsic to the testing frame)

The weight of the structure to be bent also increases for the tests conducted with 315 mm PVC; there is more water and more PVC. The structure moves on steel bearings, and the rolling resistance of these was calculated exploiting Equation 5.5.

$$\vec{F_r} = c \times N = c \times g \times M_{total} \tag{5.5}$$

Where $\vec{F_r}$ is the rolling resistance force [N], $c = 0.009$ (according to the manufacturer) is the dimensionless rolling resistance coefficient, and N is the normal

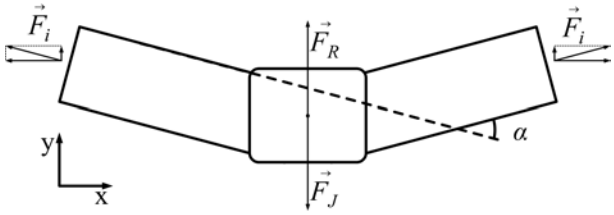

Figure 5.6: Schematic of forces in play during bending. The force applied by the hydraulic jack $\vec{F}_J$ to bend the joint, and the force created by the inner-pipe pressure $\vec{F}_i$ are indicated. Note: image is not to scale.

Table 5.3: Values of rolling resistance force for the various tests.

	Rolling resistance force [N]	
DN	Water	Air
110	16.0	14.7
315	31.1	20.3

force [N], g is the standard gravity [m.s^{-2}], and M_{total} is result of the summation of the water's mass with the structure's mass [kg]. The mass of the structure containing water is calculated (considering that the system is a perfect cylinder) using Equation 5.6.

$$M_{total} = M_{water} + M_{frame} + M_{PVC\ pipes} + M_{PVC\ joint} \tag{5.6}$$

Where M_{water} is the total mass of water inside the pipes [kg], M_{frame} is the mass of the bending frame [kg], $M_{PVC\ pipes}$ is the total mass of PVC pipes [kg], and $M_{PVC\ joint}$ is the mass of the joints [kg]. The weight of the structure containing air is calculated employing the same expression but considering that the mass of air is zero.

The values of rolling resistance are constant throughout the tests and are two orders of magnitude lower than the force applied by the hydraulic jack (Table 5.3).

Effect of pipe stiffness (intrinsic to the joint)

During joint bending, the pipes also bend longitudinally, and this produces vertical ring deflection (buckling) due to the bending moments created (Moser and Folkman, 2008). Therefore, the buckle capacity that a pipe has plays a role in joint stiffness. During laboratory tests, pipe buckling was visually detected during the laboratory tests but not otherwise quantified. Nevertheless, the bending potential of a pipe can be quantified calculating its second moment of area (Equation 5.7).

$$S = \frac{\pi}{4} \times \left[\left(\frac{Do}{4} \right)^4 - \left(\frac{Di}{4} \right)^4 \right] \tag{5.7}$$

Where S [m^4] is the second moment of area.

The 315 mm pipes possess a second moment of area more than 67 times higher than that of a 110 mm pipe. This increased pipe stiffness is also translated into increased joint stiffness.

5.4.3 Bending tests: effect of insertion (intrinsic to the joint)

Next to the diameter, insertion plays the second most significant role in defining the stiffness of a joint, and this effect is more pronounced for the 315 mm PVC than for the 110 mm.

A greater bending force was necessary to achieve the same bending angle if the pipes were more inserted (Figure 5.4 and Figure 5.5). This is related to the beginning of the contact points pipe-pipe and pipe-joint. This effect is obvious for the tests conducted with 315 mm joints where a decrease in stiffness was detected when comparing tests conducted with maximum insertion and tests conducted with half-way insertion. For the analysis of Figure 5.4 and Figure 5.5, the parameter Δ_{slope} defines the point at which a significant variation of the line's slope occurs.

For the tests with the 110 mm pipe, Δ_{slope} for the maximum insertion coincided with the beginning of the contact pipe-pipe. For the half-way test, an Δ_{slope} was detected at approximately 3°. This was not due to the contact point but should still be avoided as the joint becomes stiffer. For the minimum insertion tests, the stiffness was independent of the bending alignment.

The results were similar for the tests conducted with the 315 mm joint. For the maximum insertion tests, there were two Δ_{slope} in which one coincided with the pipe-pipe contact and the other nearer to the 5° similar to the angle defined by Dutch manufacturers. In Figure 5.5 (D), an Δ_{slope} is evident at 2°. This was accompanied by a loud noise during the tests. It appears that, after the beginning of contact at 1.4°, the force built-up in the system until, at 2°, one pipe slid over the other, and the force was alleviated. For the half-way insertion tests, the single Δ_{slope} was also at approximately 5°. For the minimum insertion tests, the joint behaved independently from the bending angle.

These results clearly demonstrate that the definition of maximum allowable joint angle following an approach similar to the formula provided by the AWWA - angle as a function of pipe length and diameter - is necessary. Nevertheless, even the AWWA approach has deficiencies since it does not address the effect of different insertions. Hence, a double parameter is required in order to characterize a joint's condition; the bending angle and a parameter defining level of insertion.

5.4.4 Bending tests: effect of pressure (constant diameter)

The joint was stiffer during the 4 bar tests than during the 0.2 bar tests. The exception was the tests conducted with the 315 mm joint with full insertion for which the joint tested with air was stiffer (Figure 5.4 and Figure 5.5). As before, the increase of inner-pipe pressure had two effects.

On the one hand, there was an increase of rolling friction due to the increase of the total mass of the structure which could be disregarded when compared to the

forces applied by the hydraulic jack (Table 5.3).

On the other hand, the component in y of the force created by the inner pressure was opposed to the direction of pull of the hydraulic jack. In Figure 5.4, and Figure 5.5 is evident that the difference between the tests conducted with air and water never surpasses 2 kN. The sum of the internal force with the rolling resistance ($Sumforces$) is calculated by Equation 5.8.

$$Sumforces = \vec{F_{iy}} + \vec{F_r} \tag{5.8}$$

According to Equation 5.8, the $SumForces$ was greater than 4 kN in the case of the 315 mm joints tested with water and 4 times lower for the same joints tested with vacuum. However, the results demonstrate smaller differences between vacuum and water tests which indicates that the effect of the water pressure ($\vec{F_{iy}}$) was over-estimated when using Equation 5.8. The explanation for this over-estimation was the counter-effect produced by the end caps. This explanation can also be extended to the constant pressure situation. During the tests made with vacuum, the force created by the inner-pressure did not experience the opposing direction to the bending force. This explains why $SumForces$ is less for the vacuum tests than for the water pressure tests. Therefore, inner-pipe pressure played a significantly less important role than the effect of diameter and of insertion.

5.5 Conclusions

Leakage and intrusion were detected in only a few tests at extreme bending angles or, for pull-out tests, after complete pull of the pipe from the joint. This indicates that for PVC joints, leakage through the rubber-gasket is mostly dependent upon the condition of the rubber. For a rubber ring in good condition, leakage can only be expected at bending angles above 10° and with complete pull-out of the pipe from the joint.

Joint stiffness increases with insertion, diameter, and pressure. An increase in stiffness is considered dangerous as the joint becomes less able to bend. Nevertheless, not all tested parameters play the same role.

Increase in diameter is the most important factor for the increase of joint stiffness. This occurs due to three factors: increase of the structure's weight; increase of the inner-pipe pressure, and due to an increase in pipe stiffness bending. Both structure weight and inner-pipe pressure played smaller roles. Pipe stiffness was ascertained to increase more than 67 times from a 100 mm to a 315 mm pipe. Pipe stiffness also played a role during bending both during and after the beginning of the contact points (pipe-pipe and pipe-joint). It should also be noted that the stiffness effect is not intrinsic to the testing frame but is a characteristic of the joint itself.

For pipes of the same diameter, insertion was ascertained to play the most important role. A pipe inserted further in the joint leads to decrease in the angle values at which the contact points begin and the start of contact will stiffen the joint. This situation is obvious for the maximum insertion tests. For the half-way insertion and minimum insertion tests, the contacts points are avoided. For the minimum insertion, the behavior of the joint appears to be almost independent from the bending

angle. This effect was specifically noted in the tests with 315 mm joints where a clear decrease in joint stiffness was discovered when comparing maximum insertion with medium insertion tests. For 110 mm pipes, the decrease was not so obvious.

Therefore, joint angle is a necessary parameter but insufficient to characterize a joint's condition. This work demonstrates the importance of also defining the insertion level of the pipe inside the joint - a double parameter assessment. During an assessment with NDE equipment for two joints with the same bending angle, the greater risk can be allocated to the one with the greater level of insertion. Additionally, from a practical perspective, these results demonstrate the significance of not installing the pipes completely inserted inside the joints as this makes the joints stiffer.

chapter 6

The index for joint condition[†]

Presenting results obtained with an NDE tool is not an easy task. Data should be presented in a clear manner whereby conclusions can be derived. Additionally, it is of the utmost importance to present the results in a way that allows comparing different pipes - a pipe condition ranking. In fact, it might be necessary to decide which of two pipes is in poorer condition, whether all joints in a pipe are in a deficient condition, or if only a few joints are responsible for a certain pipe grade.

For this, the Index for Joint Condition (IJC) for PVC push-fit joints was derived from installation guidelines and from destructive laboratory tests (Chapter 5). The IJC is presented in a graphical framework and is a powerful tool to employ in order to visualize and compare, *in-situ*, results obtained during condition assessment of PVC joint. The graphical results can also be translated into a numerical grade that allows comparing the conditions of various pipes and of individual joints. The applicability of the IJC is demonstrated in the condition assessment of 222 joints inspected in 8 different sessions that encapsulate more than 2 km of older (more than 40 years) and newer pipes (less than 2 months). While, for the new pipe, all joints were considered to be in good condition, several joints in older pipes were considered to be "at risk".

[†]This chapter is based on the following article:

Arsénio, A. M., Vreeburg, J. H. G., and Rietveld, L. (2013e). Index of joint condition for PVC push-fit joints (submitted). *Water Science & Technology: Water Supply*

6.1 Introduction

One way of preventing failures in drinking-water pipes and joints is through condition assessment (Chapter 3). It was demonstrated that the CCTV can deliver both accurate and reproducible results if employed in gap-sizing applications.

However, in order to accurately define a joint's condition in the field, an NDE is necessary but not sufficient. It is also necessary to have access to threshold conditions. With the exclusion of installation guidelines, parameters to define a joint's condition in the field throughout its service-life were not evident in the literature. Additionally, these installation guidelines were created to define optimal pipe-joint alignment during installation and provide no information regarding allowable bending angles throughout a pipe's lifetime. Dutch PVC pipe manufacturers define 6° as the maximum bending angle at a joint during installation (DYKA BV, 2012; Pipelife, 2001). The American Water Works Association (AWWA, 2002) defines a maximum joint angle as a function of the diameter and length of the installed pipe barrels.

However, these installation guidelines were created to define optimal pipe-joint alignment during installation and offer no information about allowable bending angles throughout a pipe's lifetime. In Chapter 5, the results of a large-scale laboratory tests with PVC pipes and joints were presented. These tests were performed in order to obtain parameters that can be employed to characterize a joint's condition in the field. It was concluded that the diameter and the level of insertion play major roles in the behavior of joints. Joints become stiffer with the increase of both parameters, an increase in stiffness is considered a risk as the joint is less able to bend, and stress subsequentely builds up in the pipe material. It was also indicated that a joint's condition should be defined utilizing two parameters including joint angle and the level of insertion of the pipe in the joint.

Therefore, this chapter presents the IJC and uses it to characterize the condition of the joints in eight pipes that were inspected for this project.

6.2 Materials & methods

6.2.1 The index for joint condition

Objectives

The IJC was developed to incur the following capacities:

1. Receive input produced by any NDE tool that follows the aforementioned inspection procedure;
2. Characterize the condition of all joints in an inspected pipe in-situ. This characterization can be performed, for example, to evaluate a contractor's work (after installation) or to assess the joints' condition of a pipe that is in use;
3. Compare results from inspections made for various PVC pipes: aid network managers in selecting the most appropriate pipes/joints for replacement/repair;

and

4. Compare results of different inspections made on the same joints at different time periods, *i.e.*, determine joint degradation rate. It should also be considered that changes to joint alignment are a result of soil movement, poor installation, operational factors (*e.g.* pressures), live-loads or a combination of these factors. Nevertheless, these phenomena are often not continuous and can be a one-time event. Therefore, several inspections of the same joint over a sufficiently long period of time would be required to establish an actual deterioration rate.

Implementation of the IJC

Following the results of Chapter 5, two important parameters are necessary to implement the IJC: the maximum joint bending angle and the width of the joint's ring that separates both pipes (Figure 2.2).

To define the maximum joint bending angle, tests with 110 mm and 315 mm pipes and joints were conducted in the laboratory (Chapter 5). Joint stiffness increased as well as at a faster pace at angles over 3° for 110 mm; 5° for 315 mm. These results are, for typical Dutch situations (10 m barrel pipes), more conservative than the limit defined by the AWWAL (34° for 110 mm; 12° for 315 mm) and close to the DML (6° for both diameters). The maximum angle for other diameters was extrapolated considering a linear relationship between maximum angle and diameter. This is similar to the approach of AWWA (2002).

As indicated in Chapter 5, the beginning of pipe-ring contact plays a role in joint behavior. The width of the ring (RW) separating both pipes inside of a joint varies with diameter and is manufacturer specific. For the PVC material employed in Chapter 5, the pipes from DN160 until DN500 have RW=8 mm.

The IJC is presented both in a graphical form (Figure 6.1) and as a grade given to inspected joints as well as to the entire pipe. The results presented in Figure 6.1 will be discussed in the next section; for now, only the framework will be addressed. Taking into consideration the double parameter, on the Y-axis, the minimum gap width (MGW), a surrogate measure for the level of insertion, is provided with - the gap at either 12 h or at 6 h. On the X-axis, the maximum bending angle measured in the joint is always at 12 h and 6 h. Field measurements demonstrate that there is increased variation of joint angles in the vertical plane than in the horizontal plane. It can be assumed that this occurs due to the effects of soil movement. As mentioned above, a negative bending angle indicates that the gap at 12 h is wider than the gap at 6 h, and it is important to define whether a bending angle is negative or positive to define the 3D alignment of the pipes.

The dashed horizontal line (MGW = 8 mm; annotated "Ring") represents the width of the joint's ring. For joints along this line, the pipes that they connect are touching the joint's ring; for joints below this line, the pipes are overlapping the ring. One vertical dashed-line is presented (Bending angle = ± 6.8°; annotated "Lab tests"). This is the maximum angle defined in Chapter 5 for this diameter (500 mm). In Figure 6.1, a joint inside the grey areas is considered at risk of leaking or fracturing.

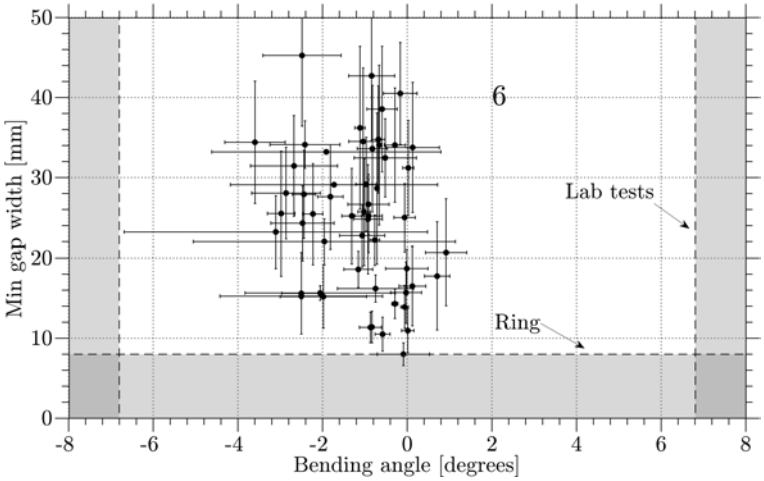

Figure 6.1: The IJC presents all of the data aggregated during a pipe inspection (500 mm). The vertical dashed line (Bending angle = ± 6.8°; annotated "Lab tests") defines the maximum angle ascertained by the laboratory tests. The dashed horizontal line (MGW = 8 mm; annotated "Ring") defines the width of the joint ring (Figure 2.2). Joints inside the grey areas (limited by the aforementioned dashed lines) are considered at risk of leaking or of fracturing. The error bars demonstrate the standard deviation of MGW and bending angle between the several repetitions of the inspection. The number 6 identifies the inspection.

Grading a pipe

Taking into consideration the location of a joint in the IJC (Figure 6.1), each joint is graded separately (joint grade). The complete pipe length is also graded by aggregating joint grades of all pipe joints within that pipe length (pipe grade). This grading procedure is similar to the process of grading distress indicators presented by Kleiner et al. (2006a). The grade of joint i (dimensionless and normalized) is presented by the summation of two factors - a higher grade identifies a joint in worst condition (Equation 6.1).

$$JG_i = \frac{1}{2} \times G1_i + \frac{1}{2} \times G2_i \tag{6.1}$$

Where $G1_i$ accounts for the angle and $G2_i$ accounts for the level of insertion. Both factors are considered to have the same weight (1/2).

The factor $G1_i$ (dimensionless) is indicated by Equation 6.2 and increases with joint angle α (Figure 3.3).

$$\begin{aligned} G1_i &= 0 && \text{if } \alpha < TA \\ G1_i &= \tfrac{\alpha}{max} && \text{if } \alpha > TA \end{aligned} \tag{6.2}$$

Where TA [°] is the maximum angle provided in Chapter 5 which depends on the joint diameter, α is the joint angle measured in the field and max [°] is the aforementioned maximum angle (= 12°). This angle was selected as it was the maximum angle tested in Chapter 5, and no higher angle has been ascertained in the field.

The value of $G2_i$ is calculated by Equation 6.3.

$$G2_i = \frac{1.1 - \frac{MGW_i}{RW_i}}{1.1} \tag{6.3}$$

Where RW_i is the width of the joint's i inner ring [mm] and MGW_i is the minimum gap width [mm] of joint i. $G2_i$ is maximum (= 1) when MGW_i=0 mm. This expression is implemented in this manner so that i) the results are dimensionless, and normalized, ii) the grade increases with the decrease of MGW_i. Overlapping pipes are assumed to be in the same condition as pipes with MGW_i=0 as the inspection procedure with the NDEs (Chapter 3) employed for this work cannot quantify the length of overlapping pipe (measure negative gaps). Since both $G1_i$ and $G2_i$ range from 0 (good condition) to 1 (worst condition), JG_i also varies in the same range.

Finally, the grade of pipe j, PG_j, is calculated by Equation 6.4.

$$PG_j = \frac{1}{3} \times \left[\sum_{i=1}^{n} \frac{1}{n} \left(G1_i + G2_i \right) \right] + \frac{1}{3} \times \left[\sum_{i=1}^{n} \frac{1}{n-1} \left(G3_{i,neg} + G3_{i,pos} \right) \right] \tag{6.4}$$

Where $G3$ is a parameter that accounts for the number of contiguous joints with α of the same sign, and n is the number of inspected joints. Each one of the three factors is considered to have the same weight (1/3). Therefore, if two consecutive joints achieve negative angles, $G3_{i,neg}$ is calculated by Equation 6.5

$$G3_{i,neg} = \frac{|\alpha_n| + |\alpha_{n+1}|}{2 \times max} \tag{6.5}$$

Where $|\alpha_n|$ and $|\alpha_{n+1}|$ are, respectively, the absolute values of the angles of contiguous joints n and n+1. A similar formula is exploited in order to calculate $G3_{i,pos}$; this parameter accounts for contiguous joints with positive α. This approach is followed because two contiguous joints with angles with the same sign are considered dangerous. For example, if the two joints are negative, the pipe buckles and the joints are sagging. Thus, both values are to quantify the situation since two contiguous joints with 1° can be considered less dangerous than two contiguous joints with 5°. The expression is divided by $2 \times max$ to obtain normalized and dimensionless results. Therefore, since all three factors range from 0 (good condition) to 1 (worst condition), PG_j also varies in the same range.

6.2.2 PVC joints inspection

Eight pipes were inspected for this project employing the CCTV system Argus 4. The CCTV was introduced in the pipe, and the gap widths at 12 h, 3 h, 6 h and 9 h were measured.

6.3 Results

In total, 222 joints in approximately 2,100 m of PVC pipe were inspected (Table 6.1, Figure 6.2). The pipe grades are depicted in Table 6.1, and the joint grades are exhibited in Figure 6.3 where the joint number is demonstrated in the X-axis, and the joint grade is given in the Y-axis. A black dot represents the grade of an inspected joint.

6.3.1 The Index for Joint Condition

As can be ascertained in Figure 6.2, the position of the dashed-horizontal line is constant because all inspected joints have RW=8 mm. The position of the vertical dashed-lines, ascertained by the laboratory tests varies between $\pm$ 4.4° for the smallest pipe (pipe 4, DN250) and $\pm$ 6.8° for the largest (pipe 6, DN500) (Table 6.1).

6.3.2 PVC joints inspection

Inspection 4 was conducted on a 2-month old pipe. All angles were close to 0° and all gaps ranged from 20 to 30 mm - small variations in α and MGW. This pipe received one of the lowest grades (3.8×10^{-2}). Nevertheless, the grade is higher than the grade of pipe 3 ($2.5 \times 10^{-}2$) that had several joints at risk. These results emphasize the significance of not relying on one parameter separately but performing a complete analysis of the IJC taking into consideration the condition of individual joints and of the entire pipe.

For inspections 1, 2, 5, and 7, several joints were at risk (inside the grey area), with inspections 1, 5, and 7 having joints with angles above the limit indicated by the destructive laboratory tests. In fact, pipes 1, 2, and 5 have the highest grades (Table 6.1). As mentioned before, the IJC allows ranking the pipes according to their condition.

Inspection 6 was conducted on a pipe that had burst in the same week. After the burst, considering that the pipe was very fragmented, it was impossible to define the cause and exact location (joint or barrel) of the burst. The pipe received a high grade (4.6×10^{-2}). This inspection is thoroughly discussed in Arsénio et al. (2012b).

The analysis of a pipe can also be made based on the condition of individual joints. For example, given the results for pipe 5, a network manager could act in different ways, either replacing/repairing the whole pipe or only the cluster of joints from 20 to joint 28 (highest grades). This last option, considering that the new joints would be installed with α=0° and MGW=25 mm (average MGW of pipe 4, newly installed), would reduce the pipe grade down from 7.3×10^{-2} (second highest) to 3.0×10^{-2} (second lowest).

The homogeneity in the gap widths for pipe 4 and the variation for the older pipes should be noted. It can be hypothesized that the alignment of the joints varies over time and that these changes might play a role in their condition. This hypothesis is made assuming that that the i) pipes are installed with aligned joints and that ii) the workmanship level of different contractors is comparable in quality.

Nevertheless, this demonstrates the importance of inspecting several pipes following installation and of inspecting the same pipe in different occasions.

The remaining pipes and joints are assumed to be in good condition.

Table 6.1: Overview all NDE field-inspections done with CCTV. TA is the maximum angle given in Chapter 5 which is a function of diameter. Pipe grade is defined by Equation 3.1 and varies between 0 (good condition) and 1 (bad condition). The grade allows ranking the pipes according to their condition.

Inspection	Access	Diameter [mm]	TA [°]	Length [m]	Joints [#]	Repetitions [#]	Grade (× 100)
1	2 m section cut	315	5	364	48		6.4
2	Flanged door	315	5	65	10	2 runs +	7.8
3	Flanged door	400	5.8	240	14	2 controls	2.5
4	Flanged door	250	4.4	200	20		3.8
5	2 m section cut	400	5.8	410	33		7.3
6	Burst point	500	6.8	510	54	1 run +	4.6
7	2 m section cut	315	5	180	21	1 control	3.1
8	2 m section cut	315	5	120	22		6.0

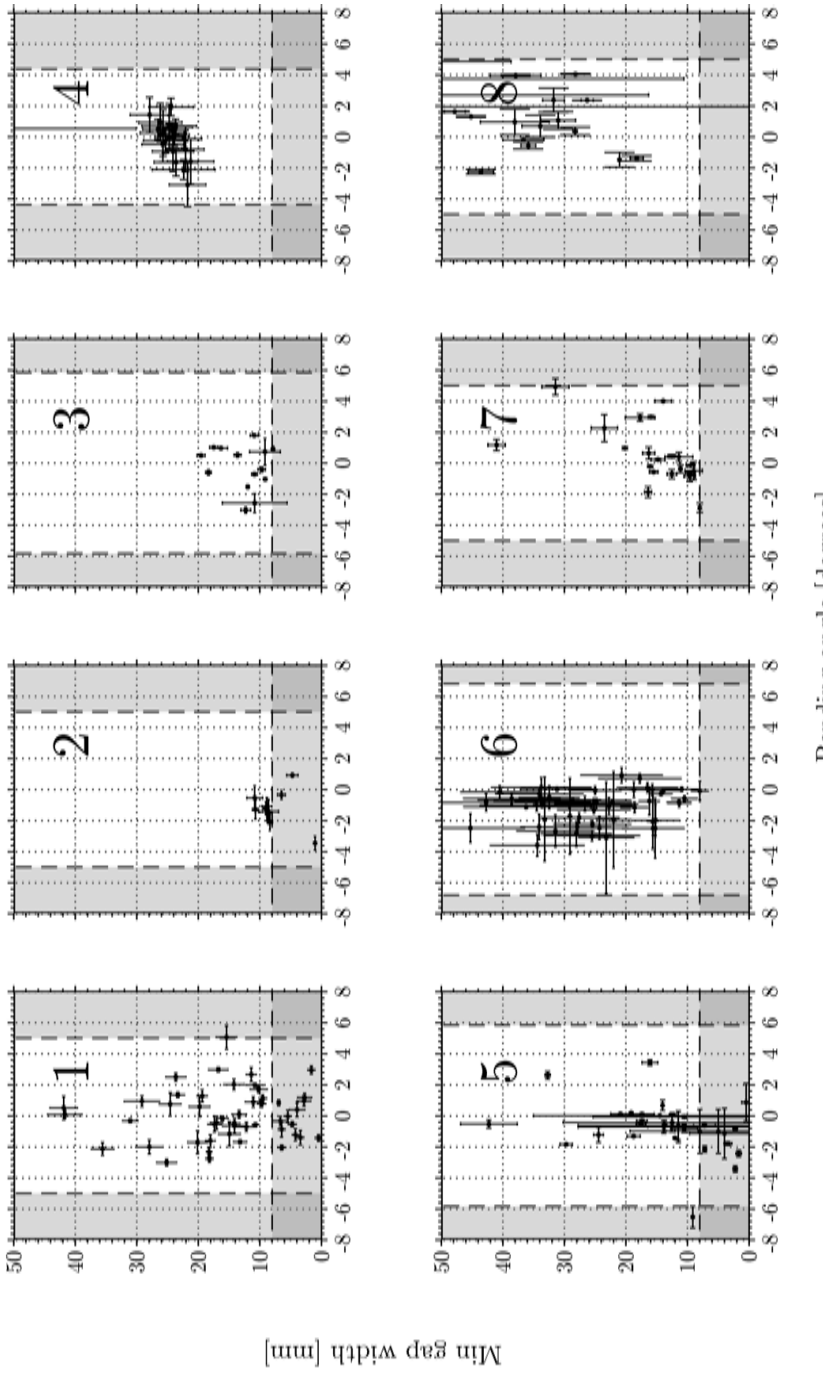

Figure 6.2: Results of the field inspections for eight inspections. A black dot identifies an inspected joint and the error bars for both the MGW and angle are given. The error bars give the standard deviation of MGW and bending angle of the several runs. Relevant information about the inspections is given in Table 6.1.

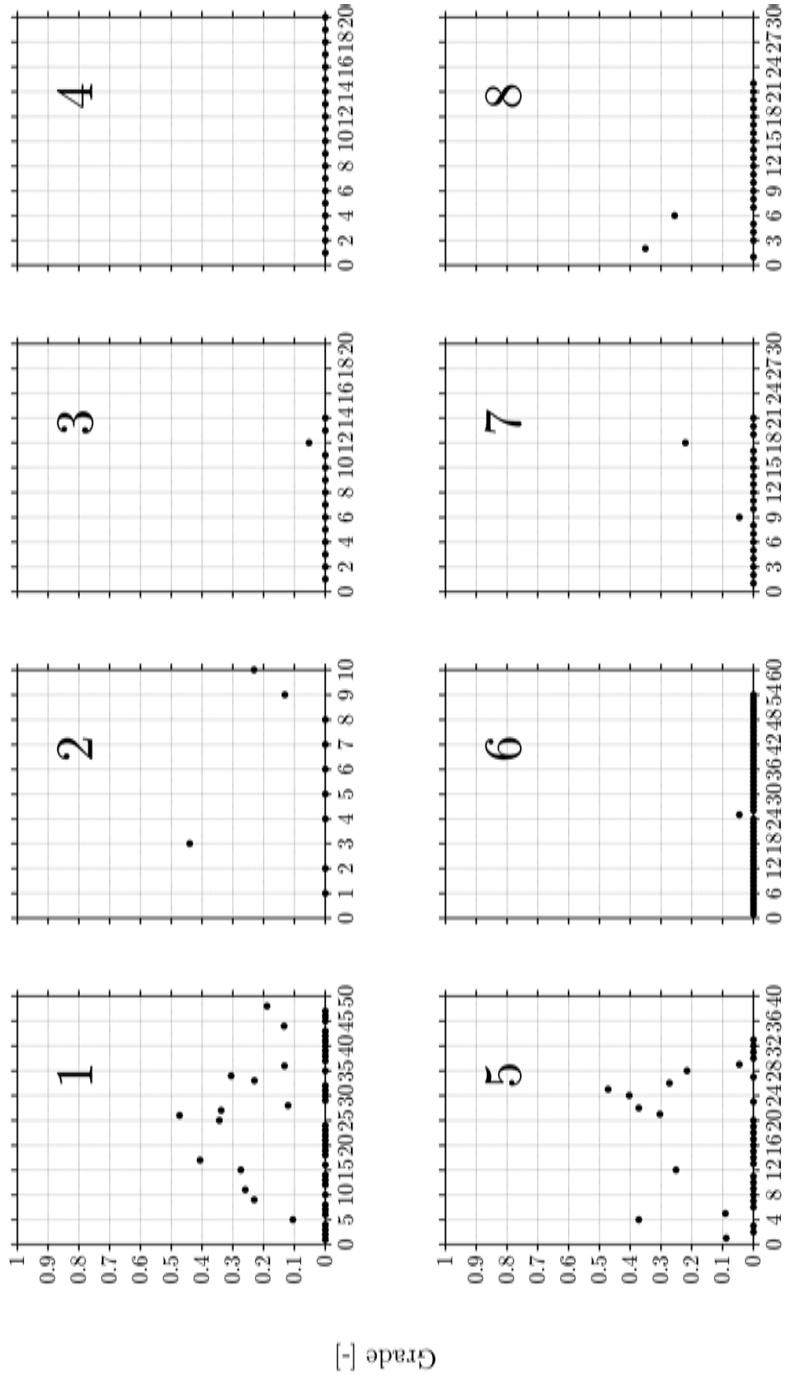

Figure 6.3: Grade of each inspected joint. A dot indicates an inspected joint.

6.4 Conclusions

The IJC has been implemented by employing installation guidelines and data from destructive laboratory tests. When using the IJC, a grade can be assigned to both the pipe and to each joint. The grade makes the results of the IJC less prone to interpretation and more reproducible.

The results demonstrated that, given the degrees of freedom in a pipe system, assessing the condition of joints cannot be performed with one parameter. For this reason, both the individual joint grades and the overall pipe grades should be analyzed in conjointly. This approach also provided a better perspective of the condition of individual joints and their role in the condition of the entire pipe.

Results of eight different CCTV inspections were presented. While a great dispersion of angle and gap values were ascertained for the older pipes, minimal dispersion was ascertained for the 2-month old. Two conclusions can be drawn from this. First, the alignment of pipes inside the joints varies throughout the years. Second, performing inspections on newly installed pipes can be utilized to assess the work of contractors following pipe installation. Furthermore, the IJC has been proven to be a powerful tool to compare the condition of different pipes. The importance of individual joint grading is demonstrated by the possibility of a network manager to perform selective repairs in certain joints in order to reduce the total pipe grade.

chapter 7

Correlating pipe failures & ground movement†

In this chapter, the approach to predict pipe failure in drinking water networks is presented. Ground movement is believed to play a crucial role in the onset of failures in underground infrastructure. In the Netherlands, due to its geological characteristics, this role is expected to be even more pronounced. This chapter demonstrates a methodology that generates a risk map for underground drinking water pipe networks employing ground movement data.

A segment of the distribution network of a Dutch drinking water company was selected as the study-area. A USTORE (Section 1.6.3) data-set for this area was obtained. The data-set was comprised of 868 failures registered throughout 40 months. The utility also supplied geographical network data. Ground movement was estimated using satellite-borne radar data.

Two types of analyzes were made: cell and pixel-based. For the cell-based analysis, AC pipes exhibited the highest failure rates. Older AC pipes were also shown to fail more often. Conversely, failure rates for PVC were the lowest of the test. For the pixel-based, analysis ground movement was also demonstrated a role in the failure of all of the materials combined.

Therefore, a risk-map for AC was generated which combined ground movement data and pipe-age data. This methodology can be a beneficial resource for the network managers for maintenance and continuous monitoring.

†This chapter is based on the following article:

Arsénio, A. M., Dheenathayalan, P., Hanssen, R., Vreeburg, J. H. G., and Rietveld, L. (2013b). Pipe failure prediction in drinking water systems using satellite observations (submitted). *Structure and Infrastructure Engineering*

7.1 Introduction

Drinking water supply networks are part of a myriad of underground infrastructures that underpin modern civilization. Much of this infrastructure is located underground, and its fate is intimately related to that of the surrounding soil (O'Rourke, 2010). A factor expected to play a role in the failure of drinking water pipes is non-uniform ground movement also indicated as differential ground movement (Budhu, 2010). In this process, ground movement creates stress on the pipe and may lead to failure. Damage to one facility (*e.g.* water main) can culminate into damage to surrounding facilities (*e.g.* gas or telecommunications) with system-wide consequences (O'Rourke, 2010).

Ground movement can be especially damaging to older pipelines (Olliff et al., 2001) and older, rigid joints (Silva et al., 2001). Hu et al. (2008) argued that changes in soil volume can induce differential ground movement that can subsequently cause the development of stresses in asbestos cement (AC) pipes. The effect of ground movement can also be potentiated in pipes whose integrity may have already been compromised by other factors, for example, chemical attacks from inside water and/or outside soils (Hu et al., 2008). According to Breen (2006), provided that PVC pipes are properly manufactured, installed, and free of scratches of more than 1 mm depth, they can endure for more than 100 years in operation. However, the same authors argued that non-uniform soil settling can cause enormous local stresses in a PVC pipe and lead to preliminary failure, and such condition can decrease the lifetime of a PVC pipe to 10 years. Dingus et al. (2002) surveyed 46 of the largest AwwaRF member utilities. For the distribution systems, according to 25% of the survey respondents, frost heave/ground motion was the number-one problem.

Folkman (2012) surveyed 188 North American utilities. According to the authors, 55.3% of respondents identified CI as the most common failing pipe material followed by AC at 17.0%. Furthermore, the utilities were asked to choose the most common type of failure in their networks, and 50% answered that circumferential crack was the main cause. In detail, the authors indicated that circumferential crack was the primary failure mode for CI, concrete, and AC. Corrosion was the primary failure mode of Ductile Iron and Steel. A longitudinal crack was the primary failure mode of PVC.

It is evident that one of the causes for circumferential breaks is longitudinal loading (Rajani and Kleiner, 2001) and that longitudinal loading can be originated by ground movement (Moser and Folkman, 2008). According to O'Rourke (2010), geohazards (*e.g.* soil subsidence, earthquakes, hurricanes) have generated substantial interest in lifeline systems (*e.g.* water, gas and telecommunications). Keeping this in mind, O'Rourke et al. (2008) examined the response of the Los Angles water supply network during the 1994 Northridge earthquake, which was the beginning point of developing a decision support model for the city's distribution network. More recently, O'Rourke (2010) expanded the previous work and analyzed and modeled the response of three North-American networks to earthquakes (San Francisco and Los Angeles), the effect of Katrina in New Orleans, and in the Mississippi river and Gulf of Mexico.

In the past centuries, the Netherlands has not been affected by earthquakes or

hurricanes. However, according to Rietveld (1984), "there is no stable rock on the surface of the country and approximately half of its surface is covered by Holocene sediments of clay, sand, and peat which attain thicknesses up to 20 m. In these areas, soil compaction can be relatively significant in relationship to the tectonic movements". Thus, in the country, the role of ground movement in failures of water pipes, as for other aspects, is expected to be noticeable.

Therefore, the objective of this chapter is twofold. The first is to study the influence of ground movement in failures occurring in a Dutch drinking water network. While failure related data is provided by a water utility, the ground movement data is obtained from satellite-borne radar surveys. The second is to, from these conclusions, create a risk map for network management. This map will assist this company in addressing potential problems created by soil-movement related failures and in pin-pointing pipes installed in risky areas. This approach is similar to those followed by O'Rourke et al. (2008) and O'Rourke (2010). Finally, the pipes installed in risky areas should be non-destructively inspected as discussed in Chapter 3.

It should be mentioned that ground movement can have several origins, for example, peat compaction, ground water level changes, and anthropogenic activities. Nevertheless, in this work, quantitatively quantifying ground movement is the main goal, not defining its origin.

7.2 Materials & methods

7.2.1 Ground movement data

Persistent scatterer points

Interferometric Synthetic Aperture Radar (InSAR) measures the change in distance between a satellite and the earth's surface over a given time frame. Given the satellite's position, changes in earth surface (ground movement) are measured along the line of sight (viewing direction) of the satellite (Hanssen, 2001). When compared to other measuring techniques, for example, leveling (Dirksen et al., 2010), InSAR possess a relatively high temporal and spatial sampling, which is a significant advantage of this technology. InSAR is also beneficial in measuring the movement of the earth's surface and modeling the signal source at a few kilometers beneath the surface (Fukushima et al., 2005; Pritchard and Simons, 2002). Therefore, it is feasible to consider that movement of the soil surface also has an effect on underground water pipes installed at depths of around 1 m, which is typical in the Netherlands.

In the late 1990s, the Persistent Scatterer Interferometry (PSI) technique was introduced to process stacks of images and extract ground movement by exploiting coherent pixels known as Persistent Scatterers (PS) points (Ferretti et al., 2001). These PS-points are usually man-made objects (*e.g.* buildings, bridges, lamp posts). In this work, PS-points are also referred to as pixels. Therefore, PSI is an opportunity based technique so the settlement estimation at any desired, specific location or object cannot be guaranteed. However, this technique provides relatively high density of such coherent pixels in urban regions and millimeter precision in surface movement estimation. In fact, the number of PS-points per square kilometers (PS

density) varies from area to area and depends on the satellite used. In general, a density from 100-1000 PS-points.km^{-2} in urban environments can be expected.

The PSI technique requires a reference in time and space to estimate ground movement. The reference in time is solved by selecting a reference image, referred to as the master image and comparing other images to the master for estimating the changes in surface. The reference in space is obtained by taking a point in the master image as a reference point. All of the estimations are then provided with a reference to this reference point, and the most stable point in the image is normally chosen as a reference point.

For this analyzes, 99 TerraSAR-X* strip-map ascending mode images of the study-area were processed employing PSI technique to estimate the ground movement rate (expressed in mm.year^{-1}) per pixel. For this satellite, a pixel, or PS-point, indicates an area of 3×3 m (approximately). The satellite data used in this work encompasses the period from February 2009 until May 2012.

Probability of differential motion

Probability of differential motion (PDM), expressed in a percentage, is defined as probability that a given PS-point experiences relative motion with respect to its surrounding PS-points (Dheenathayalan et al., 2011; Dheenathayalan and Hanssen, 2011). Thus, where ground movement is dominantly experienced (measured), PDM is a derived metric obtained from it. To calculate PDM, every PS-point is compared with the surrounding PS-points (within 200 m) to detect relative motion above a certain threshold. The value of 200 m was selected in order to guarantee enough PS-points in the vicinity. The threshold for the ground movement rate employed in this work was 1 mm.year^{-1}. This low threshold was selected to ensure that even very minimal ground movement difference between two points was detected. Therefore, by comparing a given PS-point with other neighboring PS-points, this probability of the given point experiencing relative ground movement is computed (PDM). This procedure is repeated for every PS-point so that PDM is obtained per PS.

PDM per PS-point is computed according to Dheenathayalan et al. (2011) and Dheenathayalan and Hanssen (2011). Then, following the work of Dheenathayalan and Hanssen (2013), PS-points are classified to ascertain those lying on ground surface; these represent the differential ground movement signal of the ground surface. In our study of underground water pipe network analysis, only PDM for PS-points lying on the ground surface are considered.

7.2.2 Failure registration data

The failure registration data-set consisted of 868 failures comprising all available data for this utility during this period. The exploited failure data-set encompasses the period from January 2009 until April 2012 which is consistent with the period covered by the satellite data. During this period, there was no occurrence of natural hazards (*e.g.* earthquakes or landslides). For each failure, the date, the longitude

*TerraSar-X is presented as the "most accurate high-resolution radar satellite in orbit" (Astrium, 2013).

and latitude, and the pipe material were known. These data were obtained from USTORE (Section 1.6.3). USTORE provides more relevant information, for example, regarding the origin of the failure (ground movement, inner/outer-corrosion, etc.), diameter, type of soil, or presence of trees in the vicinity. Nevertheless, the reliability of these data have not yet been assessed, hence these data were not exploited.

7.2.3 Study-area

The study-area is approximately half of the supply region of a Dutch drinking water company. The total length of network in that area is more than 4,500 km, with PVC (∼50%), AC, and cast iron (CI) (both 16%) being the most common materials. This network supplies more than 1.2 million people. This study-area was selected for the following reasons:

1. Availability of failure registration data;
2. Anticipated ground movement above the national level (Lange et al., 2012); and
3. Availability of high-resolution radar-borne satellite data.

7.2.4 Data analysis

To produce the risk-map, it is possible to follow a pixel-based approach or a cell-based approach. Each approach will now be presented and discussed. For both approaches, the available data is analyzed, and the conclusions of this analysis are used to discuss the implementation of the risk-map. Irrespective of the approach, it is expected that failure rate increases with the level of ground movement.

Pixel-based approach

This approach analyzes the vicinity (< 25 m) of PS-points. The vicinity is expected to be affected by the local differential ground movement, quantified by PDM. In the Netherlands, drinking water pipes are usually are 10 m long. Two pipes are connected with stand-alone pieces referred to as joints that feature two rubber-gaskets (Section 2.2.2). These gaskets keep the system sealed and are expected to sustain some of the ground movement. If a PS-point is located on top of a pipe, it is hypothesized that localized ground movement will impact the pipes connected to the two subsequent joints in each direction (25 m). For longer distances, the effect of ground movement will be dissipated by the joints.

Nevertheless, it is noteworthy to mention that it can be argued that ground movement may be the result of pipe failure (*e.g.* leakage) and not the cause. It cannot be, indeed, concluded what occurred first - ground movement or pipe failure. Therefore, in this work, it is assumed that ground movement is the cause of failure and not the result.

For this approach, the distribution of PDM values in the vicinity of failures will be compared with the distribution of PDM values away from failures. To produce the

risk map, detailed GIS data is required, *i.e.*, the exact coordinates of the pipe network. However, these data were not available. Thus, the analysis will be conducted, but the risk-map will not be produced.

Cell-based approach

The study-area was divided in a virtual matrix (451×320 cells). Each cell represents an area of 100×100 m. This cell size was selected to allow obtaining cells with 20-30 pixels each to allow significant results in the subsequent calculations.

It can be expected that pipes installed in different backfills will respond differently to ground movement. Nevertheless, the soil in each cell is considered to possess homogeneous characteristics. This approach was followed due to the lack of more detailed soil data; Dutch water companies do not register the characteristics of the soil where the pipes are installed. In this approach, the ground movement in a cell is hypothesized to play a role in the cell's failure rate.

All PS-points within a cell can be collectively calculated for an average PDM (Equation 7.1).

$$\overline{PDM_i} = \frac{\sum PDM_j}{n} \tag{7.1}$$

Where $\overline{PDM_i}$ is the average PDM cell i [%] $\sum PDM_j$ is the PDM of pixel j in cell i [%], and n is the number of pixels in cell i.

Furthermore, each failure was allocated to the specific cell where it occurred and the failure rate per cell was calculated using Equation 7.2

$$\lambda_{i,m} = \frac{\sum f_{i,j}}{\sum L_{i,m} \times \Delta t} \tag{7.2}$$

Where $\lambda_{i,m}$ is indicative of the failure rate [#.km^{-1}.year^{-1}] in cell i for material m; $f_{i,j}$ is the j^{th} failure in cell i; $\sum L_{i,m}$ is the pipe length [km]† of pipe material m in cell i; and Δt is the duration of the registration data [years]. This formulation for failure rate is similar to that presented in Equation 1.1 but is adapted in this instance to the cell situation. O'Rourke (2010) employs a similar parameter referred to as the repair rate [# repairs.km^{-1}]. This formulation, solely normalized in reference to network length, is of use in episodic situations such as earthquakes. However, for the long-term analysis of network performance, the normalization in respect to time becomes necessary.

The average pipe age per cell was calculated using Equation 7.3.

$$\overline{Age_{i,m}} = \frac{\sum age_{k,m} \times \sum L_{k,m}}{\sum L_{i,m}} \tag{7.3}$$

Where $\overline{Age_{i,m}}$ is the average age [years] of pipe material m in cell i; $\sum age_{k,m}$ is the average of age bin k (5-year bins) of material m; and $\sum L_{k,m}$ is the length [km] of material m of age k.

†Assuming that pipe length $\sum L_{i,m}$ did not change during Δt.

Table 7.1: Pipe length, number of failures (total and due to third party damage) and failure rate (λ) per pipe material within the study-area.

	Length [km]	Failures [#]	λ [#.km^{-1}.year^{-1}]	3rd party damage [#]
All mat	4565	868	0.060	279
PVC	2442	421	0.054	194
AC	740	235	0.10	51
CI	725	165	0.072	19

In this analysis, cells for which radar estimations are unavailable or that have no drinking water network are not considered in the analysis.

For this approach, a correlation between ground movement and pipe failures at a cell level will be researched. To produce the cell-based risk-map GIS data, as detailed as for the pixel-based analysis, is not necessary. In fact, knowing the total length of pipes and the number of failures per cell is enough. These data were available, and a risk map was produced.

7.3 Results & discussion

Exploiting satellite observations, an analysis of failures in drinking water networks will be conducted. Afterwards, based on the analysis, the risk map will be presented and analyzed.

7.3.1 Failure registration data

In the study-area AC experiences the highest failure rate followed by cast iron (CI) and, finally, PVC (Table 7.1). Subsequent analyzes were conducted without failures originated from third-party damage since, *a priori*, these failures are considered independent from ground movement. In total, 589 failures were included. Additionally, in this study, linear velocity obtained from the ground movement over the observation period was used. This signifies that the area experiencing a gradual ground movement pattern over a period is taken into consideration by itself. Thus, short and local ground movement related activities such as road work, seasonal effects, etc. are removed from our analysis.

The failure registration data-set was analyzed in order to study the existence of age-related trends in failure rate for the various pipe materials. Thus, Figure 7.1 presents the failure rate for the three materials per decade of installation. While PVC has an unexpected spike during the 1950s and CI one during the 1970s, the failure rates for both materials remain under 0.06 #.km^{-1}.year^{-1}. As a comparison, according to Kuraoka et al. (1996), a failure rate above 0.05 #.km^{-1}.year^{-1} can be considered "undesirably high". AC pipes experience the two highest failure rates (0.13 and 0.18 #.km^{-1}.year^{-1}) for pipes installed before the 1960s which indicates that these older pipes are more prone to failure than the newer ones. Throughout

the rest of the analysis, it is assumed that all of these pipes are older than 50 years. Comparable results have been presented by Vloerbergh et al. (2012) for the complete USTORE database (five Dutch water companies) for the failures registered in 2009 and 2010.

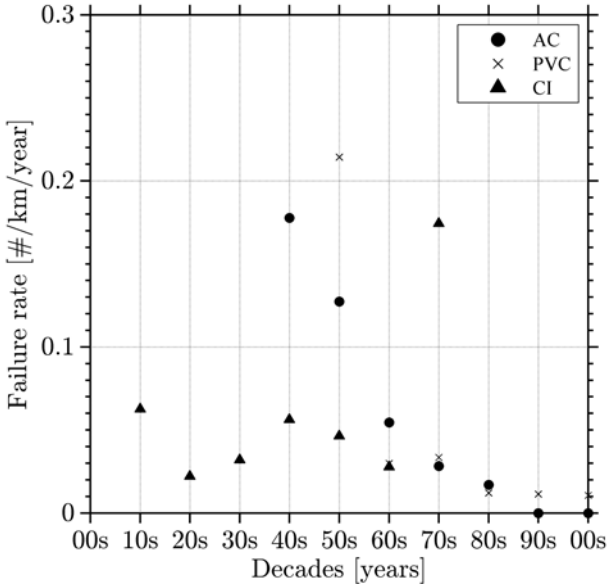

Figure 7.1: Failure rate per material and decade from 1900 until 2000.

7.3.2 Pixel-based analysis

Distribution of PDM in relation to the distance from failures

It was hypothesized that, if failures are caused due to ground movement, the distribution of PDM in the vicinity of failures (< 25 m) could be skewed to positive values (higher PDM). This analysis was conducted by including all available failures (without third-party) collectively from all materials.

A normalized histogram of the PDM for all pixels in the study-area and for the pixels in the vicinity of failures (distance < 25 m) is presented in Figure 7.2 (top and bottom). While the complete histograms are presented on the left, details of the histograms (PDM $> 50\%$) are depicted on the right.

The complete histograms show little difference between the entire area (Figure 7.2, top left) and the vicinity of failures (Figure 7.2, bottom left).

However, it is evident from the detailed histograms that, in the vicinity of failures (Figure 7.2, bottom right), there is a greater percentage of PS-points with a higher PDM (above 90%) than in the entire area (Figure 7.2, bottom left), which indicates the role of differential motion in the failures of pipes.

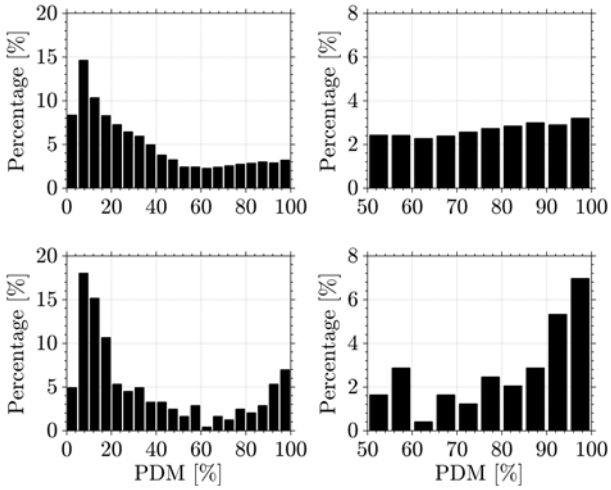

Figure 7.2: Histograms of PDM for the complete study-area and in the vicinity of registered failures (< 25 m) for all pipe materials. Top left: PDM for all pixels in the study-area. Bottom left: maximum PDM of pixels close to the failures. Top and bottom right: zoomed details of histograms on the left, presented for PDM>50%.

Risk map

Despite a trend being identified, the GIS data required to produce the risk map were not available. Thus, the pixel-based risk-map will not be produced.

7.3.3 Cell-based analysis

Analysis of PDM

Given the size of the study-area and the relative minimal number of failures, ground movement data was divided in bins. Three bins were created including low movement (LM), medium movement (MM) and high movement (HM).

A histogram of PDM per cell is illustrated in Figure 7.3. The boundaries between the bins are percentiles 33^{rd} (PDM=25.6%) and the 67^{th} (PDM=46.4%) percentiles. While LM is below PDM=25.6%, HM is above PDM=46.4%. The boundaries are represented in Figure 7.3 by dashed vertical-lines. These boundaries were selected to allow having an equal number of counts in each bin.

Age distribution

Mean age per pipe material is calculated exploiting Equation 7.3. Age distribution indicates no variation across different areas (Figure 7.4). In Figure 7.4, the error-bars represent the standard deviation of the age. For this area, PVC is the youngest material (15 years) followed by AC (45 years) and CI being the oldest (70 years).

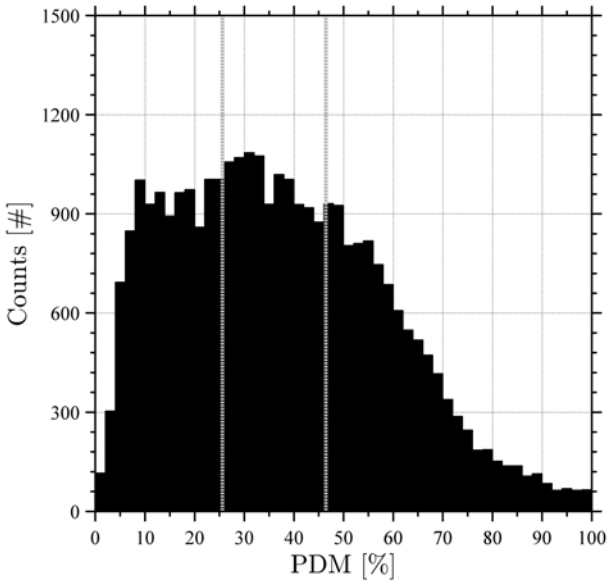

Figure 7.3: Histogram PDM. The two grey dashed vertical-lines represent the boundaries for ground movement: percentiles 33^{rd} (PDM=25.6%) and 67^{th} (PDM=46.4%). While LM is for PDM<25.6%, HM is for PDM>46.4%.

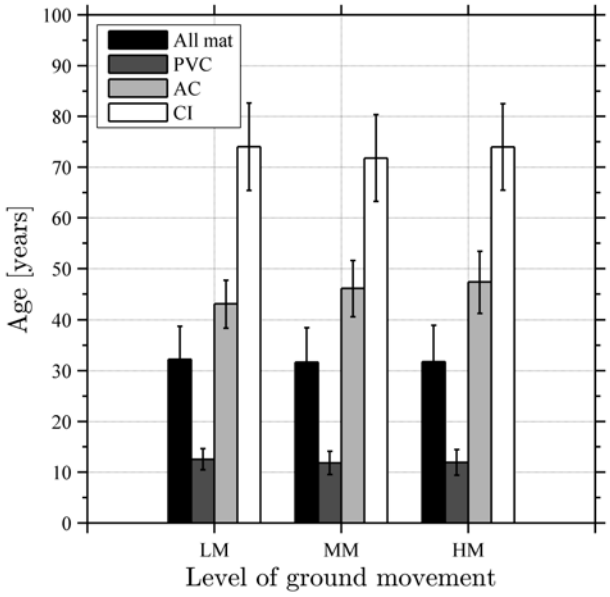

Figure 7.4: Distribution of pipe age per level of ground movement. All mat represents all materials taken as a whole. The error-bars represent the standard deviation of the age.

Length distribution

Areas with increased ground movement also have a higher percentage of PVC and lower percentages of AC and CI (Figure 7.5).

In stable areas (sand), the infrastructure was mostly installed in the late 19th Century and early 20th Century when CI was the preferred material. Due to the expansion of the population, unstable areas (peat) began to be urbanized beginning in the 1960s. Since that time, the use of PVC has been increasing among Dutch water companies (Geudens, 2012).

Given these results, it could be expected that the average pipe age in areas of HM was lower than in the other areas, which is not the case (Figure 7.4). This indicates that this water company does not use ground movement to prioritize pipe replacements.

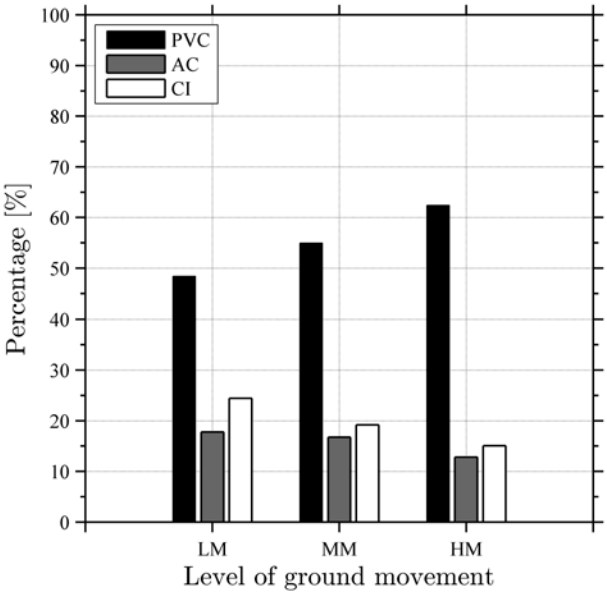

Figure 7.5: Distribution of pipe lengths per level of ground movement.

Failure rate

In Figure 7.6, the aggregated failure rate for all areas with a certain level of ground movement is plotted against level of ground movement. In Figure 7.7, the same data is presented in a scatter plot so that the slopes can be obtained. In Figure 7.7, the x-coordinates are the average between the corresponding bins. A positive slope indicates that failure rate increases with the level of ground movement. Furthermore, the material most sensitive to ground movement will also have the highest slope.

From Figure 7.6 and Figure 7.7, is it evident that PVC experiences the lowest failure rate values and is the least influenced by ground movement (slope=2.1x10^{-4}, lowest). This was expected because PVC pipes are both the youngest and the

most ductile pipes in the network. The failure rates of both CI (slope=$1.1\text{x}10^{-3}$, highest) and AC (slope=$8.5\text{x}10^{-4}$) increase with the increase of ground movement (Figure 7.7). Also, CI has the highest slope, which indicates that, in this area, CI is the most sensitive material to ground movement. Overall, the failure rates of AC are the highest in the study-area, always at least four times higher than that of PVC. Finally, no relationship between failure rate and pipe age could be ascertained since the pipe age distribution does not vary among the various areas (Figure 7.4).

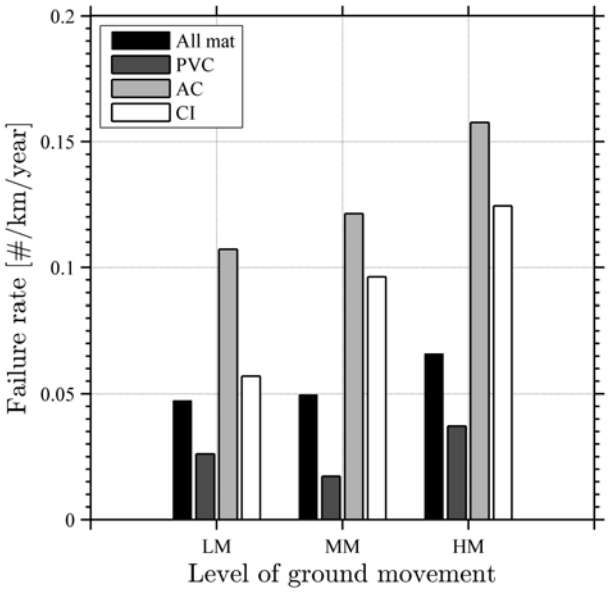

Figure 7.6: Distribution of failure rate per pipe material and per level of ground movement. All mat represents all materials taken as a whole.

Risk map

For AC pipes, two factors exhibited a role in failure: age and ground movement. On the one hand, a clear difference can be determined between the pipes older and younger than 50 years (Figure 7.1). On the other hand, the failure rate for AC pipes increases with the level of ground movement (Figures 7.6 and 7.7).

In Figure 7.8, the age distribution of AC pipes in the study-area is depicted. In Figure 7.9, the distribution of ground movement data in the study-area is demonstrated. In both figures, white indicates the nonexistence of network. While there are two clusters of older pipes, 52.02°N, 4.3°E and 52.07°N, 4.37°E (Figure 7.8), the distribution of ground movement data is random across the study-area (Figure 7.9).

Both AC pipe age and level of ground movement were employed to create an impact matrix (Table 7.2) based on the approaches described in order to produce risk matrices to manage wastewater networks Salman (2010) and was the foundation of the risk-map. For this approach, a cell is prescribed age-points and area-points; a higher grade indicates a higher risk for pipes in the cell due to ground movement.

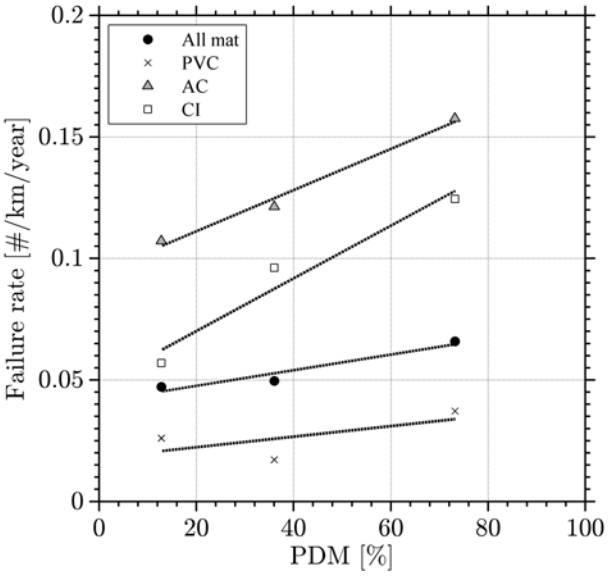

Figure 7.7: Failure rate per pipe material against PDM. All mat represents all materials taken collectively.

Thus, zero age-points were assigned to AC pipes younger than 50 years (lower probability of failure) and one age-point to AC pipes that are older (higher probability of failure). Similarly, zero area-points were assigned to pipes installed in LM areas (lower probability of failure), one area-point in MM areas (higher probability of failure), and two area-points in HM areas (highest probability of failure). The total score per cell was determined by adding the age-points and the area-points. Therefore, the lowest risk (0 points, green) was assigned to cells with the majority of young AC pipes in areas of LM and the highest risk (3 points, red) was assigned to cells with majority of old AC pipes installed in HM areas.

Using the impact matrix, the risk map was produced for AC pipes (Figure 7.10, left). To validate the assumptions of the risk-map, the distribution of failure rate in the study-area for AC pipes is depicted in Figure 7.10 (right). While, in Figure 7.10 (left), white indicates the nonexistence of pipe network and/or soil ground movement data, in Figure 7.10 (right), white indicates the absence of failures and of pipe network.

The cells that contain older pipes (Figure 7.8 in red) are also cells of higher-risk (Figure 7.10, left in red). Furthermore, the most number of failures (Figure 7.10, right) were registered inside or close to the cells of higher risk. It should be noted that there are high-risk cells without failures inside or in the vicinity. This indicates that not all high-risk areas lead to failures, but that all failures are located inside or in the vicinity of high-risk cells. Therefore, despite needing further validation, this work suggests that the areas that are presented in Figure 7.10 (left) in red, could be selected by the water utility to be inspected as discussed in Chapter 3 as they represent a greater risk for the pipes installed inside or in their vicinity.

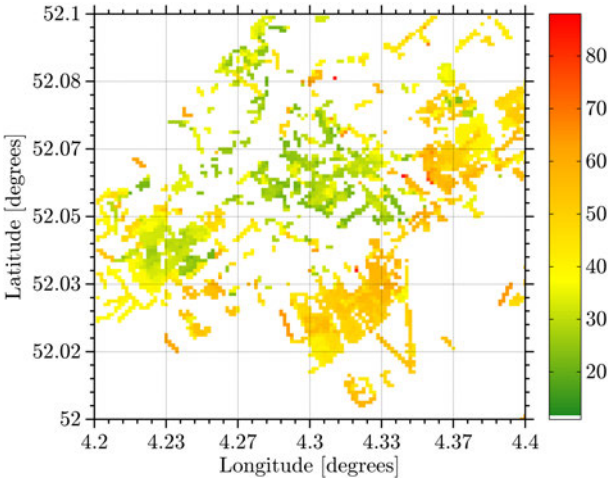

Figure 7.8: Age distribution of AC pipes in the study-area (10×10 km). The scale, illustrated in years, varies from green for cells (100×100 m) where the pipes are, in average, younger pipes until red for cells with older pipes (in average). A white dot indicates the nonexistence of AC network in that cell.

Table 7.2: Impact matrix for AC pipes created to produce the risk map. A higher grade indicates higher probability of failures. Each cell matrix is determined by adding the area-points (top) and age-points (left).

	LM	MM	HM
Young ($<$ 50 years)	0	1	2
Old ($>$ 50 years)	1	2	3

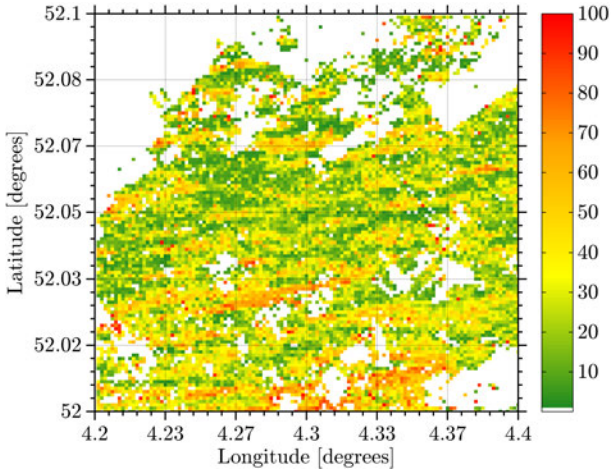

Figure 7.9: Distribution of ground movement in the study-area (10×10 *km). The scale, given in a percentage (PDM), varies from green for more stable cells (*100×100 *m) until red for more unstable cells. A white dot indicates the nonexistence of ground movement data within that cell.*

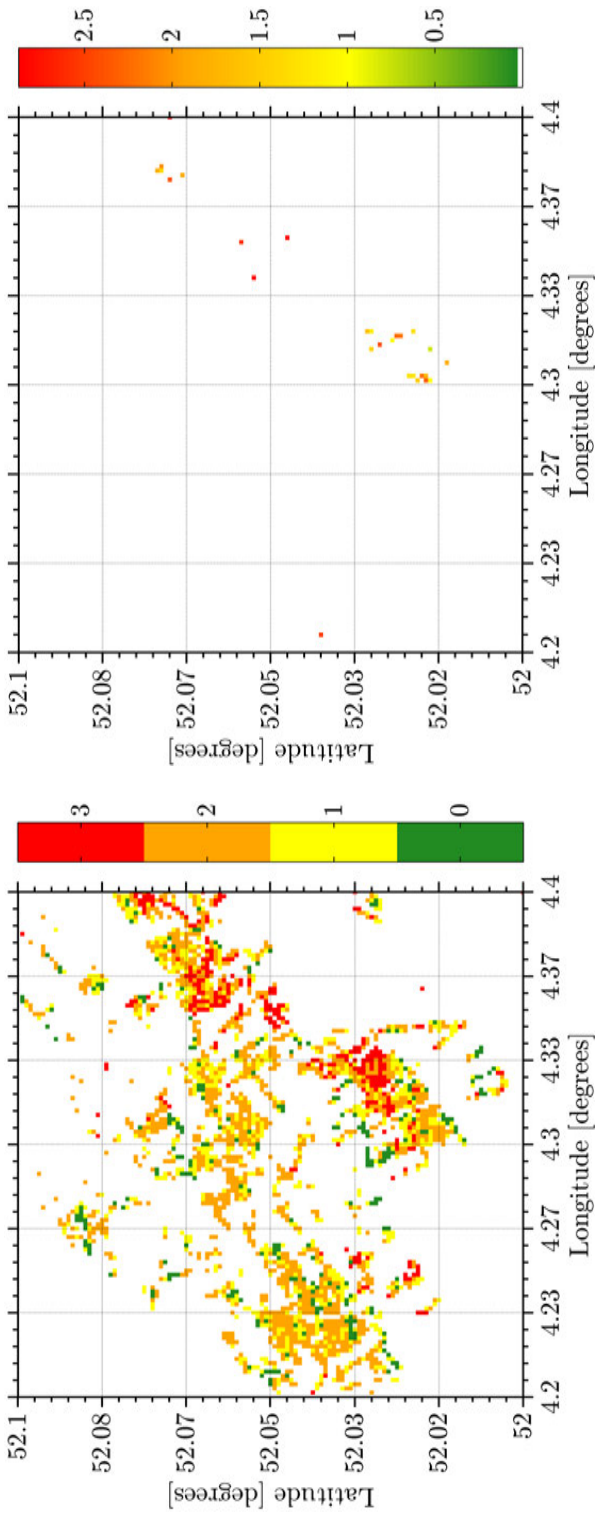

Figure 7.10: Left: risk map for AC for part of the study-area (10×10 km). The risk varies from low (green) to high (red). Right: failure rate distribution in the same area, the scale ($\#.km^{-1}.year^{-1}$) varies from green for cells with low failure rate until red for cells with higher failure rate. In both plots, a colored dot represents a cell (100×100 m) in which there is pipe network and for which ground movement data was available. A white dot indicates a cell without AC network and/or failures.

7.4 Conclusions

In this Chapter, it was hypothesized that ground movement leads to stresses on the pipes which increases the number of pipe failures. Therefore, areas with more ground movement would indicate zones that are prone to high risk for pipe failure.

The analysis of the failure registration data together with the ground movement data clearly demonstrated that the failure rate of all materials increases with the level of ground movement, this relationship being obvious for both CI and AC. Additionally, it was also demonstrated that the AC pipes installed prior to the 1960s fail more frequently than younger pipes.

For the pixel-based analysis, it was discovered that, for all materials in the vicinity of failures, there were relatively more pixels with high PDM ($> 90\%$) than for the entire study-area. This further demonstrates the role played by differential soil motion on the failures in an underground infrastructure. A cell-based risk map for AC was produced. The map takes into consideration both the age of the material and the level of ground movement in the soil where it was installed. Employing the risk map, pipes requiring urgent action could be identified and prioritized for condition assessment.

For this work, a total of 589 registered failures were exploited. More robust analysis will require having access to more failure registration data. For example, with access to more failure registration data, analysis can also focus on the impact of ground movement in smaller and larger diameter pipes. This emphasizes the significance of failure data registration and its importance for utility management.

Acknowledgement

The satellite data used was provided under the collaboration with the research that has been carried out as part of the TU Delft project "Monitoring Surface Movement in Urban Areas Using Satellite Remote Sensing" funded by Liander. The author would like to thank the German Aerospace Center (DLR) for their support in providing TerraSAR-X time-series images.

chapter 8

General conclusions

In the old city of Petra (ca. 300 BC), among the dramatic scenery, there are testimonies to the importance of drinking-water distribution for humankind where old versions of pipes are carved in the red sandstone. In other parts of the world, still standing Roman aqueducts not only pay homage to the Roman technical expertise*, but also emphasize the fact that urban development is only achievable with sustainable access to drinking water. Much of this knowledge was lost during the dark ages, and many of the techniques we recognize today had to be reinvented (Deadman, 2010). Currently, modern drinking water networks are constructed of plastic, ductile iron, or multi-layered cement, but several other materials have been used in the past (Savic and Banyard, 2011). Some of these older materials are still in use and, together, they underpin civilization.

*At its prime, the daily *per capita* water consumption in Rome, according to Brooke and Quinn (2013), exceeded 750 L, with Russo (2006) arguing that it reached almost 950 L.

8.1 Scope & objectives

In certain countries, failure related data are systematically registered. When available, these data-sets show that joints play a significant role in the failures registered in drinking water networks. This is not only the case for Dutch utilities, but also for utilities worldwide. Nevertheless, the focus of scientific literature has been centered on pipe (barrel) failure[†]. Therefore, it might be assumed that the role played by joints has been disregarded.

Additionally, joint failure plays a significant role irrespective of the material. PVC was the material of choice in this thesis due to being the most commonly employed material in the Netherlands due to its immunity to corrosion which facilitates condition assessment. Additionally, working with PVC in the laboratory does not possess the inherent safety/health risks as with, for example, AC.

Hence, the objective was to create a procedure that can be used to predict the remaining lifetime of PVC push-fit joints. This procedure was implemented in the following four main steps:

1. Definition of joint failure and characterization of the most common failure modes of joints;
2. Development of an inspection procedure to assess the condition of PVC push-fit joints in the field;
3. Selection of the most accurate and reproducible of the commercially-available, non-destructive evaluation (NDE) tools for the assessment of joints; and
4. Implementation of a lifetime prediction method to predict the failure of joints or, more realistically, a method that prioritizes the pipe/joint inspection or replacement programs within a drinking water distribution network.

Finally, one of the personal goals for the author was that this procedure "gained life", avoiding that it remained only a concept.

8.2 Failure modes of push-fit joints

Joint failure is the main focus of this work, and defining failure was one of the first goals. In this work, failure is defined as leakage: a joint fails when it begins leaking. Therefore, failure is easy to detect once it occurs; for example, there is a leak, and water is visible at the ground level. However, not all appurtenances fail in the same way, and not all materials fail in the same way. Additionally, characterizing the condition before failure, in particular, non-destructively, is not unambiguous. Thus, a component of this work was initially dedicated to define joint failure and to characterize different failure modes. From a literature review, seven failure modes for push-fit joints were derived:

- Joint bending;

[†]Typical examples are the physical based models that predict corrosion growth in metallic pipes.

- Horizontal displacement;
- Pipe bending;
- Vertical displacement;
- Axial displacement;
- Torsion by slight rotation/vibration; and
- Pipe ovalization.

All of these failure modes failures are mechanical and material independent. In this work, failures due to physical/chemical changes in PVC (*e.g.* embrittlement) are not considered. This choice was made because it was noticed that the characterization of PVC's physical/chemical condition is difficult to achieve non-destructively in the field. Therefore, the focus was on the alignment of the pipes inside the joints to characterize joint mechanical failures.

Of the aforementioned failure modes, the most significant for PVC push-fit are joint bending and axial pull-out. Despite pipe bending and pipe ovalization being related to joint failure, they are not intrinsic to the joint. In spite of this, both failure modes can be derived from the assessment of the joint's condition. It was discovered during the field inspections (Chapter 3) that lateral movement is minimal when compared to vertical movement and, therefore, horizontal displacement is negligible. PVC joints, due to not being fixed to the pipes (*e.g.* glued), can be considered immune to torsion[‡].

The connection between these failure modes and the joint alignment was the beginning point in implementing the non-destructive assessment procedure.

8.3 Condition assessment of PVC push-fit joints

8.3.1 Inspection method

For this approach, the alignment of both pipes inside the joint is assumed to be a surrogate measurement for the condition. Further clarified, when two pipes are connected with a double-socket PVC joint (Section 2.2.2), the two pipes are separated - a gap exists between them. Therefore, the alignment of a joint can be determined if this gap is measured at four different locations: 3 h (springline), 6 h (invert), 9 h (springline) and 12 h (crown). Two angles are calculated, one for the 12h-6h pair of gap values and a second for the 9h-3h pair (Equation 3.1). While the pair 12h-6h characterizes how well the pipe fits on a horizontal plane, the pair 9h-3h does the same for a vertical plane. All aforementioned failure modes can be detected employing this approach[§].

[‡]There are mechanically restrained PVC joints (*trekvast*, in Dutch). Nevertheless, these are only used in very specific situations and are not considered here.

[§]Except for torsion by slight rotation/vibration, which is not a relevant failure mode for PVC push-fit joints.

8.3.2 Non-destructive evaluation equipment

Given that alignment was the measurement of interest, it was necessary to select the best tool to characterize a joint's alignment. It was also realized from the beginning that this required having direct access to the joint. On-ground tools are usually exploited to detect pipes but not inspect to them; these tools also have limited image resolution that is insufficient for the aforementioned application (Liu and Kleiner, 2012). In this aspect, two options are possible. The inspection can either be on-pipe (on the pipe surface) on in-pipe (inside the pipe). On-pipe condition assessment requires uncovering the pipe, and this is an expensive and, sometimes, impractical operation. Thus, it was decided to pursue the in-pipe approach which solely requires an entry point[¶] and the flushing and disinfection of the pipe following the inspection.

It is important to state that it was never the objective of this work to project and/or build a new inspection tool. The tool would be purchased/rented from a commercial partner and employed for the purpose in mind, *i.e.*, the non-destructive evaluation of push-fit joints.

Several tools were surveyed, and the three most promising were selected to be tested in the laboratory. The tools were narrowed down to visual and ultrasound, which are typically presented as being applicable to inspect polymeric pipes. Two visual tools were selected (CCTV and Panoramo®) and were rented from the Dutch company MJ Oomen. The ultrasound equipment was rented from Applus RTD, also Dutch. Panoramo® was abandoned after the laboratory tests as the tool failed to deliver both accurate and reproducible results and struggled to produce a clear image under water due to the reflection of light on the suspended matter. The ultrasound was then discarded after the field test due to the difficulties in data interpretation, data loss, and lack of a gyroscope - throughout the inspection it was not possible to determine which ultrasound probe was facing down or up. Nevertheless, it must be mentioned that these problems with the ultrasound are not intrinsic to ultrasound itself, but to the specific ultrasound that was tested in the work. Of the three tools, the CCTV was consistently the best, delivering both accurate and reproducible results, therefore being the chosen tool to size the gaps in PVC joints. This happened in spite of CCTV being presented by different authors as "prone to interpretation". This part of the work demonstrated that CCTV can deliver the accuracy and the reproducibility necessary if employed for gap sizing.

8.4 Real-time pipe monitoring

This segment of the work was projected as an alternative to inspections employing NDEs in the case of important assets that i) present a high failure-risk[‖] and/or ii) cannot be inspected due to the intrusive nature of condition assessment.

[¶]Ultrasound requires not only a dedicated launching/entry point but also a dedicated exit.

[‖]A classical Dutch example would be a pipe installed in a dyke or, more commonly, a pipe installed adjacent to a highway.

A PVC 250 mm drinking water pipe supplying water to approximately 1,250 customers was continuously monitored from September 2011 until June 2013. The aggregated data encapsulates the strain registered on pipes and joints; the temperature registered next to these appurtenances (in the ground); and the strain registered on coupons of PVC isolated and also installed also next to the pipe.

The data exhibit an expected positive correlation between temperature and strain on PVC, which was expected. Daily water demand patterns could be detected with the strain gauges connected to the pipes and joints. Two confirmed episodes of water-hammer were also detected by the sensors. This demonstrates the accuracy of the strain gauges that were utilized and their potential in detecting dynamic loads that can be risky for a pipe.

The work also demonstrated that, from the beginning of the monitoring period until the coldest period for which data are available, the pipe contracted more than 5 mm at each end due to temperature changes. During the period of June-September, the temperature can exceed the installation temperature. At that time, contact points (pipe-pipe and pipe-joint) can begin if one considers that the pipes were installed fully inserted inside the joints. This emphasizes the significance of registering the water temperature (inside the pipe) during a non-destructive assessment. In addition to this, the results also demonstrate that a joint that is considered to be in a risky situation during winter (after inspection), for example, with both pipes almost contacting, can be in an even riskier situation during summer upon pipe expansion. This work also demonstrates that a pipe can be continuously monitored for expansion/contraction when other assessment methods are not available.

Nevertheless, some of the project practicalities were evident from early on as more than half of the sensors stopped working. Most sensors stopped working during a cold period registered throughout February 2012 when the maximum air temperature did not rise above 0 °C for more than two weeks. During this period, the batteries also became depleted. When new batteries were installed, some of the sensors were inoperative. Two strain gauges also became inoperative following an episode of water-hammer. This further emphasizes that, although such a set-up can produce beneficial and valuable data, its complexity is also its *Achilles' heel*. Therefore, when projecting such a set-up, this should be taken into consideration.

8.5 Destructive laboratory tests with PVC pipes & joints

At this point, the link between the failure modes and the condition assessment procedure was not evident. To characterize the present condition of an asset, one needs to know its threshold condition: it is only possible to say that something is in "good" condition if it is known what the "bad" condition is. Additionally, if a certain angle is obtained after a pipe inspection, one can wonder whether that is extreme or not and whether the same angle value is problematic in every situation, for example, does the maximum bending angle depend on the diameter?

To accomplish this, destructive laboratory tests with PVC pipes and joints were

conducted. The tests were planned in order to characterize the condition of joints, keeping in mind the failure modes described above. These tests were performed together with DYKA, a Dutch PVC pipe manufacturer. Pipes and joints of two diameters were tested - 110 and 315 mm. The material was tested under two different conditions - water pressure (4 bar, absolute) and air sub-pressure (0.2 bar, absolute). Both joint bending and axial pull-out tests were performed. To monitor the behavior of the joint, its stiffness was monitored in real-time using a force sensor.

Several conclusions were obtained from this component of the work. First, joint stiffness increases with bending angle, insertion, diameter, and pressure. An increase in stiffness is considered dangerous as the joint becomes less able to bend. The tests also demonstrated that the stiffness does not increase linearly with the bending angle (for the same diameter and pressure). The joint becomes stiffer after a threshold angle: 3° for 110 mm and 5° for 315 mm joints. These results are, for 10 m barrel pipes, more conservative than the limit defined by the AWWAL (34° for 110 mm; 12° for 315 mm) and close to the limit defined by the Dutch PVC manufacturers: 6° for both diameters.

Second, the significance of not installing pipes completely inside the joints cannot be stressed enough. The difference in joint behavior is obvious if the pipes are completely inserted or inserted half-way between the joint's center and the rubber gasket**.

Finally, for PVC joints, leakage through the rubber-gasket is generally dependent upon the condition of the rubber. For a rubber ring in good condition, leakage/intrusion can only be expected at bending angles above 10° and for complete pull-out of the pipe from the joint. Such extreme angles were never detected in the field (Section 3).

8.6 The index for joint condition

Now that the failure modes had been described (it was known what to "look" for), an inspection procedure was available (it was known what to "look" with) and the threshold conditions (the limits) were known, it was necessary to develop a framework that allowed presenting the results of pipe inspections in a straightforward, reproducible, and comparable way.

This was the reasoning behind the development of the Index for Joint Condition (IJC). The IJC was projected in order to be able to quantitatively characterize the joints' condition. Preferably, this framework should be usable *in-situ*. The IJC was developed utilizing installation guidelines and data from the aforementioned destructive laboratory tests. The IJC allows grading both the entire pipe and each joint separately which makes the results less prone to interpretation.

The results demonstrated that, given the degrees of freedom in a pipe system, assessing the condition of joints cannot be accomplished with one parameter. For

**As often happens in science, this last discovery, although not the primary objective of the tests, was surely one of the most relevant for the utilities and for the people in the field.

this reason, both the individual joint grades and the overall pipe grades should be adjacently analyzed. This approach also provided a better perspective of the condition of individual joints in their role in the condition of the entire pipe.

The field inspections clearly demonstrated that, first, the alignment of pipes inside the joints varies throughout the years. Second, performing inspections on newly installed pipes can be exploited in order to assess the work of contractors following pipe installation. Furthermore, the IJC is proven to be a powerful tool to compare the condition of various pipes. Finally, the importance of individual joint grading is demonstrated by the possibility of a network manager to perform selective repairs in some joints in order to reduce the total pipe grade.

8.7 Correlating pipe failures and soil movement

This was the last step in the work. Having selected the most accurate and reproducible NDE and having implemented the inspection and the data-analysis procedure (IJC), a method to prioritize pipes for inspection was not evident. It is known that soil movement is a problem in the Netherlands. On the other hand, it is believed that there is a relationship between soil movement and failures in underground infrastructures. Nevertheless, to the knowledge of the author, an investigation of the impact of soil movement in the occurrence of failures in drinking water networks has never been attempted. Thus, this was the beginning point of employing failure registration and ground movement data to prioritize pipe inspections; certain pipes installed in ground-movement prone areas are priority.

Failure registration data was aggregated from the Dutch MFD, USTORE (Section 1.6.3). These data were exploited collectively with empirical ground movement data measured by colleagues at TU Delft. The failure registration data encompassed a period of 40 months during which 868 failures were registered. The results clearly demonstrated that the failure rates for PVC, CI, and AC increase with the level of soil movement. For the study-area, while CI in the material is most affected by soil movement, AC has the greatest failure rates. What is more, there is a clear increase in failure rate in the AC pipes installed prior to and after the 1960s.

These conclusions were the beginning point in creating a risk map for the study-area. This map pin-points areas inside the distribution network that are expected to be more failure-prone. These riskier areas should either be inspected more often (pro-active on-condition AM) or replaced more often (pro-active hard-time AM). Either way, this map will aid water companies in managing their networks more efficiently.

As aforementioned, AC not only has the greatest failure rates but also an age related-failure pattern that was not detected either in PVC or CI. For this reason, AC was the selected material in order to produce the risk map. This decision was made in spite of PVC being the material of interest in the present work and, therefore, a comment must be made. First, the inspection procedure described in this work can be applied to any other pipe material as long as there is a gap between the pipes. Second, to characterize the condition of AC pipes requires only having access to

laboratory data characterizing AC joints' threshold conditions similar to the data obtained for PVC joints.

8.8 Concluding remarks, implementation & future prospects

8.8.1 Concluding remarks

The objectives of this work that have largely been accomplished include:

- The failure modes of push-fit joints have been surveyed and presented in detail;
- An inspection procedure has been developed. It is considered that the geometrical alignment of the pipes inside the joints is a surrogate measurement for joint condition. The geometrical alignment can be obtained with an NDE tool;
- The most accurate and reproducible NDE tool (CCTV) for inspection of PVC push-fit joints has been ascertained and fully characterized;
- The results of various inspections can be presented and compared side-by-side by employing the IJC. The IJC can aid the water companies in selecting those pipes needing the soonest replacement;
- Employing the risk map, risk-prone areas inside drinking water networks can be identified, and the inspection/replacement of these pipes can be prioritized; and
- The final result is a procedure that can be used to predict the remaining lifetime of PVC joints.

8.8.2 Implementation of the lifetime prediction procedure

At a utility level, this procedure can be implemented in four steps.

1. First step: selecting the best candidate pipes for condition assessment. To begin employing the procedure, a utility must have access to data allowing the selection of the best candidate pipes for inspection[††]. For this first step, the utility must have access to failure registration data (Section 1.6). If the utility is also provided access to soil movement data, a risk map (Chapter 7) can be implemented. In the case that soil movement data are not available, the utility can select the best candidate pipes solely based on failure registration data. The utility can further narrow down the best candidate by performing a risk-based analysis where both of the probability of failure and the expected cost of failure (Kleiner et al., 2009) are obtained by using, for example, GIS.

[††]It is impossible to expect all pipes belonging to a utility to be inspected - selecting a few is the only practical option.

2. Second step: inspecting the joints. Probably only part of the best candidate pipes can be inspected either due to time or financial constraints. Exploiting an NDE[‡‡] and following the procedure described in Chapter 3, the joints can be inspected.
3. Third step: evaluating the joints' condition. The condition of the joints can be evaluated employing the IJC (Chapter 6). The IJC allows detecting the most relevant failure modes as described in Chapter 2. The results produced with the IJC support the water utility with their decision of whether to replace the entire pipe or only part of it.
4. Fourth and final step: re-starting the process. The lifetime prediction procedure is iterative, and the same joints can[§§] be inspected several times throughout their lifetime. When the results of the *third step* are available, an evaluation of the procedure can be made: is it actually pin-pointing joints that are in poor condition?

8.8.3 Future prospects

Many questions arise before, during, and after a Ph.D. project, and some of them remain unanswered. The following points are potential research subjects for the future:

- Study threshold conditions for other materials and other types of joints:
  - Determine the threshold conditions for other pipe materials, for example, AC. For this, destructive laboratory tests with AC, similar to the ones presented here for PVC, would have to be performed. This would allow extending the lifetime prediction procedure to other materials.
  - Restrained joints (*trekvast*, in Dutch) are employed in very specific situations, for example, to join pipe barrels 20 m before and after 90° elbows. Due to being restrained, these joints are expected to behave differently and to withstand different loads. Therefore, it would be necessary to characterize the threshold condition of these joints in order to extend the assessment/characterization procedure.
- Development of NDE tools that can be exploited for an application of gap sizing but also others: detection of leaching is AC, corrosion in metallic pipes and aging/embrittlement in PVC pipes. This can be imagined as the *perfect tool* which might be difficult to achieve. Nevertheless, the work developed at University of Twente (Demcenko et al., 2012a,b) aiming at characterizing the physical aging of PVC with an ultrasound seems to indicate that, given commercial interest, it might be possible to develop an NDE that can assess more aspects of pipe and joint condition.

[‡‡]The selected NDE can either be a CCTV or another tool that can also deliver accurate and reproducible results

[§§]From a scientific perspective, it can be argued that the same pipes and joints (*e.g.* a test installation) should be inspected several times throughout a survey period of 5-10 years.

- Reliability of USTORE database:
  - The present work exploited data retrieved from USTORE database. Nevertheless, the reliability of the registered data has never been investigated. In order to validate research produced with the database, it is of the utmost importance to study the significance of the registration procedure through tests made to the pipe-fitters. This will demonstrate how reliable each registration is.
  - In USTORE, the location of a failure can be reported (*e.g.* pipe, joint, valve, etc.). An investigation is also necessary on how reliable these definitions are.
- This work demonstrated that the CCTV can be employed to assess the condition of pipes in the field and provide both accurate and reproducible results. Therefore, the feasibility of implementing a CCTV inspection as a standard inspection method to evaluate a contractor's work should be studied. This application would even minimize the problems associated with a CCTV inspection, *i.e.*, the need to flush and to disinfect, since these steps are standard before a newly installed pipe can be used for the first time. Additionally, beginning seasonal (once/twice per year) inspections on the same pipe would elucidate on the long term behavior of underground pipes.
- The condition of the rubber o-ring is also expected to play a role in the behavior of joints throughout their lifetime, and this topic was thoroughly discussed by Warnock (1999) in his Ph.D. thesis. According to the author, until the development of synthetic rubber, the joint's o-rings were made of natural rubber. Natural rubber not only ages but can also degrade with the action of micro-organisms. Both of these factors lead to a decrease in the sealing capacities of the joint (Warnock, 1999). Synthetic rubbers, even being immune to biodegradation, also suffer aging and, accordingly, a decrease in sealing capacities. Furthermore, the presence of impurities (*e.g.* sand from the backfill) creates an abrasion effect that diminishes the sealing capacities of the rubber ring. Nevertheless, to the author's knowledge, no NDE tool, either commercially available or in R&D phase, has the capacity to assess the condition of the rubber o-rings *in-situ*.

André Marques Arsénio
Utrecht, November 7, 2013

Bibliography

Andrews, M. E. (1998). Large diameter sewer condition assessment using combined sonar and CCTV equipment. In *APWA International Public Works Congress, NRCC/CPWA Seminar Series Innovations in Urban Infrastructures*, pages 91–103, Las Vegas (Nevada, USA).

Arai, Y., Koizumi, A., Inakazu, T., Watanabe, H., and Fujiwara, M. (2010). Study on failure rate analysis for water distribution pipelines. *Journal of Water Supply: Research and Technology-AQUA*, 59(6-7):429–435.

Arsénio, A. M., Bouma, F., Vreeburg, J. H. G., and Rietveld, L. (2013a). Characterization of PVC joints' behaviour during variable loading laboratory tests (submitted). *Urban Water Journal*.

Arsénio, A. M., Dheenathayalan, P., Hanssen, R., Vreeburg, J. H. G., and Rietveld, L. (2013b). Pipe failure prediction in drinking water systems using satellite observations (submitted). *Structure and Infrastructure Engineering*.

Arsénio, A. M., Pieterse-Quirijns, E. J., and Vreeburg, J. H. G. (2009a). Failure mechanisms of joints in water distribution networks and its application on asset management. In *Leading Edge on Strategic Asset Management (LESAM)*, Miami (Florida, USA).

Arsénio, A. M., Pieterse-Quirijns, I., Vreeburg, J. H. G., de Bont, R., and Rietveld, L. (2013c). Failure mechanisms and condition assessment of PVC push-fit joints in drinking water networks. *Journal of Water Supply: Research and Technology-AQUA*, 62(2):78.

Arsénio, A. M., Vreeburg, J., and Rietveld, L. (2013d). Quantitative non-destructive evaluation of push-fit joints. *Urban Water Journal*, pages 1–11.

Arsénio, A. M., Vreeburg, J. H. G., Bouma, F., and van Dijk, H. (2012a). Destructive laboratory tests with PVC push-fit joints. In *Water Distribution Systems Analysis (WDSA)*, Adelaide (Australia).

Arsénio, A. M., Vreeburg, J. H. G., de Bont, R., and van Dijk, H. (2011). Real-life inline inspection of PVC push-fit joints using NDE equipment. In *Leading Edge on Strategic Asset Management (LESAM)*, Mülheim an der Ruhr (Germany).

Arsénio, A. M., Vreeburg, J. H. G., de Bont, R., and van Dijk, H. (2012b). Real-life inline inspection of buried PVC push-fit joints. *Water Asset Management International*, 8(2):30–32.

Arsénio, A. M., Vreeburg, J. H. G., Pieterse-Quirijns, E. J., and Rosenthal, L. (2009b). Overview of failure mechanism of joints in water distribution networks. In Boxall, J. and Maksimović, C., editors, *Computing and Control in the Water Industry (CCWI)*, pages 607–612, Sheffield (UK). CRC Press.

Arsénio, A. M., Vreeburg, J. H. G., and Rietveld, L. (2013e). Index of joint condition for PVC push-fit joints (submitted). *Water Science & Technology: Water Supply*.

Arsénio, A. M., Vreeburg, J. H. G., van Doornik, J., Dijkstra, L., and van Dijk, H. (2010). Assessment of PVC Joints Using Ultrasound. In *Water Distribution Systems Analysis (WDSA)*, Tucson (Arizona, USA). ASCE.

Arsénio, A. M., Vreeburg, J. H. G., Wielinga, M. P. C., and van Dijk, H. (2012c). Continuous assessment of a drinking water PVC pipe. In *Water Distribution Systems Analysis (WDSA)*, Adelaide (Australia).

Asnaashari, A., Mcbean, E. A., Gharabaghi, B., and Tutt, D. (2013). Forecasting watermain failure using artificial neural network modelling. *Canadian Water Resources Journal*, 38(1):24–33.

Astrium (2013). TerraSAR-X Radar Satellite Imagery. Available from: http://www.astrium-geo.com/terrasar-x/.

AWWA (2002). *PVC pipe - Design and Installation. Manual of Water Supply Practices M23*. AWWA.

Bailey, M. and Kaufmann, C. (2006). Failure Analysis of PVC Pipe Joint Separations. *Materials Science and Technology - Association for Iron and Steel Technology*, 1:165–176.

Bernstein, H. M. and Laquidara-Carr, D. (2013). Water Infrastructure Asset Management: Adopting Best Practices to Enable Better Investments. Technical report, McGraw Hill Construction, Bedford.

Beuken, R. H. S., de Kater, H., Postmus, E. P., and Mesman, G. A. M. (2011). In-line inspection techniques for water mains put into perspective. In *Leading Edge on Strategic Asset Management (LESAM)*, Mülheim an der Ruhr (Germany).

Boersma, A. (2002). Long term performance prediction of existing PVC water distribution systems I. Literature study on relevant parameters. Technical report, TNO, Eindhoven (The Netherlands).

Boersma, A. and Breen, J. (2003). Long term performance prediction of existing PVC water distribution systems - V. Experiments and procedures. Technical report, TNO, Eindhoven (The Netherlands).

Boersma, A. and Breen, J. (2006). Long-term performance prediction of existing PVC water distribution systems - VII. Theory and modelling. Technical report, TNO, Eindhoven.

Breen, J. (2005). Long term performance prediction of existing PVC water distribution systems - VI. Evaluation and recommendation for extended validation. Technical report, TNO, Eindhoven (The Netherlands).

Breen, J. (2006). Expected lifetime of existing PVC water systems - Summary. Technical report, TNO, Eindhoven.

Breen, J., Boersma, A., Slaats, P. G. G., and Vreeburg, J. H. G. (2004). Long term performance prediction of existing PVC water distribution systems. In *XII Plastic Pipes conference*, Milan, Italy.

Breen, J. and Etsu, S. (2003). Long term performance prediction of existing PVC water distribution systems III. Physical properties of aged PVC. Technical report, TNO, Eindhoven (The Netherlands).

Brooke, K. L. and Quinn, Z. G. (2013). Aqueducts of Rome, Italy. Available from: http://blogs.umb.edu/buildingtheworld/waterworks/aqueducts-of-rome-italy/.

Buco, J., Emeriault, F., and Kastner, R. (2008a). 3D numerical analyses of the soil variability impact on longitudinal behaviour of buried pipes. In *International Association for Computer Methods and Advances in Geomechanics (IACMAG)*, Goa (India).

Buco, J., Emeriault, F., and Kastner, R. (2008b). Full-Scale Experimental Determination of Concrete Pipe Joint Behavior and Its Modeling. *Journal of Infrastructure Systems*, 14(3):230.

Budhu, M. (2010). *Soil Mechanics and Foundations*. John Wiley & Sons, Inc., 3rd edition.

Burn, S., Davis, P., Schiller, T., Tiganis, B., Tjandraatmadja, G., Candy, M., Gould, S., Sadler, P., and Whittle, A. K. (2005). *Long-term performance prediction for PVC pipes*. AwwaRF.

Chan, D., Gallage, C., Gould, S., Kodikara, J., Bouazza, A., and Cull, J. (2009). Field Instrumentation of a Water reticulation pipe buried in reactive soil. In *Ozwater'09: Australia's National Water Conference and Exhibition*, Melbourne (Australia).

Chan, D., Kodikara, J. K., Gould, S., Ranjith, P. G., Choi, X. S. K., and Davis, P. (2007). Data analysis and laboratory investigation of the behaviour of pipes buried in reactive clay. In *Common Ground Proceedings - 10th Australia New Zealand Conference on Geomechanics*, pages 206–211, Brisbane (Australia).

Cima, J. and Peters, D. (2009). *National Sewers and water mains failure database - Report Ref. No. 08/RG/05/26*. UKWIR, London.

Corder, G. W. and Foreman, D. I. (2009). *Nonparametric Statistics for Non-Statisticians: A Step-By-Step Approach*. Wiley.

Costello, S., Chapman, D., Rogers, C., and Mietje, N. (2007). Underground asset location and condition assessment technologies. *Tunnelling and Underground Space Technology*, 22(5-6):524–542.

Davis, P., Burn, S., Moglia, M., and Gould, S. (2007). A physical probabilistic model to predict failure rates in buried PVC pipelines. *Reliability Engineering & System Safety*, 92(9):1258–1266.

Deadman, C. (2010). *Strategic Asset Management: The Quest For Utility Excellence*. Troubador Publishing.

Demcenko, A., Akkerman, R., Nagy, P., and Loendersloot, R. (2012a). Non-collinear wave mixing for non-linear ultrasonic detection of physical ageing in PVC. *NDT & E International*, 49:34–39.

Demcenko, A., Ravanan, M., Visser, H., Loendersloot, R., and Akkerman, R. (2012b). Investigation of PVC physical ageing in field test specimens using ultrasonic and dielectric measurements. In *IEEE international ultrasonics symposium (IUS)*, Dresden (Germany).

Demma, A., Cawley, P., Lowe, M., Roosenbrand, A., and Pavlakovic, B. (2004). The reflection of guided waves from notches in pipes: a guide for interpreting corrosion measurements. *NDT & E International*, 37(3):167–180.

Devarajan, S., Miller, M. J., and Swanson, E. V. (2002). Goals for Development: History, Prospects and Costs. Technical report, The World Bank, Washington (DC, USA).

Dheenathayalan, P., Cuenca, M. C., and Hanssen, R. (2011). Different approaches for PSI target characterization for monitoring urban infrastructure. In *8th International Workshop on Advances in the Science and Applications of SAR Interferometry "FRINGE 2011"*, Frascati (Italy).

Dheenathayalan, P. and Hanssen, R. (2011). Target characterization and interpretation of deformation using persistent scatterer interferometry and polarimetry. In *5th International Workshop on Science and Applications of SAR Polarimetry and Polarimetric interferometry "POLInSAR 2001"*, Frascati (Italy).

Dheenathayalan, P. and Hanssen, R. F. (2013). Radar target type classification and validation. In *IEEE International Geoscience and Remote Sensing Symposium*, Melbourne (Australia).

Dingus, M., Haven, J., and Austin, R. (2002). *Nondestructive, noninvasive assessment of underground pipelines*. AwwaRF, Denver (USA).

Dirksen, J. (2013). *Monitoring ground settlement to guide sewer asset management*. Ph.d., TU Delft (Delft).

Dirksen, J., Clemens, F. H., Korving, H., Cherqui, F., Le Gauffre, P., Ertl, T., Plihal, H., Müller, K., and Snaterse, C. T. (2013). The consistency of visual sewer inspection data. *Structure and Infrastructure Engineering*, 9(3):214–228.

Dirksen, J., Veldhuis, J. A. E. T., Clemens, F. H. L. R., and Baars, E. J. (2010). Sensible sewer system rehabilitation using information on sewer system settlement. In *Novatech 2010*, pages 1–9.

Doleac, M. L., Lackey, S. L., and Bratton, G. (1980). Prediction of time-to-failure for buried cast-iron pipe. In *Proceedings of the Annual Conference of the American Water Works Association*, pages 31–38, Denver (USA).

DYKA BV (2012). Price list March 2012 (in Dutch). Technical report, DYKA BV, Steenwijk.

Edwards, R. (2010). *Asset Management - Whole-life Management of Physical Assets*. ICE Publishing, London (UK).

Eiswirth, M., Frey, C., Herbst, J., Jacubasch, A., Held, I., Heske, C., Kramp, J., Munser, R., and Wolf, L. (2001). Sewer assessment by multi-sensor systems. In *IWA World Water Congress*.

EPA (2002). The Clean Water and Drinking Water Infrastructure Gap Analysis. Technical report, US EPA.

Farley, M., Trow, S., and Lossleakage, D. W. (2003). *Losses in Water Distribution Networks - A Practitioner's Guide to Assessment, Monitoring and Control*. IWA Publishing, London.

Farley, M., Wyeth, G., Ghazali, Z. B. M., Istandar, A., and Singh, S. (2008). The Manager' s Non-Revenue Water Handbook. Technical report, USAID and Ranhill Utilities Berhad, Bangkok (Thailand).

Feeney, C. S., Thayer, S., Bonomo, M., and Martel, K. (2009). Condition Assessment of Wastewater Collection Systems. Technical Report May, US EPA, Washington, DC (USA).

Ferretti, A., Prati, C., and Rocca, F. (2001). Permanent scatterers in SAR interferometry. *IEEE Transactions on Geoscience and Remote Sensing*, 39(1):8–20.

Folkman, S. (2012). Water main breaks rates in the USA and Canada: a comprehensive study. Technical report, Utah State University Buried Structures Laboratory.

Fukushima, Y., Cayol, V., and Durand, P. (2005). Finding realistic dike models from interferometric synthetic aperture radar data: The February 2000 eruption at Piton de la Fournaise. *Journal of Geophysical Research*, 110(B3):B03206. Available from: http://doi.wiley.com/10.1029/2004JB003268.

Gaewski, P. E. and Blaha, F. J. (2007). Analysis of Total Cost of Large Diameter Pipe Failures. Technical report, AwwaRF.

Gallage, C. P. K., Chan, D., Gould, S., and Kodikara, J. (2009). Behaviour of an in-service Cast Iron water reticulation pipe buried in expansive soil. In *Ozwater'09: Australia's National Water Conference and Exhibition*.

Gallage, C. P. K., Kodikara, J., and Chan, D. (2011). Response of a plastic pipe buried in expansive clay. *Proceedings of the ICE - Geotechnical Engineering*, 165(1):45–57.

Gallage, C. P. K., Kodikara, J. K., Chan, D., and Davis, P. (2008). A comparison of the results of the numerical analysis and the physical behavior of a pipe buried in reactive clay. In *International Association for Computer Methods and Advances in Geomechanics (IACMAG)*, Goa (India).

Geudens, P. (2012). Dutch Drinking Water Statistics 2012. Technical report, VEWIN, Rijswijk (The Netherlands).

Grigg, N. S. (2006). Condition Assessment of Water Distribution Pipes. *Journal of Infrastructure Systems*, 12(3):147.

Grigg, N. S. (2009). National Mains Failure Database Project. In *World Environmental and Water Resources Congress*, pages 694–699, Kansas City (Missouri, USA).

Grigg, N. S. (2013). *Personal Communication*. Colorado State University.

Hanssen, R. F. (2001). *Radar Interferometry: Data Interpretation and Error Analysis. Vol. 2*. Kluwer Academic Publishers, Dordrecht.

Hellier, C. J. and English, T. (2001). *Handbook of Nondestructive Evaluation*. McGraw-Hill.

Herz, R. K. (1996). Aging processes and rehabilitation needs of drinking water distribution networks. *Journal of Water Supply: Research and Technology-AQUA*, 45:221–231.

Hodgins, M. (2013). *Personal communication*. Water Research Foundation.

Howard, A. K. (1977). Modulus of Soil Reaction Values for Buried Flexible Pipe. *Journal of the Geotechnical Engineering Division*, 103(GT1):33–43.

Hu, Y., Vu, H. Q., and Lotfian, K. (2008). Instrumentation of asbestos cement pipe in expansive soil. In *American Society of Civil Engineering International Pipelines Conference*, pages 1–10, Atlanta (Georgia, USA).

Hudson, W. R., Haas, R., and Uddin, W. (1997). *Infrastructure management: Design, construction, maintenance, rehabilitation, renovation*. McGraw-Hill, New York.

IAM (2012). Asset Management - an anatomy v1.1. Technical Report February, The Institute of Asset Management, Bristol (UK).

IBAK (2012). Inspection systems. Available from: http://www.ibak.de/.

IJkdijk (2009). Press release: Dike breaches predictable thanks to sensor systems. Available from: http://www.ijkdijk.nl/en/experiments/piping.

ISO 13783 (1997). Plastics piping systems - Unplasticized PVC end-load-bearing double-socket joints - Test method for leak tightness and strength while subjected to bending and internal pressure.

Jeyapalan, J. K. and Abdel-Magid, B. M. (1987). Longitudinal stresses and strains in design of RPM pipes. *Journal of Transport Engineering*, 113(3):315–331.

Kirby, R., van der Walt, T., Abbott, D., Jones, P., and Stewart, D. (2006). International Infrastructure Management. Technical report, NAMS Group Ltd.

Kirkham, R., Kearney, P. D., Rogers, K. J., and Mashford, J. (2000). PIRAT - A System for Quantitative Sewer Pipe Assessment. *The International Journal of Robotics Research*, 19(11):1033–1053.

KIWA (2007). Piping systems of PVC for the transport of drinking water and raw water. Technical report, KIWA, Rijswijk.

Kleiner, Y. and Rajani, B. (2001). Comprehensive review of structural deterioration of water mains: statistical models. *Urban Water*, 3:131–150.

Kleiner, Y. and Rajani, B. (2008). Prioritising individual water mains for renewal. In *World Environmental and Water Resources Congress*, pages 1–10, Honolulu (Hawaii, US). ASCE/EWRI.

Kleiner, Y., Rajani, B., and Sadiq, R. (2009). Drinking Water Infrastructure Assessment: The National Research Council of Canada Perspective. *World Environmental and Water Resources Congress 2009: Great Rivers*, pages 67–67.

Kleiner, Y., Rajani, B., and Wang, S. (2007). Consideration of static and dynamic effects to plan water main renewal. In *Middle East Water 2007, 4th International Exhibition and Conference for Water Technology*, pages 1–13, Manama, Bahrain.

Kleiner, Y., Sadiq, R., and Rajani, B. (2006a). Modeling Deterioration and Managing Failure Risk of Buried Critical Infrastructure. In *Building Science Insight*.

Kleiner, Y., Sadiq, R., and Rajani, B. (2006b). Modelling the deterioration of buried infrastructure as a fuzzy Markov process. *Water Supply Research and Technology - AQUA*, 55(2):67–80.

KNMI (2012). Hourly weather data in the Netherlands (in Dutch). Available from: http://www.knmi.nl/klimatologie/uurgegevens/#no.

Kuraoka, S., Rajani, B., and Zhan, C. (1996). Pipe-soil Interaction Analysis of Field Tests of Buried PVC Pipe. *Journal of Infrastructure Systems*, 2(4):162–170.

Lange, G. D. (2003). *Long term performance prediction of existing PVC water distribution systems - IV. Literature study on external load factors*. Netherlands Institute of Applied Geosciences TNO, Utrecht (The Netherlands).

Lange, G. D., Bakr, M., Gunnink, J. L., and Huisman, D. J. (2012). A predictive Map of Compression-Sensitivity of the Dutch Archaeological Soil Archive. *Conservation and Management of Archaeological Sites*, 14(1-4):284–293.

Liu, Z. and Kleiner, Y. (2012). State of the art review of inspection technologies for condition assessment of water pipes. *Measurement*, 46(1):1–15.

Liu, Z., Kleiner, Y., Rajani, B., Wang, L., and Condit, W. (2012). Condition Assessment Technologies for Water Transmission and Distribution Systems. Technical report, US EPA, Cincinnati (US), US EPA.

Mackellar, S. (2006). UKWIR National Mains Failure Database. In *International Conference of Plastics Pipes XIII*, Washington (DC, USA).

Mackellar, S. and Pearson, D. (2003). Nationally Agred Failure Data and Analysis Metholody for Water Mains. Volume 1: Overviw and Finding. Rep. No. 03/RG/05/7. Technical report, UKWIR, London (UK).

Maierhofer, C. (2003). Nondestructive Evaluation of Concrete Infrastructure with Ground Penetrating Radar. *Journal of Materials in Civil Engineering*, 15(3):287.

Makar, J. M. (1999). Diagnostic techniques for sewer systems. *Journal of Infrastructure Systems*, 5(2):69–78.

Makar, J. M. and Kleiner, Y. (2000). Maintaining water pipeline integrity. In *AWWA Infrastructure Conference and Exhibition*, Baltimore (Maryland, US).

Marlow, D., Davis, P., Trans, D., Beale, D., and Burn, S. (2009). Remaining Asset Life: A State of the Art Review. Technical report, WERF, Alexandria (US).

Meijering, T. G., Wolters, M., and Hermkens, R. J. M. (2004). The durability of a low-pressure gas distribution system of ductile PVC. In *Plastics Pipes XII*, Milan (Italy).

Mesman, G. and Wielen, J. V. D. (2005). Georadar: adequate to assess the condition of AC pipes? (in Dutch). Technical report, Kiwa Water Research, Nieuwegein.

Methods, H., Walski, T. M., Chase, D. V., Savic, D. A., Grayman, W., Beckwith, S., and Koelle, E. (2003). *Advanced Water Distribution Modelling and Management*. Haestad Methods.

Misiunas, D. (2005). *Failure Monitoring and Asset Condition Assessment in Water Supply Systems*. Ph.d., Lund University (Lund).

Moglia, M., Davis, P., and Burn, S. (2008). Strong exploration of a cast iron pipe failure model. *Reliability Engineering & System Safety*, 93(6):885–896.

Moser, A. P. and Folkman, S. (2008). *Buried Pipe Design*. McGraw-Hill Professional, 3 edition.

Najjaran, H., Sadiq, R., and Rajani, B. (2004). Modeling pipe deterioration using soil properties - an application of fuzzy logic expert sytem. In *ASCE International Conference on Pipeline Engineering and Construction*, pages 1–10, San Diego (California, US).

NETTWORK (2002). Trenchless Technology Network Underground Mapping, Pipeline Location Technology and Condition Assessment. Technical Report March, Centre, The University Of Birmingham Infrastructure Engineering And Management Research, Birmingham.

NRC-CNRC (1997). Acquisition of Field Data on the Performance of Buried PVC Pipes - Thermal Performance of Trench Backfills and Mechanical Performance of Buried PVC Water Mains for 1993-96. Technical report, NRC-NCRC.

Ofwat (2007). International comparison of water and sewerage service 2007 report. Technical report, OFWAT.

Olliff, J. L., Rolfe, S. J., Wijeyesekera, D. C., and Reginold, J. T. (2001). Soil-Structure-Pipe Interaction with Particular Reference to Ground Movement Induced Failures. In *Proceedings of Plastic Pipes XI*, pages 1127–1140, Munich (Germany).

O'Rourke, T. (2010). Geohazards and large, geographically distributed systems. *Géotechnique*, 60(7):505–543.

O'Rourke, T. and Trautmann, C. (1980). Analytical modeling of buried pipeline response to permanent earthquake displacements. Technical report, Cornell University, School of Civil and Environmental Engineering, Ithaca (NY, USA).

O'Rourke, T. D., Jezerski, J. M., Olson, N. a., Bonneau, a. L., Palmer, M. C., Stewart, H. E., O'Rourke, M. J., and Abdoun, T. (2008). Geotechnics of Pipeline System Response to Earthquakes. In *Geotechnical Earthquake Engineering and Soil Dynamics IV*, pages 1–38, Reston, VA. American Society of Civil Engineers.

Parker, J. (2010). Assets in the developing world. *Assets*, (November):14–15.

PBL (2007). Correction wording flood risks for the Netherlands in IPCC report. Available from: http://www.pbl.nl/en/dossiers/Climatechange/content/correction-wording-flood-risks.

Pipelife (2001). Technical documentation for PVC pressure networks (in Dutch). Technical report, Pipelife, Enkhuizen.

Prior, J. (1935). Investigation of bell and spigot joints in cast-iron water pipes. Part I-Pullout strength. Part II-Bell strength. Part III-Harness strength.". Technical report, College of Engineering, Ohio State University, Columbus (OI, USA).

Pritchard, M. E. and Simons, M. (2002). A satellite geodetic survey of large-scale deformation of volcanic centres in the central Andes. *Nature*, 418(6894):167–71. Available from: http://www.ncbi.nlm.nih.gov/pubmed/12110886.

Rajani, B. and Abdel-akher, A. (2013). Performance of Cast-Iron-Pipe Bell-Spigot Joints Subjected to Overburden Pressure and Ground Movement. *Journal of Pipeline Systems Engineering and Practice*, 4(2):98–114.

Rajani, B. and Kleiner, Y. (2001). Comprehensive review of structural deterioration of water mains: physically based models. *Urban Water*, 3:151–164.

Rajani, B. and Kleiner, Y. (2002). Towards pro-active rehabilitation planning of water supply systems. In *International Conference on Computer Rehabilitation of Water Networks CARE-W*, pages 29–38, Dresden (Germany).

Rajani, B. and Kleiner, Y. (2004). Non-destructive inspection techniques to determine structural distress indicators in water mains. In *Evaluation and Control of Water Loss in Urban Water Networks*, pages 1–20, Valencia, Spain.

Rajani, B. and Kuraoka, S. (1995). Field Performance of PVC Water Mains Buried in Different Backfills. In *International Conference on Advances in Underground Pipeline Engineering II*, pages 138–149, New York (NY, USA). NRC, ASCE.

Rajani, B., McDonald, S., and Félio, G. (1993). Water Mains Break Data on Different Pipe Materials for 1992 and 1993 (A-7019.1 Final). Technical report, NRC-CNRC, Ottawa (Ontario, Canada).

Rajani, B. and Tesfamariam, S. (2004). Uncoupled axial, flexural, and circumferential pipe-soil interaction analyses of partially supported jointed water mains. *Canadian Geotechnical Journal*, 1010:997–1010.

Rajani, B. and Zhan, C. (1996). On the estimation of frost loads. *Canadian Geotechnical Journal*, 33:629–641.

Rajani, B., Zhan, C., and Kuraoka, S. (1996). Pipe-soil interaction analysis of jointed water mains. *Canadian Geotechnical Journal*, 33:393–404.

Rajeev, P. and Kodikara, J. (2011). Numerical analysis of an experimental pipe buried in swelling soil. *Computers and Geotechnics*, 38(7):897–904.

Rajeev, P., Kodikara, J., Chiu, W. K., and Kuen, T. (2013). Distributed Optical Fibre Sensors and their Applications in Pipeline Monitoring. *Key Engineering Materials*, 558:424–434.

Randall-Smith, M., Russell, A., and Oliphant, R. (1992). Guidance manual for the Research, structural condition assessment of the trunk mains. Technical report, Water Research Centre, Swindon (UK).

Reed, C., Robinson, A. J., and Smart, D. (2006). *Potential techniques for the assessment of joints in water distribution pipelines*. AwwaRF, Denver (USA).

Reissner, E. (1959). On Final Bending of Pressurized Tubes. *Journal of Applied Mechanics*, pages 386–392.

Rietveld, H. (1984). Land subsidence in The Netherlands. In Johnson, A. I., Carbognin, L., and Ubertini, L., editors, *Proceedings of the Third International Symposium on Land Subsidence*, pages 455–464, Venice (Italy). IAHS.

Russo, R. (2006). Aqueduct Architecture: Moving Water to the Masses in Ancient Rome. Available from: http://www.yale.edu/ynhti/curriculum/units/2006/4/06.04.04.x.html.

Salman, B. (2010). *Infrastructure Management and Deterioration Risk Assessment of Wastewater Collection Systems*. Ph.d., University of Cincinnati.

Savic, D. A. and Banyard, J. K. (2011). *Water Distribution Systems*. Thomas Telford Ltd, 1st edition.

Scarino, J. H. (1981). Buried pipelines: providing flexibility at structures. *Transportation Engineering Journal*, 108(TE3):267–281.

Sellmeijer, H., López, J. d. l. C., van Beek, V. M., and Knoeff, H. (2012). Fine-tuning of the backward erosion piping model through small-scale, medium-scale and IJkdijk experiments. *European Journal of Environmental and Civil Engineering*, 15(8):1139–1158.

Selvadurai, A. P. S., Hu, J., and Konuk, I. (1999). Computational modelling of frost heave induced soil-pipeline interaction II. Modelling of experiments at the Caen test facility. *Cold Regions Science and Technology*, 29(3):229–257.

Sepehr, K. (1994). Frost protection of buried PVC water mains in western Canada. *Canadian Geotechnical Journal*, 31(4):491–501.

Shamir, U. and Howard, C. (1979). Analytic approach to scheduling pipe replacement. *Journal of American Water Works Association*, 71(5):248–258.

Silva, D. D., Burn, L. S., and Eiswirth, M. (2001). Joints in Water Supply and Sewer Pipelines: An Australian Perspective. In *Wagga Wagga*.

Singhal, A. C. (1984). Mechanical Characteristics of Pipeline Joints. In *ASME Pressure Vessel and Piping Conference*, San Antonio, Texas, USA.

Slaats, P. G. G., Mesman, G. A. M., Rosenthal, L. P. M., and Brink, H. (2004). Tools to monitor corrosion of cement-containing water mains. *Water science and technology*, 49(2):33–39.

Smolders, S., Verhoest, L., De Gueldre, G., and Van De Steene, B. (2009). Inspection of deteriorating asbestos cement force mains with georadar technique. *Water science and technology*, 60(4):995–1001.

Stiglitz, J. E. and Bilmes, L. (2008). *The Three Trillion Dollar War*. W. W. Norton.

Tabesh, M., Soltani, J., Farmani, R., and Savic, D. (2009). Assessing pipe failure rate and mechanical reliability of water distribution networks using data-driven modeling. *Journal of Hydroinformatics*, 11(1):1–17.

Tan, R. Y. and Yang, C. H. (1988). Structural responses of underground pipelines to dynamic loadings. *Mechanics of Structures and Machines*, 16(1):103–122.

UKWIR (2006). A comparison of leakage practice and leakage levels in UK and Netherlands (Rep. ref. no. 06/WM/08/34). Technical report, UKWIR.

UKWIR (2008). National sewers and water mains failure database water data protocol. Technical Report 1, UKWIR.

Van, M. A., Zwanenburg, C., Koelewijn, A. R., and Lottum, H. V. (2009). Evaluation of Full Scale Levee Stability Tests at Booneschans and Corresponding Centrifuge Tests. In M. Hamza et al., editor, *17th International Conference on Soil Mechanics and Geotechnical Engineering*, pages 2048–2051.

van der Helm, A. (2007). *Integrated modeling of ozonation for optimization of drinking water treatment*. Ph.d., TU Delft (Delft).

Vangdal, A. C., Reksten, K., Saegrov, S., and Ugarelli, R. (2011). Experience from inspection of water pipes - hard fact based AM - opportunities and consequences. In *Leading Edge on Strategic Asset Management (LESAM)*, Mülheim an der Ruhr (Germany).

Visconti, L. (1963). Il gattopardo.

Visser, R. (2009). *Residual lifetime assessment of uPVC gas pipes*. Ph.d., University of Twente.

Vloerbergh, I. N. and Blokker, E. J. M. (2010). Sharing failure data to gain insight into network deterioration. *Water Asset Management International*, 6(2):9–14.

Vloerbergh, I. N., Schipdam, R., van Thienen, P., and Beuken, R. (2012). Pipe fitters assist to predict investment needs for water main. *Water Asset Management International*, 8(3):12–18.

Vreeburg, J. H. G. (2007). *Discolouration in drinking water systems: a particular approach*. Ph.d., TU Delft (Delft), Delft.

Warnock, J. S. (1999). *A study of the factors influencing mechanical joint performance in water pipelines*. Ph.d., Imperial College of Science, Technology and Medicine.

Zhan, C., Goodrich, L., and Rajani, B. (1995). Thermal Performance of Trench Backfills for Buried Water Mains. In Jeyapalan, J. K. and Jeyapalan, M., editors, *Advances in Underground Pipeline Engineering II*, pages 650–661, New York (NY, USA). ASCE.

Glossary

List of symbols & notations

Below follows a list of the most frequently used symbols and notations in this thesis.

Parameter	Definition	Units
α	Joint angle	[°]
$\lvert\alpha_n\rvert$	Absolute value of α of the n^{th} joint	[°]
Ai	Inner-pipe cross-section area	[m^2]
b	Pipe barrel length	[m]
DML	Dutch Manufacturers' Limit	[°]
Do	Outside pipe diameter	[mm]
DI	Inside pipe diameter	[mm]
DN	Nominal diameter	[mm]
ϵ	Strain	[-]
$\bar{\epsilon}$	Average strain	[-]
$\bar{\epsilon}_i$	Strain recorded at position i	[-]
f	Recorded number of failures	[#]
$\vec{F_i}$	Internal force	[N]
$\vec{F_{iy}}$	Component in y of the internal force	[N]
$\vec{F_r}$	Rolling resistance force	[N]
$G1_i$	Parameter that accounts for angle of joint i	[-]
$G2$	Parameter that accounts for MGW of joint i	[-]
$G3$	Parameter that accounts for the number of joints in a row with angle of the same signal	[-]

List of symbols & notations (contd.)

Parameter	Definition	Units
g	Standard gravity	[m/s^2]
h	Displacement recorded by the LVDT	[m]
λ	Failure rate	[#/km/year]
$\sum L$	Pipe network length	[km]
L	Distance between the rotation points and the lip of the pipe inside the joint	[m]
m	Number of laboratory tests	[-]
MGW	Minimum gap width	[mm]
M_{total}	Water mass + structure mass	[kg]
M_{water}	Total mass of water inside the pipes	[kg]
M_{frame}	Mass of the bending frame	[kg]
$M_{PVC\ pipes}$	Total mass of PVC pipes	[kg]
$M_{PVC\ joint}$	Mass of the joints	[kg]
n	Number of joints in pipe j	[#]
N	Normal force	[N]
P	Inner pipe pressure	[Pa]
PG_j	Grade of pipe j	[-]
RW	Width of the joint's inner ring	[mm]
S	Second moment of area	[m^4]
$tests$	Maximum α given by the laboratory tests	[°]
Δt	Period of observation	[years]
$\overline{T}$	Average temperature	[°C]
T_i	Temperature recorded at position i	[°C]
$12h$	Pipe crown	[-]
$3h$	Springline	[-]
$6h$	Pipe invert	[-]
$9h$	Springline	[-]

List of abbreviations

The following abbreviations are used in this thesis:

AC	Asbestos cement
AM	Asset management
AWWAL	American Water Works Association Limit
CCTV	Closed-circuit television
CI	Cast iron
DI	Ductile iron
GPR	Ground-penetrating radar
IJC	Index for joint condition
LVDT	Linear variable differential transformer
MSS	Multi-sensor system
(N)MFD	(National) mains failure database
NDE	Non-destructive evaluation
PE	Polyethylene
RMSE	Root mean squared error
ROV	Remotely operated vehicle
(u)PVC	(Unplasticized) polyvinyl chloride
2D	Two dimensional
3D	Three dimensional

List of publications

Peer-reviewed journals

- Arsénio, A. M., Vreeburg, J. H. G., de Bont, R., and van Dijk, H. (2012b). Real-life inline inspection of buried PVC push-fit joints. *Water Asset Management International*, 8(2):30–32

- Arsénio, A. M., Pieterse-Quirijns, I., Vreeburg, J. H. G., de Bont, R., and Rietveld, L. (2013c). Failure mechanisms and condition assessment of PVC push-fit joints in drinking water networks. *Journal of Water Supply: Research and Technology-AQUA*, 62(2):78

- Arsénio, A. M., Vreeburg, J., and Rietveld, L. (2013d). Quantitative non-destructive evaluation of push-fit joints. *Urban Water Journal*, pages 1–11

- Arsénio, A. M., Bouma, F., Vreeburg, J. H. G., and Rietveld, L. (2013a). Characterization of PVC joints' behaviour during variable loading laboratory tests (submitted). *Urban Water Journal*

- Arsénio, A. M., Vreeburg, J. H. G., and Rietveld, L. (2013e). Index of joint condition for PVC push-fit joints (submitted). *Water Science & Technology: Water Supply*

- Arsénio, A. M., Dheenathayalan, P., Hanssen, R., Vreeburg, J. H. G., and Rietveld, L. (2013b). Pipe failure prediction in drinking water systems using satellite observations (submitted). *Structure and Infrastructure Engineering*

Conference proceedings

- Arsénio, A. M., Vreeburg, J. H. G., Pieterse-Quirijns, E. J., and Rosenthal, L. (2009b). Overview of failure mechanism of joints in water distribution networks. In Boxall, J. and Maksimović, C., editors, *Computing and Control in the Water Industry (CCWI)*, pages 607–612, Sheffield (UK). CRC Press

- Arsénio, A. M., Vreeburg, J. H. G., van Doornik, J., Dijkstra, L., and van Dijk, H. (2010). Assessment of PVC Joints Using Ultrasound. In *Water Distribution Systems Analysis (WDSA)*, Tucson (Arizona, USA). ASCE

- Arsénio, A. M., Vreeburg, J. H. G., de Bont, R., and van Dijk, H. (2011). Real-life inline inspection of PVC push-fit joints using NDE equipment. In *Leading Edge on Strategic Asset Management (LESAM)*, Mülheim an der Ruhr (Germany)

- Arsénio, A. M., Vreeburg, J. H. G., Bouma, F., and van Dijk, H. (2012a). Destructive laboratory tests with PVC push-fit joints. In *Water Distribution Systems Analysis (WDSA)*, Adelaide (Australia)

- Arsénio, A. M., Vreeburg, J. H. G., Wielinga, M. P. C., and van Dijk, H. (2012c). Continuous assessment of a drinking water PVC pipe. In *Water Distribution Systems Analysis (WDSA)*, Adelaide (Australia)

Posters in conferences

- Arsénio, A. M., Pieterse-Quirijns, E. J., and Vreeburg, J. H. G. (2009a). Failure mechanisms of joints in water distribution networks and its application on asset management. In *Leading Edge on Strategic Asset Management (LESAM)*, Miami (Florida, USA)